Identification and Characterization of M2 Macrophage-targeting Peptide M2pep for the Delivery of Pro-apoptotic Peptides to Tumor-associated Macrophages

Mary Elise Cieslewicz

A dissertation
submitted in partial fulfillment of the
requirements for the degree of

Doctor of Philosophy

University of Washington

2015

Reading Committee:

Suzie Pun, Chair

André Lieber

Elaine Raines

Patrick Stayton

Program Authorized to Offer Degree:
Bioengineering

University of Washington

Abstract

Identification and Characterization of M2 Macrophage-targeting Peptide M2pep for the Delivery of Pro-apoptotic Peptides to Tumor-associated Macrophages

Mary Elise Cieslewicz

Chair of the Supervisory Committee
Professor Suzie Pun, Ph.D.
Bioengineering

Activated macrophages are made up of two broad subsets, M1 "classically activated" macrophages and the M2 "alternatively activated" macrophages. These subsets present diverse functional phenotypes, with M1 macrophages exhibiting a pro-inflammatory and microbicidal functions while M2 macrophages possess functional roles in resolution of inflammation and tissue remodeling. An imbalance in M1 versus M2 macrophages can contribute to disease progression. In cancer, populations of tumor-associated macrophages (TAMs) mediate immunosuppression and possess M2-like qualities such as poor antigen presentation, promotion of angiogenesis and tissue remodeling and repair. In addition, TAMs may promote the exhausted phenotype of CD8+ T cells, resulting in their inability to eliminate tumor cells. Not surprisingly, the extent of TAM accumulation within tumors generally correlates with poor disease prognosis. Despite the growing interest in tumor immunotherapy, there continues to be a dearth of TAM-specific targeting agents.

In this work, an M2-selective peptide was isolated via a subtractive phage biopanning technique against whole cells. The phage biopanning resulted in identification of M2pep, a peptide that selectively binds and is internalized by murine M2 macrophages. Next, M2pep was characterized for binding to TAMs extracted from CT-26 syngeneic tumors as well as accumulation in TAMs *in vivo*. Administration of a fusion peptide of M2pep with KLA, a pro-apoptotic peptide, resulted in delayed tumor growth, increased mouse survival, and selective elimination of TAMs.

Unfortunately, M2pep did not bind human M2 macrophages derived from peripheral blood mononuclear cells (PBMC), and consequently, whole-cell phage display biopanning against human macrophages was performed to obtain a similar human M2pep peptide. Despite six separate whole-cell panning attempts against human PBMC-derived M2 macrophages, no peptide with selective binding to human M2 macrophages was isolated. In addition, biopanning against Legumain and PD-L1 immobilized proteins, targets selected for their high expression on tumor-associated macrophages, failed to distinguish peptides with selective binding to their target protein. Work to discover peptides with selective human M2 macrophage binding properties is ongoing in the lab.

TABLE OF CONTENTS

Work appearing in this thesis was published in the following manuscript:
M Cieslewicz, J Tang, JL Yu, H Cao, M Zavaljevski, K Motoyama, A Lieber, EW Raines, and SH Pun. Targeted Delivery of Proapoptotic Peptides to Tumor-associated Macrophages Improves Survival. *Proceedings of the National Academy of Sciences.* October 2013. 110(40): 15919 - 15924.

LIST OF FIGURES

CHAPTER 1

CHAPTER 2

CHAPTER 3

ACKNOWLEDGEMENTS

At the culmination of PhD you hardly know where to begin in thanking those people who helped you at every stage of your life in achieving this goal. It is an accomplishment that could only have been achieved with the help and support of my family, friends, and mentors who inspired my interest in medical research, developed my scientific and laboratory skills, supported my career choices, and also kept me company along the way.

I foremost want to thank Suzie for her support over the last five years. As an advisor, Suzie has the incredible ability to mentor her students in a supportive yet hands-off manner. After every conversation with Suzie, I was amazed that an individual could be so smart yet approachable. While primarily invested in the development of her students' scientific skills, Suzie also takes an active interest in our personal interests and career choices. As my career goals evolved over the last five years, Suzie worked to help me discover the right fit, first helping me acquire an internship in the biotechnology industry and then supporting me through the management consulting interview process. Her support of alternative career choices for PhDs was invaluable to me.

I also want to thank my committee members, André Lieber, Elaine Raines and Patrick Stayton, who served as research collaborators and resources for scientific discussions. Your input was instrumental to the completion of this work.

There are also several individuals who guided my interest in math and science as well as introduced me to laboratory work. I would like to thank my high school teachers, Christine Lucas and Marisa Roberts, who inspired me to pursue an engineering degree in college and solidified my commitment to encourage other women to do the same. I would also like to thank Kelly Orcutt who, as a graduate student at MIT, mentored me in the lab for two years and supported me through the graduate school application process.

Several past and current Pun Lab Members (Punions!) also contributed to my thesis through scientific and non-scientific discussions:

- Leslie Chan (my partner in crime): Completing graduate school with Leslie was a treat. Leslie was my first friend in Seattle. I'll never forget our Friday Night Frying Session… because the best way to finish a long week in lab is to deep-fry everything in your fridge, of course!

- Julie Shi: As a senior graduate student above me and my office mate, Julie was my lab confidant, always willing to discuss confusing data and lend a supportive word when science didn't go my way.

- Dave Chu: Dave always made lab fun, affectionately giving me my lab nickname and providing stimulating conversation across our benches.

- Christine Wang and Kevin Tan: Christine and Kevin were my podcast and pop culture gurus, respectively! They were always able to keep me up to date on NPR and Taylor Swift.

- Chayanon Ngambenjawong: I am always so impressed by Chayanon, probably the most hard-working person I have ever met. I am amazed by Chayanon's thoughtful approach to research and constant willingness to help others in lab.

- Bob Lamm, Gary Liu, and Brynn Livesay (the dynamic trio!): Starting their graduate career during my fourth year of graduate school, Brynn, Gary and Bob brought such a great attitude to the lab. The three of them truly made me want to be a better, more positive person, and I feel so good leaving the lab in such great future hands!

- Nataly Kacherovksy: Thank you to Nataly for her mentorship during my rotation project, and her molecular biology expertise!

- Jonathan Yu: As an undergraduate working with me for three years, I saw Jonathan blossom from a recently graduated high school senior to a full-blown scientist. I cannot thank Jonathan enough for his hard work, great attitude and flexibility in lab. His contribution to this work is truly incredible.

I would also like to thank friends who offered fun distractions from lab along the way. I truly enjoyed playing Seven Wonders with friends Joe Phan, Austin Day and Tom Long. Talyn Chu was my Seattle expert, always knowing the best place to get dinner or the quirkiest, "only in Seattle" activity to do. Lastly, Jenna Sullivan has been a genuine friend who counseled me through grad school strife, always up for grabbing dinner and offering advice on subjects ranging from life lessons to flow cytometry lessons.

I would like to thank my siblings, John and Catherine Cieslewicz. John left for college when I was 12 years old, and started his PhD when I was 16 years old. Seeing John's education and career path unfold as I grew up made me think about what I wanted out of school, and I feel I owe so much to John for introducing me to the idea that I could get a PhD, too. Catherine has always been such a supportive and accommodating sister! Growing up, she never seemed embarrassed or annoyed by her "little sister," and it means so much to me that I can still call Catherine whenever I need encouragement.

My fiancé, Daniel, has been my rock from a distance. Preparing to graduate in 2010 and begin a 5-year long distance relationship, I told Dan that I might be too busy in grad school to talk every day on the phone. He jokingly replied, "That's ok, just pencil me in." Dan's mellow attitude has kept me mellow, and in the end we often talked more than once each day. Doing a rough calculation, I discovered that Dan has likely flown over 70,000 miles to visit me over the last five years, which is almost 3 times the circumference of the earth. I'm so grateful to Dan for enduring these tough last five years so that I could come to UW to work for Suzie. And I am so excited to be marrying a man who would fly around the world to see me.

Lastly, this PhD would not have been possible without the unconditional love and support of my parents, Mike and Mary Cieslewicz. As I grew up, they always supported whatever career I thought I wanted to pursue – even when, as a 12 year old, I thought I wanted to be a chef. In many ways, lab work is a lot like cooking, so that support prepared me for work they had no clue I would do in the future! They exemplified what hard work looks like and always encouraged a love of learning. They provided every opportunity for me to try new things and find out what I am passionate about. This thesis is dedicated to them because it is truly an extension of the love and opportunities they gave to me.

DEDICATION

to my parents, Mary and Michael

my fiancé, Daniel

Chapter 1

IDENTIFICATION AND CHARACTERIZATION OF THE MURINE M2 MACROPHAGE TARGETING PEPTIDE M2PEP

Abstract

Activated macrophages are made up of two broad subsets, the M1 “classically activated” macrophages and the M2 “alternatively activated” macrophages. The M1 macrophage phenotype is induced by endogenous, pro-inflammatory mediators such as interferon-γ or exogenous molecules such as lipopolysaccharide, resulting in a pro-inflammatory and microbicidal functional phenotype. In contrast, M2 macrophages are activated by IL-4 and IL-13, and possess functional roles in resolution of inflammation and tissue remodeling. An imbalance in M1 vs M2 macrophages can contribute to disease progression. Despite utilizing ligands such as mannose or folate, which bind receptors that are more highly expressed on M2 macrophages, no truly M2 macrophage-specific targeting moiety existed prior to this work. To identify an M2-selective peptide, a subtractive phage biopanning technique against whole cells was employed. The phage biopanning resulted in identification of M2pep, a peptide that selectively binds and is internalized by murine M2 macrophages.

1.1 Introduction and Rationale

1.1.1 The Role of the Immune System In Disease Prevention and Progression

Both innate and adaptive immunity play an important role in host defense against pathogens. Immunological recognition of a pathogen is achieved by both white blood cells of the innate immune system and lymphocytes of the adaptive immune system.

The first line of defense against an invading pathogen is physical barriers such as mucosal surfaces, and chemical toxins such as antimicrobial peptides secreted by cells at these barriers. In addition, phagocytic cells such as macrophages, can ingest and degrade invading pathogens. The innate immune response occurs quickly to react to an infectious organism, while the adaptive immune response occurs on a longer time scale.

Lymphocytes of the adaptive immune system achieve highly specific elimination of pathogens due to antigen receptors expressed on the surface of these cells. Thus the adaptive immune response is much more efficient. In addition, adaptive immune cells can endure even after the infection has been resolved, creating long-term immunity to invading pathogens. Typically an adaptive immune response occurs over the course of hours to days, while an innate immune response can occur within minutes of exposure to a pathogen. The adaptive immune response to an invasion can last for weeks, and pathogen memory may last a lifetime.

While the immune system is critical for eradication of infection, it can also play a role in various chronic inflammatory diseases. For example, patients with the autoimmune disease multiple sclerosis develop T cells that are reactive against the myelin sheath that protects axons, resulting in a coordinated inflammatory response that damages this protective layer [1]. Multiple sclerosis patients exhibit decreased motor function that includes loss of limb mobility, impaired vision and incontinence. While in multiple sclerosis, the immune system is activated to target destruction of healthy tissues, in other diseases the immune system can become deactivated and result in unchecked disease progression. This thesis discusses such immune system dampening that occurs in cancer progression (Chapter 2), and suggests methods of targeting immune cells that play a role in tumor growth.

1.1.2 The Genesis and Polarization of Macrophages

All cellular components of the blood are derived from the same progenitor cell, the pluripotent hematopoietic stem cell, found in the bone marrow. The pluripotent hematopoietic stem cell gives rise to the common lymphoid progenitor and common myeloid progenitor, which are precursors to T cells and macrophages, respectively, among other cell types. The common myeloid progenitor gives rise to monocytes that, after circulating in the peripheral blood, extravasate into tissues where they differentiate into macrophages. Depending on their tissue of residence, macrophages take on different titles and diverse functional roles. Macrophages are one of the phagocytic cells of the immune system, and play a major role in engulfing and killing invading pathogens. Macrophages also initiate inflammation in response to a microorganism, activating and recruiting other immune cells. Outside of their role in host defense, macrophages are also scavengers that clear dead cells from the body [2].

Tissue macrophages can be shifted to diverse functional phenotypes by local environmental cues [3]. These polarization states are broadly categorized as classically-activated M1 macrophages or alternatively-activated M2 macrophages. The M1 macrophage phenotype is induced by endogenous, pro-inflammatory mediators such as interferon-γ or exogenous molecules such as lipopolysaccharide, resulting in a pro-inflammatory and microbicidal functional phenotype [4].

In contrast, M2 macrophages are activated by IL-4 and IL-13, and possess functional roles in resolution of inflammation and tissue remodeling [5]. In addition to the IL-4/IL-13 activated M2 macrophage (also known as M2a), other M2-like cells have been identified, including the M2b (activated by immune complexes and agonists of toll-like receptors), and M2c (activated by IL-10 and gluccocorticoid hormones) cells [6]. Macrophages exhibit both heterogeneity and plasticity, with dynamic changes in polarization as inflammation or disease progress.

1.1.3 Dearth of Targeting Moieties for M1 and M2 Macrophages

Several ligands have been used to target macrophage populations. The small molecules mannose and folate, which are ligands for the mannose receptor and folate receptor β, respectively, have been conjugated to drugs or drug carriers for macrophage delivery [7, 8]. However, receptors for both molecules are highly expressed in other cell types. Mannose receptor is a pathogen recognition receptor that is also used by dendritic cells [9]. In addition to activated macrophages, folate binds to receptors on normal epithelial cells and tumor cells [10]. Segers and colleagues reported the use of phage display to identify a peptide that binds the scavenger receptor-A on macrophages found within atherosclerotic plaques [11], but scavenger receptor-A is also expressed on dendritic cells.

1.1.4 Identification of Targeting Ligands Via Phage Display

Peptide phage library screening is a common method of identifying novel targeting ligands, and has been used to identify peptides for applications targeting tumor vasculature [12], colon cancer [13], brain endothelial cells and neurons [14, 15], and cardiomyocytes [16], among several others. Commonly, phage display is conducted against a known antigen that is immobilized onto a surface. This method offers many benefits, as the purified protein offers a homogeneous target population for panning and increases the likelihood of identifying a selective phage. Furthermore, the target antigen is known, which simplifies follow-up characterization of the peptide's affinity for its target.

However, phage panning against whole cells or *in vivo* targets, while more challenging, offers the opportunity to identify novel targets on a particular cell population, or isolate peptides with the ability to bind a target *in vivo.* Recently, work by Li and colleagues used a subtractive whole cell panning technique to identify a peptide that bound selectively to a cell line of esophageal adenocarcinoma [17]. This peptide was then tested for binding to human esophageal specimens, and shown to preferentially bind dysplasia in Barret's esophagus. This type of peptide could possible be used for early detection of cancerous cells.

1.2 Materials and Methods

1.2.1 Materials

Recombinant Mouse Macrophage Colony Stimulating Factor (M-CSF) (Shenandoah Biotech); mouse recombinant interferon-γ (R&D Systems); lippopolysaccharide (InvivoGen); mouse recombinant interleukin-4 (R&D Systems); recombinant mouse interleukin-10 (R&D Systems); rabbit anti-ovalbumin IgG (Polysciences); recombinant mouse interleukin-1β (R&D Systems); anti-mouse F4/80 FITC antibody (AbDserotec); anti-mouse CCR2 PE antibody (R&D Systems); anti-mouse CCR9 FITC antibody (eBioscience); anti-mouse CD11c PE antibody (eBioscience); anti-mouse CD301 FITC antibody (AbDserotec); Phosphate Buffered Saline (made in house); PhD-C7 and PhD-12 Phage Libraries (New England Biolabs); Biotin-PEG NovaTag resin (EMD Millipore); NovaPEG Rink Amide resin (EMD Millipore); Fmoc-Cys(Trt) Wang resin (EMD Millipore); AlexaFluor660-maleimide (Life Technologies); anti-M13 phage antibody (Sigma); goat anti-rabbit FITC antibody (Sigma); streptavidin-FITC (eBioscience); streptavidin-PEcy7 (eBioscience); anti-mouse Ly6G FITC/PE antibody (BD Pharmingen); anti-mouse B220 FITC/PE antibody (BD Pharmingen); anti-mouse CD3 PE antibody (BD Pharmingen); anti-mouse CD45 APC antibody (BD Pharmingen); anti-mouse CD11c PE antibody (eBioscience); anti-mouse F4/80 PEcy5 antibody (eBioscience); anti-mouse F4/80 unlabeled antibody (Abcam); anti-rat AlexaFluor555 antibody (Life Technologies); chloroquine (Sigma); methyl-β-cyclodextrin (Sigma); cytochalasin D (Sigma); dynasore (Sigma); nocodazole (Sigma); Hanks Balanced Salt Solution (ThermoScientific); Cell Tracker Violet BMQC (Life Technologies); Far Red Live Dead Fixable Dye (Life Technologies)

1.2.2 Generation of Bone Marrow-derived Macrophages

All protocols for animal handling were approved by the UW Institutional Animal Care and Use Committee. Bone marrow-derived macrophages were generated as previously described using mouse M-CSF [18]. Briefly, bone marrow was harvested from female C57bl/6 mice and 5 million cells per dish plated in non-tissue culture treated petri dishes in RPMI media supplemented with 20% Horse Serum, 1% Antibiotic/Antimycotic (AbAm) and 20 ng/mL

recombinant mouse macrophage-colony stimulating factor (M-CSF). Cells were supplemented with additional media on day 4 of differentiation. 7-day differentiated macrophages were activated for 48 hours in media containing cytokines as follows: M1 cells used 25 ng/mL interferon-γ (IFNγ) and 100 ng/mL lipopolysaccharide (LPS), M2a cells used 25 ng/mL interleukin-4 (IL-4), and M2c cells usd 10 ng/mL interleukin-10 (IL-10). M2b macrophages were generated as previously described [19]. Briefly, non-tissue culture treated 6-well plates were coated with 0.6 mg/mL of anti-OVA IgG for 2 hours at room temperature, with shaking, and then washed three times with warmed Phosphate Buffered Saline (PBS) supplemented with 1% Bovine Serum Albumin (PBS/1%BSA). 7-day differentiated macrophages were plated at 2 million cells/well in activation media containing 20 ng/mL interleukin-1β (IL-1β) for 24 hours. All cells were cultured at 37°C in a 5% CO_2 atmosphere.

1.2.3 Flow Cytometry Characterization of Polarized Macrophages

M1, M2 and resting macrophages were incubated at 4°C for 10 minutes with Fc Block. Fc Block was removed, and cells incubated for 15 minutes with anti-F4/80 FITC antibody, or anti-CCR2 PE and anti-CCR9 FITC antibodies, or anti-CD11c PE and anti-CD301 FITC antibodies. Cells were washed three times with PBSA and analyzed on a FACScan Flow Cytometer (Becton Dickinson).

1.2.4 Subtractive Panning Method

The first round of panning was conducted only on M2 macrophages to select for all M2 macrophage binding phage. All phage incubations were done for 1 hour at 4°C, rotating. First a 2-hour receptor-clearing period was performed by removing media from M2 cells and replacing with warmed RPMI. Next, cells were lifted and incubated with PhD-C7 and PhD-12 libraries ($2x10^{11}$ Plaque Forming Units (PFU)) in PBS/1%BSA. Cells were washed five times using PBS/1%BSA, then resuspended in 1 mL 0.2 M Glycine-HCl on ice for 15 minutes. Cell solution was neutralized with 150 μL of 20 mM Tris pH 9.1, and then underwent three freeze-thaw

cycles. Cell solution was then titered and amplified according to the NEB protocol. For subsequent subtractive pans, $2x10^{11}$ PFU of the amplified eluate was first applied to receptor-cleared M1 macrophages. M1 macrophages were centrifuged and the supernatant applied to M2 macrophages. Phage was eluted from M2 cells and amplified. Subtractive panning was repeated three times, using the amplified eluate from the previous pan as the starting library for each round. Ten plaques from the third round of panning were selected for DNA sequencing.

1.2.5 ELISA Phage Binding Study

M1, M2 and unactivated macrophages and dendritic cells were plated in a 96-well plate. Cells were incubated for 2 hours with $1x10^{5}$ PFU/μL M2pep Phage or Phage Library in Hanks Buffered Saline Solution (HBSS) supplemented with 1% BSA at 4˚C. Cells were washed twice with HBSS supplemented with 1% BSA and fixed for 15 minutes with 4% paraformaldehyde at 4˚C. Cells were washed twice, and incubated for 30 minutes at 4˚C with a 1:2000 dilution of rabbit anti-M13 antibody in HBSS supplemented with 1%BSA. Cells were washed twice, and incubated with a 1:12000 dilution of anti-rabbit HRP antibody for 30 minutes at 4˚C. Cells were washed twice, substrate was added, quenched and absorbance at 450 nm and 540 nm read on a Safire^{2} plate reader (Tecan). Developed substrate was removed and cellular protein quantified by a bicinchoninic acid assay.

1.2.6 Titering Phage Binding Study

$2x10^{11}$ PFU M2pep Phage were incubated with 10^{6} cells of resting, M1, M2, and dendritic phenotype in 200 μL total volume for 2 hours at 4˚C. Cells were then washed three times with PBS/1%BSA and resuspended in 1 mL of Triton1X, and underwent one freeze-thaw cycle. Thawed cells were passed through a 25 g needle to facilitate cell lysis and titered according to the NEB protocol.

1.2.7 Solid Phase Peptide Synthesis and Fluorophore Conjugation

For use in dissociation constant measurement studies, biotinylated M2pep with a PEG linker (sequence: YEQDPWGVKWWY) was synthesized using standard Fmoc solid phase peptide synthesis on a PS3 peptide synthesizer (Protein Technologies) using a Biotin-PEG NovaTag resin. For use in all other binding studies, peptides (M2pep and scM2pep with sequence WEDYQWPVYKGW) synthesized with a C-terminal biotin tag were purchased from Elim Biopharmaceuticals Inc (Hayward, CA) at >95% purity. A Lys_3Gly_3Ser linker was appended to the C-terminus of the phage-displayed sequence to assist in solubility and peptide display. For use in confocal imaging studies, M2pep was synthesized on a Fmoc-Cys(Trt) Wang resin, which adds a C-terminal cysteine to the synthesized peptide. AlexaFluor660-maleimide was conjugated to the free thiol of the cysteine-terminated peptide.

1.2.8 Flow Cytometry Peptide Binding Study

Primary murine macrophage cell types were activated as described above, neutrophils were obtained from the bone marrow, and B and T cells were obtained from the spleen. Neutrophils, B cells, and T cells were identified by anti-mouse Ly6G PE, anti-mouse B220 PE, and anti-mouse CD3 antibodies respectively. Cells were also isolated from the peritoneal cavity of a thioglycollate-injected mouse and probed with anti-mouse CD45 APC, anti-mouse CD11c PE, anti-mouse CD301 FITC, and anti-mouse F4/80 PEcy5 antibodies. For each binding study, 10^5 cells were incubated with Fc Block for ten minutes, then Fc Block was removed and cells incubated with 200 μM of M2pep for 30 minutes at 4°C. Cells were washed three times, fixed with 4% paraformaldehyde, and probed with either streptavidin-FITC or streptavidin-PEcy7 antibodies. Cells were analyzed on a BD Canto flow or Miltenyi MACSQuant cytometer.

1.2.9 Flow Cytometry Peptide Binding Study in Mixed Population of M1 and M2 Macrophages

M2pep binding M2 macrophges in populations of cells with varying ratios of M1 or M2 macrophages was assessed via flow cytometry. Plates of M2 macrophages were first stained

with Cell Tracker Violet BMQC dye via the manufacturers instructions. M1 macrophages or violet-stained M2 macrophages were then lifted from culture plates via cell lifter and aliquoted into a 96-well, round bottom, black plate in varying ratios of M1 and M2 macrophages: 10%, 20%, 30%, 40%, 50%, and 100% M2 macrophages in 100,000 total cells per well. Cells were then incubated with 200 μM of biotinylated-M2pep for 30 minutes at 4˚C and washed twice. Cells were stained with the Far Red Fixable Live/Dead dye according to manufacturer's instructions and fixed for 15 minutes at 4˚C with 4% paraformaldehyde. Cells were then washed once followed by staining with Streptavidin-PEcy7 for 15 minutes at 4˚C. Cells were washed twice and analyzed on a MACSQuant Flow Cytometer.

1.2.10 Measurement of M2pep Dissociation Constant on Cells

The Kd of M2pep with an oligoethyleneglycol-biotin tag was quantified in a titration flow cytometry assay. 10^5 M2 macrophages per sample were incubated with varying concentrations of M2pep in PBSA for 1 hour at 4˚C. Cells were washed three times with PBS/1%BSA, then fixed with 0.5% methanol free formaldehyde for 15 minutes at 4˚C. After one wash, M2pep was probed with a FITC-conjugated Streptavidin for 15 minutes at 4˚C, followed by three washes with PBS/1%BSA. Cells were analyzed on a FACSCanto flow cytometer (Becton Dickinson). The median fluorescence intensities were fit by least squares regression to the following equation: $\mathrm{MFI}_{\mathrm{expected}} = \mathrm{MFI}_{\mathrm{min}} + \mathrm{MFI}_{\mathrm{range}}\left(\frac{[\mathrm{peptide}]}{[\mathrm{peptide}]+K_d}\right)$, to calculate K_D.

1.2.11 M2pep Phage Competition Study

M2 macrophages were incubated with 10^9 PFU of M2pep Phage for 20 minutes at 4˚C. Then unbound phage was removed and replaced with M2pep or scM2pep at varying concentrations for 30 minutes at 4˚C. Cells were washed twice with PBS/1%BSA, then fixed for 15 minutes at 4˚C with 0.5% methanol free formaldehyde, followed by one wash with PBS/1%BSA. Bound phage was probed using a 1:2000 dilution of rabbit anti-M13 Phage antibody for 30 minutes at 4˚C,

followed by two washes with PBS/1%BSA. Then, anti-M13 antibody was probed using a 1:80 dilution of goat anti-Rabbit-FITC antibody, followed by two washes with PBS/1%BSA. Cells were analyzed using a MACSQuant flow cytometer (Miltenyi).

1.2.12 M2pep-Streptavidin Complex Internalization Study

To generate a 500 nM solution of M2pep-Streptavidin-PEcy7 complexes, 4x molar excess of biotinylated M2pep was incubated with PEcy7-labeled streptavidin in RPMI media supplemented with 20% Horse Serum for 30 minutes at room temperature. Then, a 1:60 dilution of anti-F4/80 APC was added, and complex solution incubated with M1 and M2 macrophages plated on coverslips for 1 hour at 37°C. Cells were washed with HBSS supplemented with 1% BSA (HBSS/1%BSA) three times, followed by fixation with 4% paraformaldehyde for 15 minutes at room temperature. Cells were washed once with HBSS/1%BSA, followed by staining with 2 μg/mL DAPI. Cells were washed twice with HBSS and mounted onto coverslips

1.2.13 Fluorophore-conjugated M2pep Internalization Study

M1 and M2 macrophages and CT-26 cells were plated on glass coverslips. Cells were incubated with 20 μM of AlexaFluor660-labeled M2pep or scM2pep and a 1:200 dilution of rat anti-F4/80 antibody in RPMI media supplemented with 10% Horse Serum. Cells were incubated for 1 hour at 37°C. Cells were washed three times with HBSS/1%BSA, then incubated for 20 minutes at room temperature with an anti-rat AlexaFluor555 antibody. Cells were washed three times, then fixed for 15 minutes at room temperature with 4% paraformaldehyde. Cells were stained with 5 μg/mL DAPI, washed and mounted onto glass slides. Slides were imaged using a Zeiss LSM 510 META confocal microscope.

1.2.14 M2pep Mechanism of Internalization Inhibitor Study

To identify the mechanism of internalization of M2pep, M2 macrophages were stained for both confocal imaging and flow cytometry analysis after exposure to chemical compound inhibitors of various internalization pathways. To stain for confocal imaging, M2 macrophages were plated on glass slides in a 24 well plate. Cells were then subjected to a 2 hour incubation at 37°C with 5 mM methyl-β-cyclodextrin, 10 μM cytochalasin D, or 100 μM chloroquine, or a 1 hour incubation at 37°C with 1 μM Dynasore or 100 μM nocodazole in RPMI media supplemented with 2% horse serum. Then, inhibitor compounds were removed and cells incubated for 1 hour at 37°C with RPMI media containing 20 μM fluorescein-labeled M2pep and the same concentrations of inhibitors indicated above. Cells were then washed three times with ice cold HBSS/1%BSA and fixed for 15 minutes at room temperature with 4% paraformaldehyde. Cells were stained with 5 μg/mL DAPI, washed and mounted onto glass slides. Slides were imaged using a Zeiss LSM 510 META confocal microscope.

Staining cells for flow cytometry analysis proceeded in a similar fashion. M2 macrophages were seeded in a 24 well plate and subjected to the inhibitor compound pre-incubation described above, followed by incubation with fluorescein-labeled M2pep and inhibitor compounds. Cells were then washed, lifted from the plate using trypsin, stained with the live/dead dye propidium iodide, and analyzed on a flow cytometer.

1.2.15 Statistics

Differences between groups were assessed via a Student's T Test.

1.3 Results

1.3.1 Characterization of Bone Marrow-derived Macrophages

Although M1 and M2 macrophage phenotypes are observed in diseased tissues, cultured macrophages polarized toward the M1 or M2 phenotype *in vitro* show a more homogeneous response Therefore, M1 and M2 cells were generated for biopanning by polarizing murine bone marrow-derived macrophages with interferon (IFN)-γ and lipopolysaccharide (LPS), and with interleukin (IL)-4, respectively. Immunophenotyping confirms that two distinct macrophage populations are generated: $F4/80^{+}CCR2^{+}CCR9^{+}$ M1 and $F4/80^{+}CD301^{+}CD11c^{+}$ M2 cells (Figure 1.1). These markers have been previously reported for their respective subset [20].

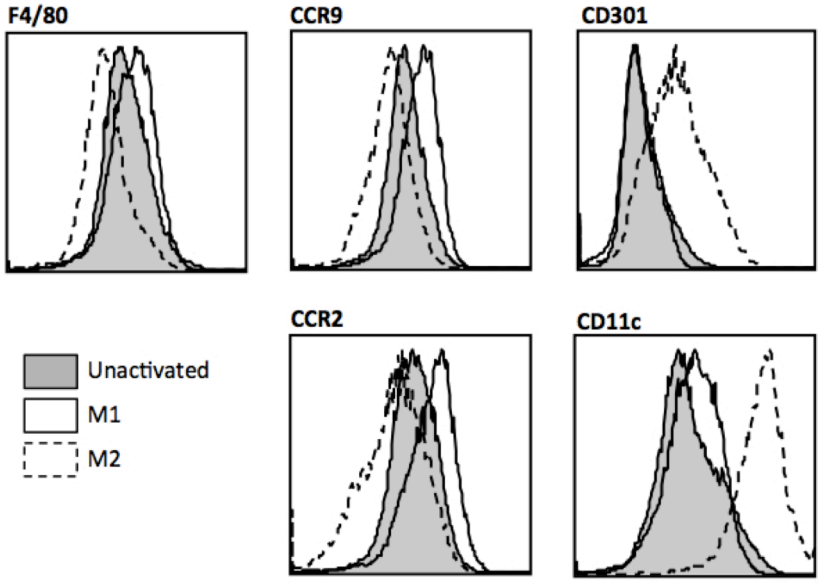

Figure 1.1: Immunophenotyping of murine M1 and M2 macrophages via flow cytometry. While both types of cells express the macrophage marker F4/80, M1 Macrophages preferentially express CCR9 and CCR2, and M2 Macrophages preferentially express CD301 and CD11c. Histograms representative of two experiments.

1.3.2 Subtractive Panning Technique Yields Two Consensus Sequences

M2 macrophage-binding peptides were identified using three successive rounds of subtractive phage panning to select for phage that bind preferentially to M2 over M1 macrophages. The titer of phage eluted from M2 cells increased in each successive selection round (Figure 1.2). Sequencing of ten random clones from the third round reveals two unique sequences: YEQDPWGVKWWY (M2pep), appearing in 8 of 10 clones, and HLSWLPDVVYAW, appearing in 2 of 10 clones.

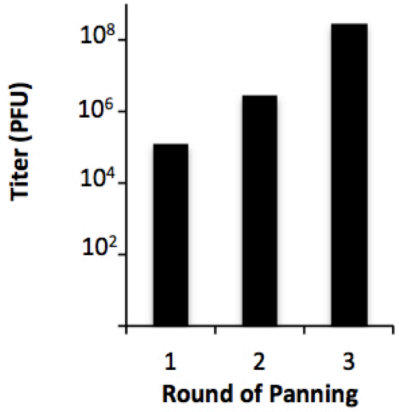

Figure 1.2: Phage titers from successive subtractive panning rounds increase, suggesting the enrichment of a consensus sequence.

1.3.3 M2pep Phage Exhibits Selective Binding to Murine M2 Macrophages

Selectivity of the phage clone displaying M2pep, hereafter called "M2pep Phage," for M2 macrophages was confirmed by titering (Figure 1.3A) and whole cell ELISA (Figure 1.3B). By both assays, M2pep Phage demonstrates higher affinity for M2 compared to M1 macrophages and dendritic cells ($p<0.05$). The titering binding study revealed that M2pep phage exhibited 2.7-fold higher binding to M2 macrophages over M1 macrophages, as well as 35-fold higher binding over the phage library. The ELISA binding study confirmed this result, demonstrating 2-fold higher binding of M2pep Phage to M2 macrophages over M1 macrophages, and 4-fold higher binding of M2pep Phage over the phage library.

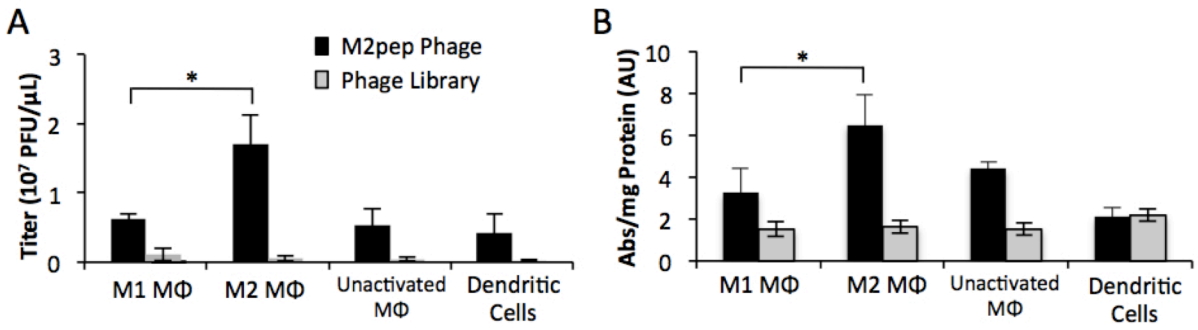

Figure 1.3: Characterization of M2pep Phage Binding. A) Titering and B) Whole-Cell ELISA binding studies indicate that M2pep phage exhibits selective binding to mouse M2 macrophages over M1 macrophages, unactivated macrophages and dendritic cells. n = 3. * p < 0.05

1.3.4 M2pep Exhibits Selective and Specific Binding to Murine M2 Macrophages

M2pep and a control peptide with a scrambled M2pep sequence (scM2pep) were synthesized with a Ser-Gly_3-Lys_3-Biotin C-terminal tag and tested for selectivity of M2 macrophage binding by flow cytometry using a labeled streptavidin probe (Figure 1.4A). M2pep exhibited significantly higher binding to M2 macrophages over all other cells types, including M1 macrophages ($p = .001$). Furthermore, scM2pep exhibited negligible binding to all cell types, demonstrating the sequence specificity of M2pep for M2 macrophages. M2pep exhibits 10.8 fold higher binding to M2 macrophages over scM2pep, as well as 5.7 fold higher binding to M2 over M1 macrophages. The equilibrium dissociation constant (K_D) of the M2pep with an oligoethyleneglycol-biotin tag for M2 macrophage was determined from a binding saturation curve to be roughly 90 μM (Figure 1.4B). The K_D of the untagged M2pep by competitive binding experiments was unable to be determined due to the solubility limits of this peptide.

A competitive binding experiment for M2pep phage with M2pep and scM2pep was performed to further demonstrate sequence-specific binding of M2pep. Phage bound to M2 macrophages were quantified by flow cytometry using an anti-M13 antibody. Competition with M2pep resulted in concentration-dependent inhibition of M2pep Phage binding with approximately 50% reduction in binding obtained with 10 μM peptide (Figure 1.5). Furthermore, competition with 200 μM of scM2pep exhibited no knock down of M2pep Phage binding ($p = .887$). Together the

direct and competitive binding studies demonstrate that M2pep exhibits both selective and specific binding to M2 macrophages.

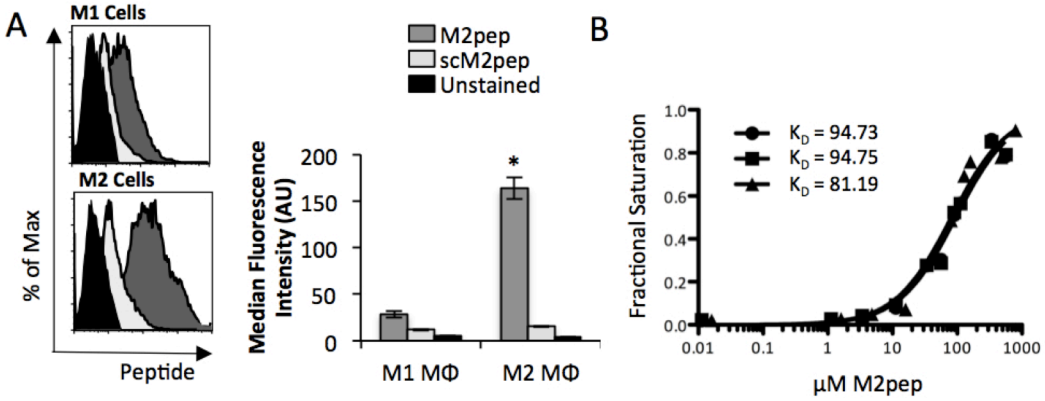

Figure 1.4: Biotinylated M2pep selectively binds M2 Macrophages. (A) Biotinylated M2pep exhibits higher binding to M2 macrophages over M1 macrophages, and greater binding than scM2pep. n = 3. * p < 0.01. (B) The dissociation constant of M2pep is estimated to be approximately 90 μM. Data from three separate experiments is shown.

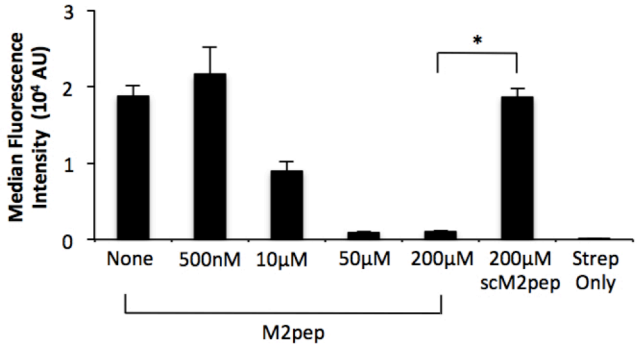

Figure 1.5: M2pep competition with M2pep Phage demonstrates specific binding of M2pep to M2 macrophages. Bound M2pep Phage was competed with M2pep or scM2pep and remaining bound phage was quantified by flow cytometry. n = 3. * p < 0.05.

1.3.5 M2pep Exhibits Binding to M2a and M2b Cells with Lower Binding to M2c Cells

M2 macrophages can be further divided into three subsets. M2a macrophages are activated by IL-4/IL-13, M2b macrophages are activated by immune complexes and agonists of toll-like receptors, and M2c macrophages are activated by IL-10 and gluccocorticoid hormones. M2b and

M2c macrophages are known to have increased expression of CD86 and CCR2, respectively [6]. Flow cytometry characterization confirms these phenotypes of M2b and M2c macrophages generated *in vitro* (Figure 1.6A). M2pep exhibits selective binding to M2a and M2b macrophages, with lower binding to M2c macrophages (p = .046) (Figure 1.6B).

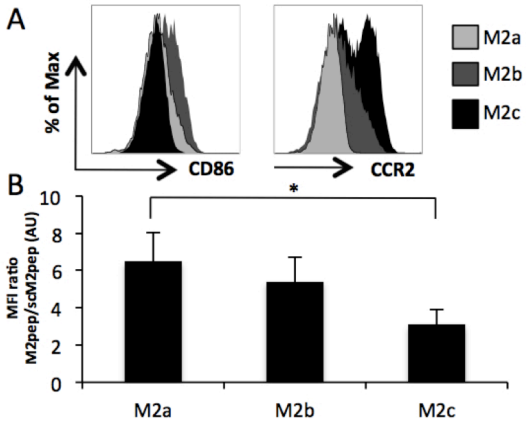

Figure 1.6: M2pep exhibits binding to M2a and M2b cells. (A) M2b and M2c macrophages are characterized by increased expression of CD86 and CCR2, respectively. Histograms representative of three experiments. (B) M2pep exhibits binding to M2a and M2b macrophages, with lower binding to M2c macrophages. n = 3. * p < 0.05.

1.3.6 M2pep Exhibits Selective Binding to M2 Macrophages in Mixed Populations of Cells

To test the utility of M2pep in recognizing M2 macrophages when exposed to a diverse milieu of cells, M2pep was exposed to varying ratios of M1 and M2 macrophages in a mixed population and analyzed for binding to M2 macrophages. Briefly, M2 macrophages were stained with Cell Tracker Violet dye before being mixed with unstained M1 macrophages in varying ratios: 1:9, 2:8, 3:7, 4:6, 5:5, or 10:0 M2 to M1 macrophages. M2 macrophages within these populations were then identified via the Cell Tracker Violet dye and assessed for median fluorescence intensity of M2pep binding. Among all ratios of M2:M1 macrophages tested, there was no statistical difference in the median fluorescence intensity of M2pep binding to M2

macrophages, suggesting that M2pep is able to recognize M2 macrophages even when they are a minority in a cell population (Figure 1.7).

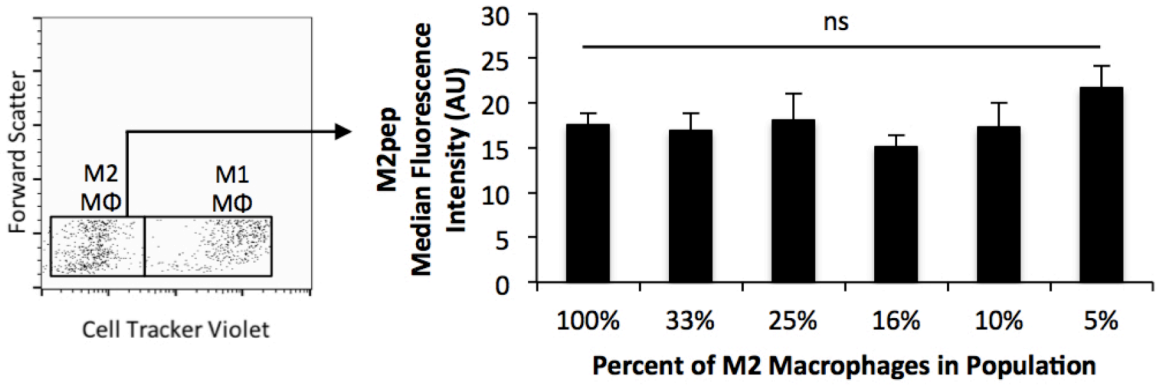

Figure 1.7: M2pep exhibits preferential binding to M2 macrophages in mixed populations of cells, even when the percent of M2 macrophages within the population is as low as 5%. n = 3. ns p > 0.05.

Because M2pep successfully bound to bone marrow derived, *in vitro* generated M2 macrophages in mixed population of cells, M2pep binding to mixed populations of primary cells was also tested. Mice were administered the sterile irritant thioglycollate by intraperitoneal injection, and peritoneal cells were harvested after 4 days for flow cytometric analysis. $CD45^+$ leukocytes (Figure 1.8Ai) were analyzed for expression of F4/80, CD11c (Figure 1.8Aii) and CD301 (Figure 1.8Aiii), and binding to M2pep. M2pep exhibits higher binding to $CD45^+F4/80^+$ cells that were $CD11c^+$ (Gate 1, p = .00001) or $CD301^+$(Gate 3, p = .002). M2pep exhibits 3.5 fold higher binding to $CD45^+F4/80^+CD11c^+$ M2 cells over $CD45^+F4/80^+CD11c^-$ cells, as well as 9.1 fold higher binding to $CD45^+F4/80^+CD301^+$ M2 cells over $CD45^+F4/80^+CD301^-$ cells (Figure 1.8B).

Binding of M2pep to mixed populations of cells isolated from the spleen and bone marrow was also tested. M2pep demonstrates higher binding to bone marrow-derived M2 macrophages, relative to splenic B cells (p = .004) and T cells (p = .002), and bone marrow-derived neutrophils (p = .003) (Figure 1.9). B cells, T cells, and neutrophils also exhibit high nonspecific binding of scM2pep, while M2 macrophages do not.

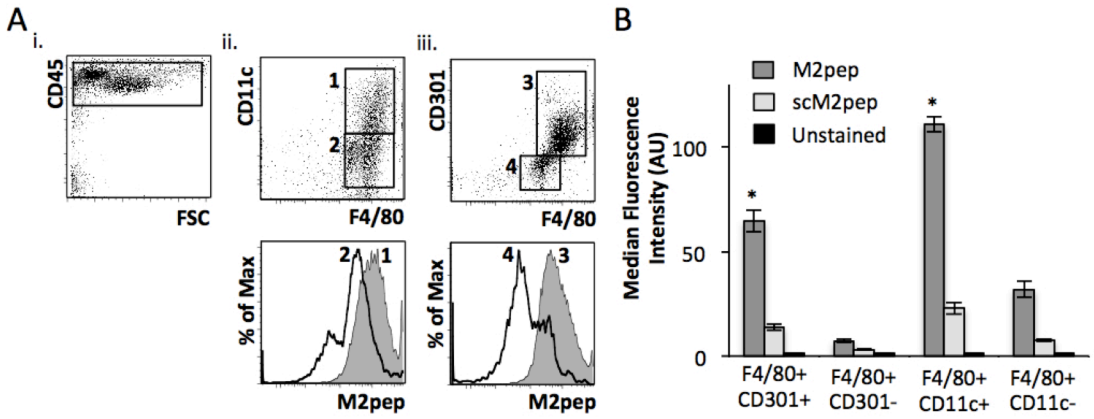

Figure 1.8: M2pep preferentially binds M2 macrophages isolated from the peritoneal cavity of mice. (A) M2pep preferentially binds F4/80+CD11c+ cells (ii) or F4/80+CD301+ cells (iii). Histograms representative of three experiments. (B) Median Fluorescence Intensity of populations depicted in part A. * $p < 0.01$.

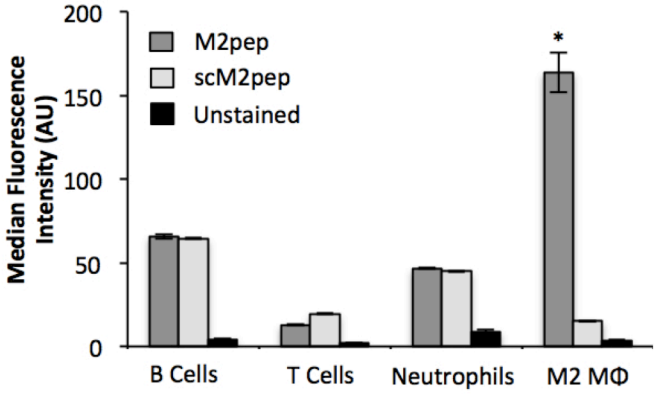

Figure 1.9: M2pep lacks binding to B cells, T cells, and neutrophils isolated from the spleen, but exhibits binding to bone-marrow derived, in vitro activated M2 macrophages. n = 3. * $p < 0.01$.

1.3.7 M2pep is Internalized by Murine M2 Macrophages but not M1 Macrophages or CT-26 Colon Carcinoma Cells

Binding studies by flow cytometry indicated that M2pep binds selectively to M2 macrophages relative to both M1 macrophages as well as CT-26 cancer cells ($p = .005$) (Figure 1.10).

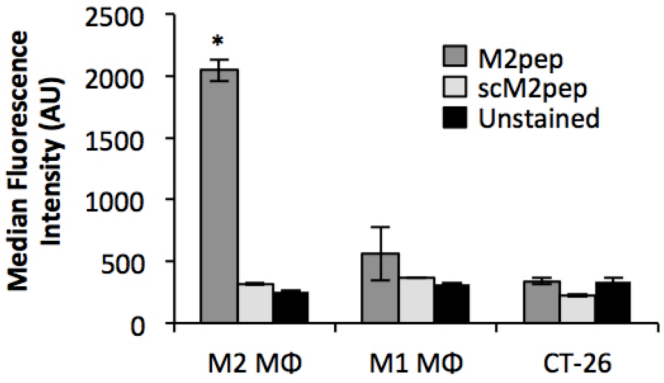

Figure 1.10: M2pep lacks binding to CT-26 colon carcinoma cells. n = 3. * p < 0.01.

To evaluate the ability of M2pep to mediate targeted intracellular delivery to M2 cells, AlexaFluor660-labeled M2pep and scM2pep were incubated at 37 ˚C with *in vitro*-derived M1 and M2 macrophages, and CT-26 colon carcinoma cells (Figure 1.11A). Confocal imaging demonstrates positive staining of M1 and M2, but not CT-26 cells, for F4/80, a macrophage marker (red). M2pep (green) is efficiently internalized in M2 macrophages relative to M1 macrophages ($p = .0002$) or CT-26 cells ($p = .000003$). scM2pep is not internalized in any of the tested cell types. Mean fluorescence intensity of M2pep binding to M2 macrophages is 3.8 fold higher ($p=0.0002$) and 5.3 fold higher ($p=0.000003$) than M1 macrophages and CT-26 cells, respectively (Figure 1.11B).

By similar methods, M2pep was tested for its ability to mediate delivery of a model biologic drug. Biotinylated M2pep or scM2pep was incubated with PEcy7-labeled Streptavidin to generate protein complexes. The complexes were then applied to M1 and M2 macrophages and imaged using a confocal microscope. The images show that M2pep mediates the delivery of streptavidin selectively to M2 macrophages and not M1 macrophages. Furthermore, scM2pep-streptavidin complexes show no uptake (Figure 1.12). This data illustrates the potential usefulness of M2pep as an M2-selective agent for intracellular delivery of cargo.

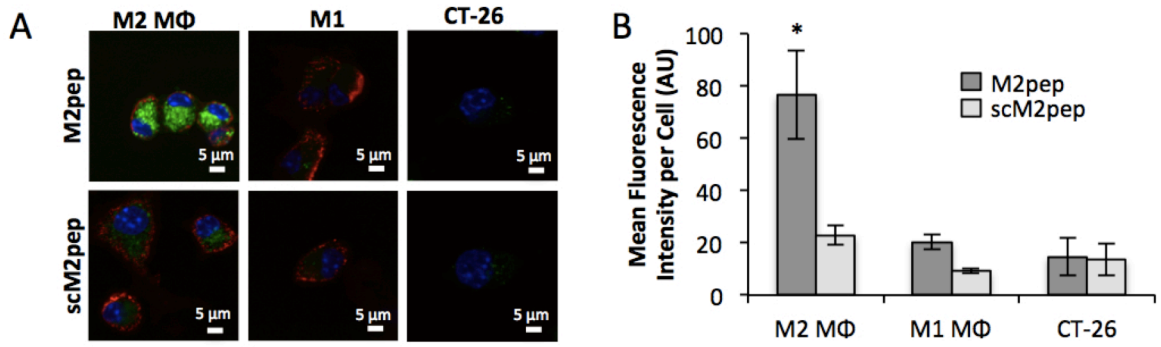

Figure 1.11: M2pep is internalized by M2 macrophages but not M1 macrophages or CT-26 colon carcinoma cells. (A) Cells were plated on coverslips and incubated with 20 µM of AlexaFluor660-labeled M2pep or scM2pep (green), an anti-F4/80 antibody (red), and DAPI nuclear dye (blue), and imaged using a confocal microscope. Images representative of two experiments. (B) Mean Fluorescence Intensity of imaged cells in part A were quantified. Cell counts for analysis: M2pep/M2MΦ n = 8, M2pep/M1MΦ n = 3, M2pep/CT26 n = 5, scM2pep/M2MΦ n = 5, scM2pep/M1MΦ n = 3, scM2pep/CT26 n = 2. * $p < 0.01$.

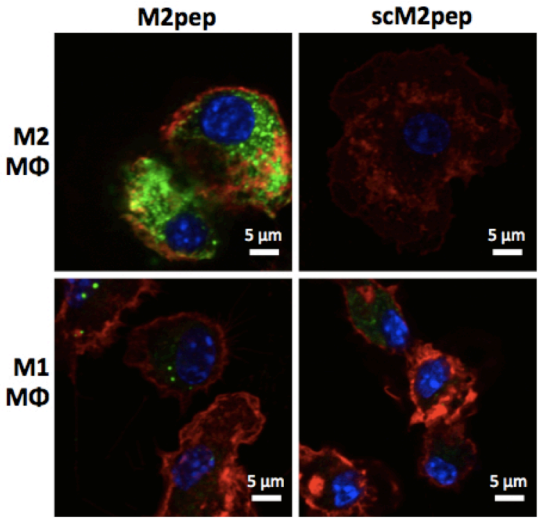

Figure 1.12: M2pep mediates the intracellular delivery of a biologic. M2pep-Streptavidin complexes (green) and an anti-F4/80 antibody (red) were incubated with M1 and M2 macrophages. Cells were stained with DAPI and imaged on a confocal microscope.

1.3.8 M2pep Is Internalized by Macropinocytosis

The mechanism of M2pep internalization was elucidated in order to provide insight into potential cell surface receptors that bind M2pep. Briefly, M2 macrophages were pre-incubated with various inhibitors of internalization pathways, followed by incubation with inhibitors plus fluorescently labeled M2pep. These cells were then imaged via a confocal microscope or analyzed on a flow cytometer for uptake of M2pep. Cells were incubated with the inhibitors of clathrin-independent internalization mechanisms chloroquine, methyl-β-cyclodextrin and cytochalasin D, which act by raising endosomal pH, depleting cholesterol, and disrupting actin filaments, respectively. Cells were also incubated with inhibitors of clathrin-dependent internalization mechanisms nocodazole and dynasore, which act by inhibiting microtubule polymerization or the GTPase activity of dynamin, respectively. As seen in confocal images, uptake of M2pep was potently inhibited by incubation with methyl-β-cyclodextrin and cytochalasin D (Figure 1.13). Methyl-β-cyclodextrin is an inhibitor of clathrin-independent mechanism of internalization and Cytochalasin D is a known inhibitor of macropinocytosis, also a clathrin-independent mechanism of internalization. Thus M2pep is internalized via macropinocytosis.

Results of the confocal imaging of M2 macrophages treated with various inhibitors of internalization pathways was further supported by a similar study using flow cytometry analysis. M2 macrophages treated with methyl-β-cyclodextrin and cytochalasin D exhibited a significant reduction in uptake (63% and 53% reduction, respectively) of fluorescein-labeled M2pep ($p = 0.0004$ and $p = 0.0006$, respectively). There was also a smaller, yet statistically significant reduction in M2pep uptake (14% reduction) in M2 macrophages treated with nocodazole ($p = 0.0215$).

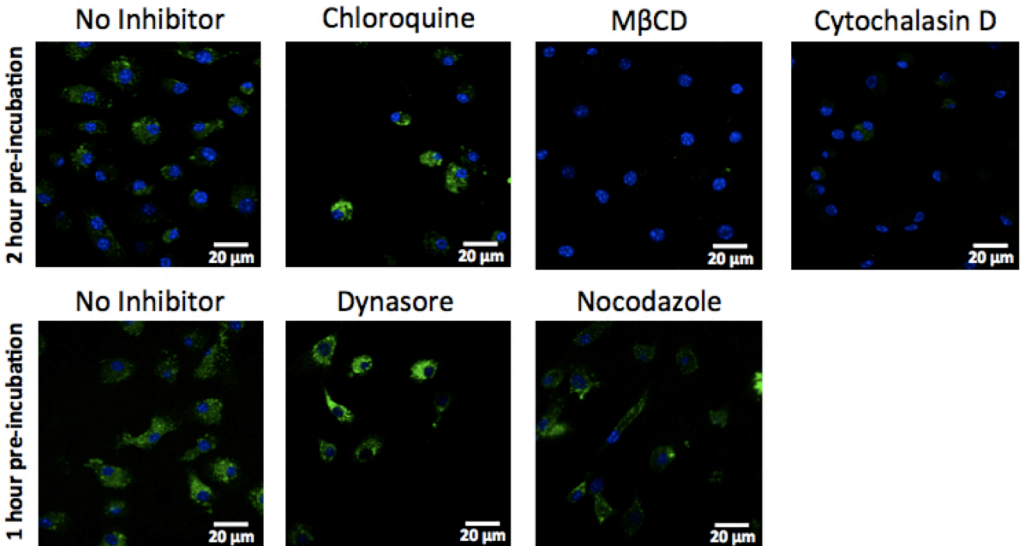

Figure 1.13: Confocal images of uptake of M2pep in M2 macrophages treated with various inhibitors of internalization pathways demonstrates reduced uptake in methyl-β-cyclodextrin and cytochalasin D treated cells, suggesting M2pep is taken up via macropinocytosis. Images representative of two experiments.

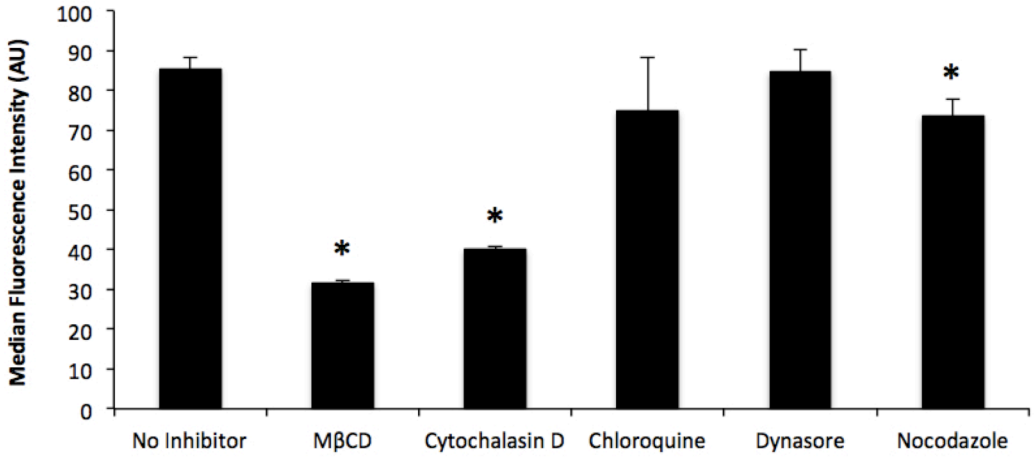

Figure 1.14: Flow cytometry assessment of mechanism of internalization demonstrates significant reductions in M2pep uptake in M2 macrophages treated with methyl-β-cyclodextrin or cytochalasin D. n = 3. * $p < 0.05$.

1.4 Discussion

In the work described in this chapter, a subtractive phage panning method was used to identify a novel peptide sequence that demonstrates selective binding and internalization in M2 macrophages. A peptide library selection approach was used because peptide ligands generally offer higher binding affinity and specificity for their receptors compared to small molecules and are typically less immunogenic and cheaper to scale and manufacture compared to antibodies. Peptides can be easily conjugated to vehicles carrying therapeutic payloads or imaging agents. For example, the LyP-1 peptide has been conjugated to superparamagnetic iron oxide nanoworms and used, via intravenous injection, to image atherosclerotic plaques with high resolution [21, 22]. Similar M2pep-based diagnostics may be developed to identify M2 macrophages in disease states and offer insight into disease progression. Additionally, M2pep may be conjugated to drugs for macrophage-targeted therapies (see Chapter 2). Work to identify the cell surface receptor that M2pep binds is on going in the lab. Identification of this receptor could provide a valuable new target for M2 macrophage selective therapies.

Increased macrophage polarization to the M2 phenotype is associated with the progression of a number of other pathologies including cancer, asthma, allergic inflammation, and fibrosis [18, 23]. Alternatively activated macrophages are important cells in the resolution of parasitic infection. Specifically, M2 macrophages have also been suggested to play a role in dampening the inflammation that leads to septic shock in an experimental infection of mice with *S. mansoni*, a trematode [21]. While M2 macrophages play a positive role in fighting diabetes and parasitic infection, some studies indicate that M2 macrophages can play a detrimental role in diseases like asthma. For example, in a mouse model of chronic inflammatory lung disease, Kim and colleagues demonstrated the role of M2 macrophages in the progression of mucous cell metaplasia [24]. The researchers also reported increased numbers of IL-13 producing, alternatively activated macrophages in human subjects with severe asthma when compared to healthy patients. Thus, delivery of agents that alter the ratio of M2 to M1 macrophages may be valuable for treatment of other conditions in which the balance between M1 and M2 macrophages is disturbed.

1.5 Acknowledgements

Thank you to David Chu and Russell Johnson for helpful discussions regarding phage panning methods. Thank you to Jingjing Tang for characterization of bone marrow derived, *in vitro* generated murine M1 and M2 macrophages as well as intraperitoneal cavity, thioglycollate elicted macrophages. Thank you to Cara Comfort for the isolation and cell culturing of bone marrow derived macrophages. Thank you to Julie Shi for helpful discussions in the development of mechanism of internalization inhibitor studies. Thank you to Greg Martin in the Keck Microscopy center for help in confocal imaging methods.

1.6 References

1. Steinman L (1996) Multiple sclerosis: a coordinated immunological attack against myelin in the central nervous system. Cell 85:299–302.

2. Murphy KM (2012) Janeway's Immunobiology 8th Ed.

3. Gordon S, Taylor P (2005) Monocyte and macrophage heterogeneity. Nat Rev Immunol 5:953–964.

4. Mosser DM, Edwards JP (2008) Exploring the full spectrum of macrophage activation. Nat Rev Immunol 8:958–969. doi: 10.1038/nri2448

5. Gordon S (2003) Alternative activation of macrophages. Nat Rev Immunol 3:23–35.

6. Mantovani A, Sica A, Sozzani S, et al. (2004) The chemokine system in diverse forms of macrophage activation and polarization. Trends Immunol 25:677–686. doi: 10.1016/j.it.2004.09.015

7. Low PS, Henne WA, Doorneweerd DD (2008) Discovery and Development of Folic-Acid-Based Receptor Targeting for Imaging and Therapy of Cancer and Inflammatory Diseases. Acc Chem Res 41:120–129. doi: 10.1021/ar7000815

8. Hashida M, Nishikawa M, Yamashita F, Takakura Y (2001) Cell-specific delivery of genes with glycosylated carriers. Adv Drug Deliver Rev 52:187–196.

9. Sallusto F, Cella M, Danieli C, Lanzavecchia A (1995) Dendritic cells use macropinocytosis and the mannose receptor to concentrate macromolecules in the major histocompatibility complex class II compartment: downregulation by cytokines and bacterial products. J Exp Med 182:389–400.

10. Ross JF, Chaudhuri PK, Ratnam M (1994) Differential regulation of folate receptor isoforms in normal and malignant tissues in vivo and in established cell lines. Physiologic and clinical implications. Cancer 73:2432–2443.

11. Segers FME, Yu H, Molenaar TJM, et al. (2012) Design and validation of a specific scavenger receptor class AI binding peptide for targeting the inflammatory atherosclerotic plaque. Arterioscl Throm Vas 32:971–978. doi: 10.1161/ATVBAHA.111.235358

12. Arap W, Pasqualini R, Ruoslahti E (1998) Cancer treatment by targeted drug delivery to tumor vasculature in a mouse model. Science 279:377–380.

13. Hsiung P-L, Hardy J, Friedland S, et al. (2008) Detection of colonic dysplasia in vivo using a targeted heptapeptide and confocal microendoscopy. Nat Med 14:454–458. doi: 10.1038/nm1692

14. Liu JK, Teng Q, Garrity-Moses M, et al. (2005) A novel peptide defined through phage display for therapeutic protein and vector neuronal targeting. Neurobiol Dis 19:407–418. doi: 10.1016/j.nbd.2005.01.022

15. Pasqualini R, Ruoslahti E (1996) Organ targeting in vivo using phage display peptide libraries. Nature 380:364–366. doi: 10.1038/380364a0

16. McGuire MJ, Samli KN, Johnston SA, Brown KC (2004) In vitro selection of a peptide with high selectivity for cardiomyocytes in vivo. J Mol Biol 342:171–182. doi: 10.1016/j.jmb.2004.06.029

17. Li M, Anastassiades CP, Joshi B, et al. (2010) Affinity peptide for targeted detection of dysplasia in Barrett's esophagus. Gastroenterology 139:1472–1480. doi: 10.1053/j.gastro.2010.07.007

18. Martinez FO, Helming L, Gordon S (2009) Alternative activation of macrophages: an immunologic functional perspective. Annu Rev Immunol 27:451–483. doi: 10.1146/annurev.immunol.021908.132532

19. Sironi M, Martinez FO, D'Ambrosio D, et al. (2006) Differential regulation of chemokine production by Fcgamma receptor engagement in human monocytes: association of CCL1 with a distinct form of M2 monocyte activation (M2b, Type 2). J Leukoc Biol 80:342–349. doi: 10.1189/jlb.1005586

20. Becker L, Liu N-C, Averill MM, et al. (2012) Unique proteomic signatures distinguish macrophages and dendritic cells. PLoS ONE 7:e33297. doi: 10.1371/journal.pone.0033297

21. Herbert DR, Hölscher C, Mohrs M, et al. (2004) Alternative macrophage activation is essential for survival during schistosomiasis and downmodulates T helper 1 responses and immunopathology. Immunity 20:623–635.

22. Hamzah J, Kotamraju VR, Seo JW, et al. (2011) Specific penetration and accumulation of a homing peptide within atherosclerotic plaques of apolipoprotein E-deficient mice. Proc Natl Acad Sci USA 108:7154–7159. doi: 10.1073/pnas.1104540108

23. Sica A, Mantovani A (2012) Macrophage plasticity and polarization: in vivo veritas. J Clin Invest 122:787–795. doi: 10.1172/JCI59643

24. Kim EY, Battaile JT, Patel AC, et al. (2008) Persistent activation of an innate immune response translates respiratory viral infection into chronic lung disease. Nat Med 14:633–640. doi: 10.1038/nm1770

Chapter 2

DEVELOPMENT AND CHARACTERIZATION OF M2PEPKLA FOR TARGETED DEPLETION OF TUMOR-ASSOCIATED MACROPHAGES AND MODULATION OF THE TUMOR MICROENVIRONMENT

Abstract

The immune system plays an intimate role in both protection from tumor formation and tumor progression. In cancer, populations of tumor-associated macrophages (TAMs) mediate immunosuppression and possess M2-like qualities such as poor antigen presentation, promotion of angiogenesis and tissue remodeling and repair. In addition, TAMs may promote the exhausted phenotype of CD8+ T cells, resulting in their inability to eliminate tumor cells. Not surprisingly, the extent of TAM accumulation within tumors generally correlates with poor disease prognosis. Despite the growing interest in tumor immunotherapy, there continues to be a dearth of TAM-specific targeting agents. In this work, M2pep was characterized for binding to TAMs extracted from CT-26 syngeneic tumors. In addition, fluorophore-labeled M2pep intravenously injected into tumor-bearing mice was shown to accumulate selectively in TAMs. Administration of a fusion peptide of M2pep with KLA, a proapoptotic peptide, resulted in delayed tumor growth, increased mouse survival, and selective elimination of TAMs. Despite reported literature describing the T cell exhaustion-promoting effects of TAMs, elimination of TAMs via M2pepKLA administration did not alter populations of exhausted CD8+ T cells within the tumor environment.

2.1 Introduction and Rationale

2.1.1 The Immunoeditting Hypothesis of Cancer

The immune system plays an intimate role in both protection from tumor formation and tumor progression. Recently, researchers have come to accept the hypothesis of immunoediting of cancer, by which the immune system progresses through three stages during tumor development: elimination, equilibrium, and escape [1].

In the elimination stage, a developing tumor is recognized by the immune system and destroyed before it grows to an appreciable size. The methods by which the immune system identifies and eliminates tumors is poorly understood, however some mechanisms may include the presence of “danger signals” early in tumor development that activate dendritic cells, the release of damage-associated molecular patterns by dying tumor cells or tissue surrounding the tumor, or the expression of stress ligands on the surface of tumor cells that activate innate immune cells. Effective elimination is thought to require both an innate and adaptive immune response.

In the equilibrium stage, the immune system maintains tumor cells in a state of dormancy that can last years before cells resume growth. CD4+ and CD8+ T cells of the adaptive immune response are required for a tumor to enter equilibrium. The equilibrium stage effectively molds the immunogenicity of the tumor cells, with only those cells that circumvent the adaptive immune response able to escape and resume growth.

In the escape stage, tumor cells begin unchecked growth either by their own cellular changes that allow them to circumvent the immune system, or through changes in the host immune system due to cancer-induced immunosuppression. Tumor cells may induce upregulation of oncogenes or decrease expression of antigenic proteins. They may also lose expression of MHC proteins that present antigens to T cells or the machinery that loads the peptide onto the MHC. In addition, secretion by the tumor cells of factors that generate an immunosuppressive environment and recruit immune cells that contribute to immunosuppression aids in escape.

The roles of some of these cells, including exhausted CD8+ T Cells and Regulatory T cells, are described in sections below.

The immunoediting hypothesis depicts the integral role the immune system plays in not only protecting the host from the formation of cancer cells, but also in shaping the type of cancer cell that develops. After escape, the immune system continues to contribute to the progression of the disease, with some cell subsets, including tumor-associated macrophages (TAMs), promoting tumor invasiveness. Thus, modulating the immune system is an important approach to cancer therapy.

2.1.2 TAMs are M2 Macrophage-Like Cells and Play a Role in Cancer Progression

In cancer, populations of tumor-associated macrophages (TAMs) mediate immunosuppression and possess M2 macrophage-like qualities such as poor antigen presentation, promotion of angiogenesis and tissue remodeling and repair, although there is heterogeneity in pathways and phenotypes in different tumors [2]. TAMs also secrete factors Milk Fat Globule-E8 and interleukin-6 that lead to tumorigenicity and drug resistance of cancer stem/initiating cells [3]. The extent of TAM accumulation within tumors generally correlates with poor disease prognosis [4, 5]. Indeed, the role of M2 macrophages in chronic inflammation and disease is increasingly appreciated, and the ability to modulate specific subsets of macrophage populations is a major focus of macrophage-targeted therapy [6]. This motivates the use of targeting agents like M2pep to specifically deliver therapeutic agents to TAMs to abrogate their role in tumor progression.

2.1.3 T Cell Subsets in the Tumor Microenvironment

The tumor stroma is made up of diverse cell subsets, each contributing to the immunoediting of cancer cells. Below is a brief description of some of the types of T cells that play an important role in anti-tumor immunity or tumor progression.

CD8+ Cytotoxic T Lymphocytes (CTLs)

Cytotoxic T Lymphocytes (CTLs), a subset of CD8+ cells, have long been regarded as a cell population responsible for the elimination of cancer. In fact, the presence of CTLs in solid tumors correlates with increased survival of patients [7]. In addition to secreting factors such as interferon-γ (IFN-γ) or tumor necrosis factor-α (TNF-α) that induce an anti-tumor response in other cells subsets, CTLs also produce cell-killing granzymes in response to antigen-mediated activation [8].

T Helper Cells

Th1 T Helper Cells are important for the priming of CTLs to induce an anti-tumor response, and their presence within tumors has been implicated in a lower chance of tumor recurrence [9, 10]. Through interactions with antigen presenting cells and secretion of IFN-γ and interleukin-12 (IL-12), Th1 cells support the CTL anti-tumor response. Th1 cells can also play a direct role in tumor elimination through production of IFNγ, TNFα and cytolytic granules [11]. Th2 T Helper Cells have generally been implicated in a more tumor-protective role by promoting T cell anergy, inhibiting apoptosis of cancer cells and promoting their proliferation. Many studies have revealed a skewed T Helper cell subset balance towards the Th2 phenotype within tumors, likely induced by the high levels of interleukin-10 (IL-10) secreted by tumor cells [12, 13]. Often this imbalance in T helper cell subsets correlates with poorer disease prognosis [14].

Regulatory T Cells (Tregs)

Regulatory T cells (Tregs) also typically play an immunosuppressive role in tumor progression, through targeted effects on antigen presenting cells and other T cells. Within the tumor, Tregs have been shown to suppress APCs and T cells through secretion of IL-10 or transforming growth factor-β (TGF-β) [15, 16], as well as kill antigen presenting cells (APCs) and T cells through granzyme production [17]. Through these and other mechanisms, Tregs induce tolerance of cancer cells and their presence in the tumor environment has a profound effect on

patient survival [18]. In myriad types of cancer, presence of Tregs correlates with disease progression and decreased survival [19]. Of particular significance to this work is the interaction of Tregs with antigen presenting cells. Tregs have been shown to inhibit functions of antigen presenting cells through various pathways [20], including binding of cytotoxic T-lymphocyte-associated protein 4 (CTLA-4) to CD80/86 on APCs, and stimulating APCs to upregulate the immunosuppressive enzyme indolamine 2,3-dioxygenase (IDO).

T cell Exhaustion

T cell exhaustion was first identified in patients with chronic infection, and is described as antigen-specific CD8+ T cells that do not produce cytokines [21]. T cell exhaustion occurs in stages, with the cells first losing the ability to produce interleukin-2 (IL-2), high proliferative capacity, and ex vivo killing capabilities. In intermediate stages of exhaustion, cells will lose the ability to produce tumor necrosis factor-α (TNFα), and in later stages lose the ability to produce IFNγ or degranulate [21]. Recently, T cell exhaustion has been identified in mouse models of cancer and human samples. Researchers have described the dysfunction of exhausted CD8+ T cells in epithelial ovarian cancer [22], melanoma [23, 24], and hepatocellular carcinoma patients [25]. CD8+ T cell dysfunction has been observed in several mouse models of cancer as well [26-28].

Common cell surface markers that identify exhausted CD8+ T cells in cancer include Programmed Cell Death-1 (PD-1), T Cell Immunoglobulin Mucin 3 (TIM-3), and Lymphocyte Activation Gene 3 (LAG-3), among others. Sakuishi and colleagues showed that in mice, CD8+ cells that are double positive for PD-1 and TIM-3 expression display the greatest impairment in production of IL-2, TNFα, and IFNγ cytokines, indicative of an exhaustive T cell phenotype. In that same study, the researchers demonstrated that simultaneous blockade of both cell surface markers via antibodies had a dramatic effect on tumor growth reduction, with 50% of mice achieving complete remission. Similarly, Matsuzaki and colleagues showed that $CD8^{+}PD\text{-}1^{+}LAG\text{-}3^{+}$ tumor infiltrating lymphocytes from human epithelial ovarian cancer patients exhibited lower IFNγ and TNFα production [22]. Studies have shown that for some types of cancer, the

presence of $CD8^{+}PD\text{-}1^{+}$ exhausted T cells correlates with poor disease prognosis for patients [29, 30].

Role of Antigen Presenting Cells in T Cell Exhaustion

Antigen presenting cells may play a role in the induction of exhausted T cells in tumors. The ligand for PD-1, PD-L1 (also known as B7-H1) is expressed on the surface of antigen presenting cells, and studies have implicated the interaction between APC-displayed PD-L1 and CD8+ T cells in T cell exhaustion and tumor tolerance. In the Matsuzaki ovarian cancer study described above, researchers cocultured peripheral blood lymphocytes with peripheral blood-derived APCs and tumor-derived APCs, and reported that tumor-derived APCs induce PD-1 expression on T cells, while peripheral blood-derived APCs do not. In addition, coculturing $CD8^{+}PD\text{-}1^{+}$ T cells with tumor-derived APCs results in T cells exhibiting upregulation of LAG-3 and a limited ability to proliferate. A separate study of patients with hepatocellular carcinoma, showed that tumor kupffer cells (liver macrophages) display greater cell surface expression of PD-L1 than surrounding normal liver tissue kupffer cells, and that higher expression of PD-L1 on tumor kupffer cells correlated with poorer patient disease prognosis [25]. The work also showed that $CD8^{+}PD\text{-}1^{+}$ T cells are found in close proximity to $PD\text{-}L1^{+}$ kupffer cells, suggesting an interaction between these cell subsets. Indeed, recent clinical trials have used antibodies to target the PD-1/PD-L1 interaction for cancer therapy [31].

Franklin and colleagues published work exploring the origin of TAMs within the tumor microenvironment and how phenotypes of T cells change in their absence [32]. Using a $CD11c^{cre}Rbpj^{fl/fl}$ mouse, these researchers were able to deplete TAMs from the tumor environment, leaving resident macrophages untouched. In this mouse model, PD-1 expression decreased and GranzymeB expression increased on CD8+ T cells, demonstrating that TAMs may contribute to CD8+ T cell exhaustion.

Mounting evidence supports an integral role for TAMs in the exhaustion of T cells and immune tolerance to tumors. Thus agents, like M2pep, that may be able to selectively deliver

cytotoxic agents to TAMs for elimination, may be useful tools for further exploring the interaction between TAMs and T cells.

2.1.4 KLA Pro-apoptotic Peptide and Use in Cancer Therapies

The KLA peptide $_{D}(KLAKLAK)_{2}$ is a pro-apoptotic motif first used by Pasqualini and coworkers to initiate apoptosis in mammalian cells via disruption of the mitochondrial membrane [33]. KLA is not plasma membrane permeable and requires facilitated intracellular delivery for optimal activity. KLA fusion peptides with a targeting sequence have been previously used to selectively kill tumor cells. Ellerby and colleagues used the CNGRC "tumor-homing" peptide fused to the KLA peptide to induce selective apoptosis of tumor cells, resulting in delayed tumor growth and prolonged survival in tumor-bearing mice [33]. Similarly, Mai and colleagues fused a protein transduction domain to the KLA peptide, and demonstrated tumor reduction upon local delivery [34]. The use of targeting peptides fused with the KLA peptide suggest that KLA is able to retain pro-apoptotic function in the presence of targeting agents, and motivates the use of KLA with M2pep. Overall, treatment with KLA is well tolerated, and its requirement for assisted delivery into cells makes it a good candidate for peptide-fusion materials with targeting peptides.

2.2 Materials and Methods

2.2.1 Materials

CT-26 colon carcinoma cells (American Type Culture Collection); Balb/c mice (Charles River Laboratories); Tumor Dissociation Kit (Miltenyi); Collagenase I (Sigma); Dispase II (Roche); anti-mouse CD11b eFluor450 antibody (eBioscience); anti-mouse Ly6C APCcy7 antibody (BD Pharmingen); anti-mouse Ly6G PerCPcy5.5 antibody (BD Pharmingen); anti-mouse Ly6G FITC antibody (BD Pharmingen); anti-F4/80 AlexaFluor647 antibody (Life Technologies); anti-mouse CD8a APC antibody (Biolegend); anti-mouse CD4 AlexaFluor488 antibody (Biolegend); anti-mouse CD25 PE antibody (eBioscience); anti-mouse FoxP3 eFluor450 antibody (eBioscience);

anti-mouse PD1 eFluor450 antibody (eBioscience); anti-mouse TIM3 PE antibody (eBioscience); CyTrack Orange (eBioscience); Transcription Factor Staining Buffer Kit (eBioscience); AlexaFluor660-maleimide (Life Technologies); Heparin-HCl (APP)

2.2.2 CT-26 Tumor Inoculation and Tumor Cell Suspension Harvest For M2pep Binding Study

All animal protocols were approved by the UW Institutional Animal Care and Use Committee. Subcutaneous tumors were formed by injection of 10^6 CT-26 cells into the right flank of BALB/c mice. Tumor-bearing mice were used 2-weeks post inoculation, at a maximum tumor diameter of 1.5 cm. For flow cytometry analysis, tumors were harvested and single cell suspensions recovered using the Tumor Dissociation Kit (Miltenyi). 10^5 cells were incubated with Fc Block for 30 minutes at 4˚C. Cells were pelleted by centrifugation at 200 g for 10 minutes and resuspended in PBS supplemented with 5% BSA and the following antibodies: anti-mouse CD11b eFluor450, anti-mouse Ly6C APCcy7, anti-mouse Ly6G PerCPcy5.5 and anti-mouse F4/80 AlexaFluor647. Cells were washed twice, and resuspended in PBS supplemented with 5% BSA and 200 μM of M2pep, scM2pep, or no peptide. Cells were washed three times, followed by fixation with 4% paraformaldehyde for 15 minutes at 4˚C. Cells were washed once and incubated with Streptavidin-FITC and CyTRAK Orange for 15 minutes at room temperature. Cells were washed and analyzed using a MACSQuant Flow Cytometer (Miltenyi) and FlowJo Analysis software (TreeStar).

2.2.3 Intravenous Injection of AlexaFluor660 Labeled M2pep and Imaging by Xenogen and Confocal Microscopy

For intravenous injections, 50 μg of AlexaFluor660 labeled M2pep, scM2pep or injection media (saline, 200 μL) were injected via tail vein into tumor bearing mice. At 30 minutes, live anesthetized mice were perfused with PBS and tumors and organs harvested. Tissues were imaged on a Xenogen Imager (Caliper) and fixed overnight using 4% paraformaldehyde. Tissues

were cryosectioned, stained using an anti-F4/80 antibody with AlexaFluor555 secondary and DAPI, and imaged on a Zeiss LSM 510 META confocal microscope.

2.2.4 Solid Phase Peptide Synthesis

Peptides were synthesized via standard Fmoc solid phase peptide synthesis using a NovaPEG Rink Amide resin and purified at >95% purity by RP-HPLC in house as follows: M2pepKLA (YEQDPWGVKWWYGGGS-$_D$[KLAKLAK]$_2$), scM2pepKLA (WEDYQWPVYKGWSGGGS-$_D$[KLAKLAK]$_2$), and KLA ($_D$[KLAKLAK]$_2$).

2.2.5 M2pepKLA Survival Study

Subcutaneous tumors were formed by injection of 10^6 CT-26 cells in RPMI and Matrigel into the right flank of BALB/c mice. After tumors reached approximately 50 mm^3 in volume, peptides (2.5 nmole/g) or Injection Buffer (PBS/5%DMSO) were administered by tail vein injection four times over the course of one week. Tumor volume was determined by caliper measurements (using volume = (a)(b^2) where a is the longer of the two tumor dimensions) every 1-2 days, and mouse weight recorded. Mice were sacrificed when tumor volume exceeded 10% of body weight or ulceration occurred.

2.2.6 Flow Cytometry Analysis of Tumor Macrophage and T Cell Populations

Subcutaneous tumors were formed by injection of 10^6 CT-26 cells into the right flank of BALB/c mice. Seven days after tumor inoculation, mice were dosed via retro-orbital injection with 5 nmol/gram M2pepKLA, scM2pepKLA or injection buffer every other day for a total of four injections. Tumors were collected one day after the last injection and dissociated into a single cell suspension for flow cytometry analysis. Tumors were minced in the presence of complete media. Next, half of tumor suspension was placed in a C-tube (Miltenyi), 150 μL of 10,000 CDU/mL Collagenase I and 150 μL of 32 mg/mL Dispase II added, and incubated at 37C

for 1 hour. The other half of the tumor mixture was further dissociated via scraping against a 70 μm cell strainer using the plastic end of a 3 mL syringe plunger. Collagenase/Dispase dissociated cells were stained with anti-mouse CD11b eFluor450, anti-mouse F4/80 AlexaFluor647, and anti-mouse Ly6G-FITC antibodies, and CyTRAK Orange as a nuclear dye to identify nucleated cells. Mechanically dissociated cells were stained with two separate antibody panels to identify tumor infilatrating lymphocyte and exhausted CD8+ T Cell populations. The tumor infilatrating lymphocyte panel consisted of anti-mouse CD8a APC, anti-mouse CD4 AlexaFluor488, anti-mouse CD25 PE, and anti-mouse FoxP3-eFluor450 antibodies. Intracellular FoxP3 staining was performed using the Transcription Factor Staining Buffer Kit (eBioscience) according to the manufacturers instructions. The CD8+ T Cell Exhaustion marker panel consisted of anti-mouse CD8a APC, anti-mouse PD1 eFluor450, and anti-mouse TIM3 PE antibodies. Cells were permeabilized for PD-1 and TIM-3 staining. Cells were analyzed on a MACSQuant Flow Cytometer (Miltenyi) and FlowJo Analysis Software (TreeStar).

2.2.7 M2pepKLA Toxicity Studies

Balbc mice were inoculated with CT-26 tumors as previously described. 8 days after tumor inoculation mice were administered 2.5 nmol/gram M2pepKLA or Injection Buffer (PBS/5%DMSO). Blood samples from 3 mice in each treatment group were taken at 6 hour and 24 hour time points and submitted to the UW Medical Center for a Comprehensive and Hepatic Blood Panel analysis. Briefly, the mouse intraperitoneal cavity was opened to reveal the portal vein. An incision was made in the portal vein and blood permitted to pool in the IP cavity. Pooled blood was transferred to a microcentrifuge tube containing 200 μL 1000 USP units/mL Heparin. Tubes were spun at 2000 rpm for 5 minutes, supernatant transferred to a fresh tube and repeated once. For the 24 hour time point animals, animals were perfused and tissues (liver, lung, spleen and kidneys) were harvested following blood collection. Tissues were placed in 4% paraformaldehyde and submitted to UW Comparative Pathology Department for analysis by a veterinary pathologist.

2.2.8 Statistics

Differences between groups were examined using Student's T-test, except for survival data, which was examined using the Log-rank Mantel-Cox test. Error bars are reported as standard deviations except where noted.

2.3 Results

2.3.1 M2pep Binds TAMs Extracted from CT-26 Tumors

To test whether M2pep binds TAMs, biotinylated M2pep was incubated with dissociated cells harvested from CT-26 syngeneic tumors in BALB/c mice (Figure 2.1A).

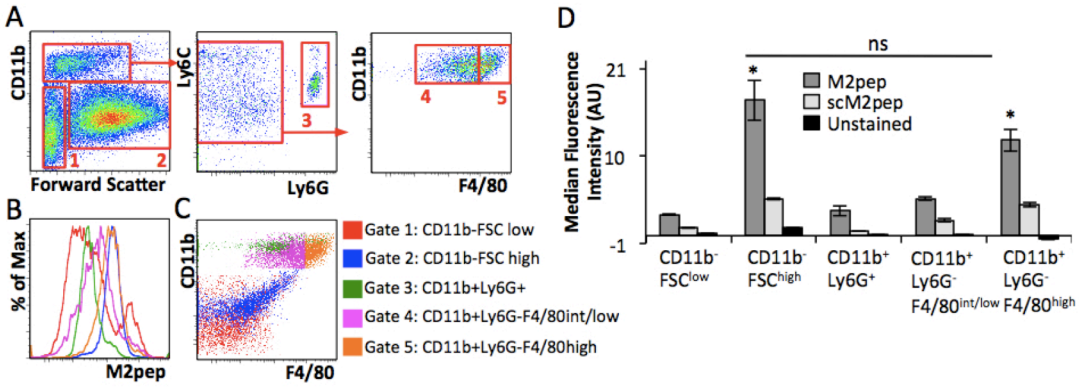

Figure 2.1: M2pep binds TAMs extracted from CT-26 tumors. (A) CT-26 tumors from BALB/c mice were dissociated and stained for flow cytometry analysis using 200 µM M2pep. Dot plots and histograms are representative of three biological replicates. (B) M2pep exhibits higher binding *ex vivo* to $CD11b^{+}Ly6G^{-}F4/80^{high}$ TAMs compared to other $CD11b^{+}$ cells, but also binds $CD11b^{-}FSC^{high}$ cells. (C) Gated cell populations displayed on a CD11b vs F4/80 dot plot. (D) Median fluorescence intensity of populations depicted in part B. * $p < 0.05$.

M2pep exhibits high binding to $CD11b^{+}Ly6G^{-}F4/80^{high}$ M2-like TAMs compared to $CD11b^{+}Ly6G^{-}F4/80^{int/lo}$ M1-like macrophages (p=0.01), per markers defined previously by Spence et al [35]. Binding of M2pep to $CD11b^{+}Ly6G^{-}F4/80^{high}$ M2-like TAMs is also significant relative to $CD11b^{+}Ly6G^{+}$ neutrophils (p = .003) and $CD11b^{-}FSC^{low}$ cells (p = .007) (Figure 2.1B and D).

However, M2pep also exhibits binding to $CD11b^{-}FSC^{high}$ cells, which are likely the CT-26 tumor cells due to their high frequency in the overall population (~70%).

2.3.2 M2pep Injected Via Tail Vein Accumulates in TAMs In Vivo

To test M2pep homing to TAMs *in vivo,* AlexaFluor660-labeled M2pep and scM2pep were injected into the tail vein of syngeneic tumor-bearing BALB/c mice. Tissues harvested 30 min post-injection were imaged using a Xenogen imager. Tumors were cryosectioned, stained with an anti-F4/80 antibody and DAPI, and imaged. Confocal images from mice treated with M2pep show high fluorescence within the tumor-associated macrophages, but low signal in other cells, and tumors from mice treated with scM2pep and PBS controls have low fluorescence in all cells (Figure 2.2A). The mean fluorescence intensity per $F4/80^{+}$ cell is 4.1-fold (p=0.002) and 3.4-fold (p=0.003) higher in tumors from M2pep injected mice compared to scM2pep or PBS injected mice (Figure 2.2B). Additional images from M2pep-injected mice confirm the uptake into $F4/80^{+}$ cells (Figure 2.2C). These results demonstrate that *in vivo,* M2pep does not bind tumor cells and selectively accumulates in TAMs.

Xenogen images of tissues demonstrate greater accumulation of M2pep in tumor tissue as compared with heart, lung, and spleen tissue in three mice injected with peptide (Figure 2.3A and B). Liver and kidneys show high fluorescence, likely due to clearance of peptide and fluorophore from these organs (not shown). Sulfonated cyanine dyes like the AlexaFluors have been shown to accumulate in and be cleared from liver [36]. We therefore imaged liver sections of treated mice. Diffuse fluorescence was seen throughout the liver in M2pep and scM2pep-injected mice, with less fluorescence in PBS-injected mice, suggesting that liver fluorescence is due to dye clearance and not Kupffer cell accumulation of peptide (Figure 2.3C). Spleen confocal images show no peptide accumulation in any cell type, including $F4/80^{+}$ cells (Figure 2.3D). Thus, M2pep accumulates in TAM populations but not resting tissue macrophages.

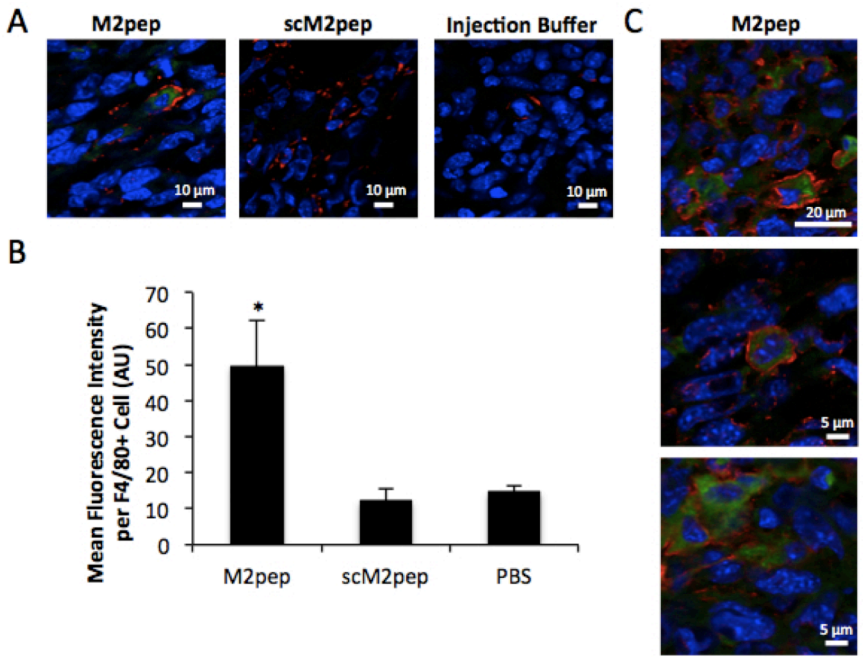

Figure 2.2: M2pep binds F4/80+ cells in vivo. BALB/c mice bearing 2-week CT-26 tumors were injected via tail vein with 50 µg AlexaFluor660-labeled M2pep, scM2pep, or PBS injection buffer. At 30 minutes mice were perfused, and tumors and organs were harvested. (A) Tumors were cryosectioned, stained and imaged on a confocal microscope using the same settings. Blue = DAPI; Red = F4/80; Green = Peptide. Images are representative of three biological replicates. (B) Mean Fluorescence Intensity per F4/80+ cell was quantified. * $p < 0.05$. (C) Additional images from M2pep-injected mice illustrate the selective accumulation of M2pep in TAMs.

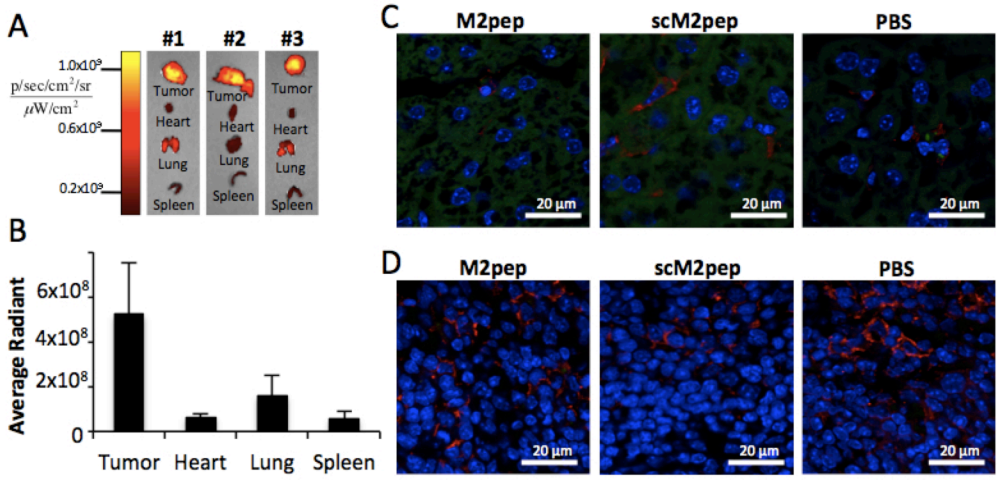

Figure 2.3: M2pep exhibits accumulation in tumors compared to other organs. (A) Xenogen images of organs excised from three mice injected with AlexaFluor660-labeled M2pep demonstrates uptake in tumors. (B) A trend towards greater uptake of M2pep by tumors is observed as compared with heart, lung and spleen, but it does not reach statistical significance. (C) Both M2pep and scM2pep display diffuse uptake in liver. (D) Both M2pep and scM2pep lack uptake in splenic cells.

2.3.3 M2pepKLA Delays Mortality in Mice

The specific accumulation of M2pep in TAMs *in vivo* demonstrated the utility of M2pep to deliver cargo to these cells. Because TAMs are known to play a role in tumor-promotion, a fusion peptide of M2pep with KLA, a pro-apoptotic peptide, was synthesized with the goal of selectively depleting TAMs *in vivo* in tumor-bearing mice. Tumor-bearing mice received four injections of peptides (2.5 nmole peptide per gram body weight per dose of either M2pepKLA, scM2pepKLA or M2pep) or Injection Buffer every other day. Multiple doses of peptide were administered due to the rapid elimination of peptides with MW < 5 kDa [37]. Mouse tumor size was measured every 2-3 days by caliper measurements and mouse weight was recorded. Mice were sacrificed when ulceration occurred or tumor volume reached 10% of animal body weight. The untreated mouse groups tended to have the greatest number of tumors that ulcered: injection buffer (6/8 mice tumors ulcered), M2pep (3/10), scM2pepKLA (5/8), M2pepKLA (1/10). The fast growing nature of the untreated groups in this immunocompetant animal model may have contributed to the increased ulceration rate. Due to the high rates of ulceration in the injection buffer and scM2pepKLA groups, tumor growth rates in the M2pep and M2pepKLA groups were compared and found to demonstrate slower tumor growth in the M2pepKLA groups ($p<0.04$ on days 9 and 10, Figure 2.4A). Furthermore, survival of mice receiving M2pepKLA is significantly longer than those receiving other treatments ($p = .0032$) (Figure 2.4B).

M2pepKLA is well tolerated, with little weight change in the treated mice over the course of the study. The trends in reduced tumor growth rate and prolonged survival from M2pepKLA treatment were reproducible in a second independent study that utilized three doses spread over seven days (Figure 2.5A and B). The improved outcome in tumor-bearing mice receiving M2pepKLA strongly supports the potential use of M2pep-targeted agents as an adjuvant to anti-cancer therapies.

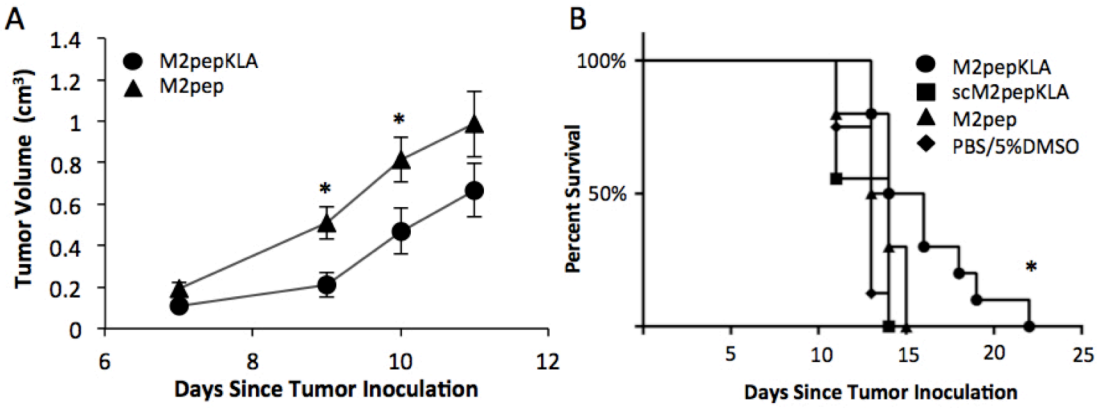

Figure 2.4: M2pepKLA administration improves survival. (A) Treatment with M2pepKLA described in figure 6 mediates delayed tumor growth compared to M2pep, with statistically different tumor size at day 9 (p = .009) and day 10 (p = .038). (B) Seven days after tumor inoculation, mice were administered 2.5 nmole/gram of M2pepKLA (n=10), scM2pepKLA (n=8), M2pep (n=10), or PBS/5%DMSO (n=8) four times every other day. Mice receiving M2pepKLA had significantly longer survival compared to other groups.

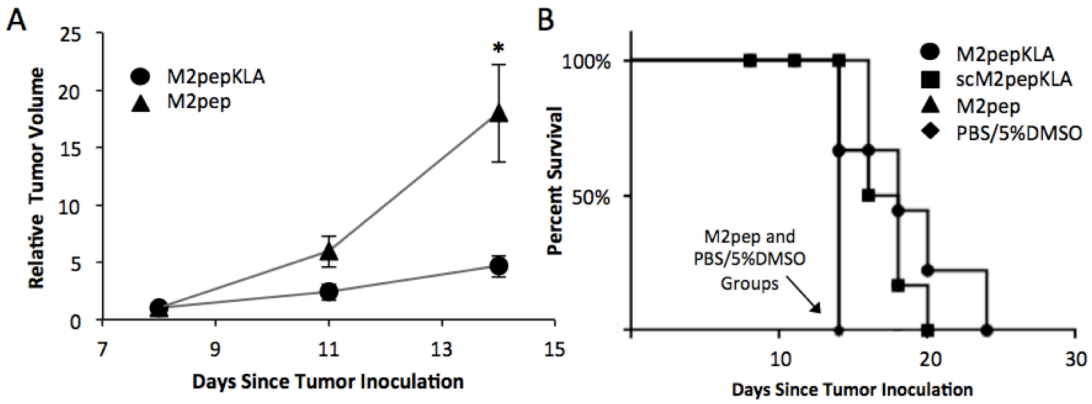

Figure 2.5: Additional survival studies confirm ability of M2pepKLA to delay tumor growth and improve survival. (A) In a separate study, mice (n = 6 per group) were dosed with M2pepKLA 3 times over 7 days, resulting in a statistically significant tumor growth delay at day 14 (p = .025). (B) In the separate study with dosing three times over seven days, there was a trend for delayed mortality in the group treated with M2pepKLA.

2.3.4 M2pepKLA Selectively Depletes TAMs in Mice

To confirm the hypothesized mechanism of M2pepKLA efficacy, tumors were analyzed for selective elimination of TAMs after M2pepKLA treatment. Tumor-bearing mice received 3 injections of 2.5 nmole peptide/g or injection buffer every other day. The day following the last

injection, mice were sacrificed, their tumors excised and cell composition was analyzed by flow cytometry. M2-like, $CD11b^{+}F4/80^{hi}$ TAMs decreased from 64% in the injection buffer mice to 38% in the M2pepKLA mice (p = .018) (Figure 2.6A). $CD11b^{+}F4/80^{hi}$ cells decreased from 9.40% to 5.97% of the total population (p = .007), while $CD11b^{+}F4/80^{int/lo}$ cells increased from 5.33% to 10.33% (p = .042) and $CD11b^{-}$ cells remained unchanged at approximately 84% (p = .308) when treated with M2pepKLA (Figure 2.6B). The $CD11b^{+}F4/80^{lo}$ population consisted primarily of $CD11b^{+}Ly6G^{+}$neutrophils. Therefore, the ratio of M2- to M1-like cells was determined as the ratio of $CD11b^{+}F4/80^{hi}Ly6G^{-}$ to $CD11b^{+}F4/80^{int/lo}Ly6G^{-}$. Compared to injection buffer-treated mice, M2/M1 ratio was significantly reduced by M2pepKLA treatment (M2/M1=1.6 for buffer vs M2/M1=0.6 for M2pepKLA; p=0.0017 for n=5). This demonstrates the ability of the M2pepKLA fusion peptide to selectively reduce TAMs *in vivo*.

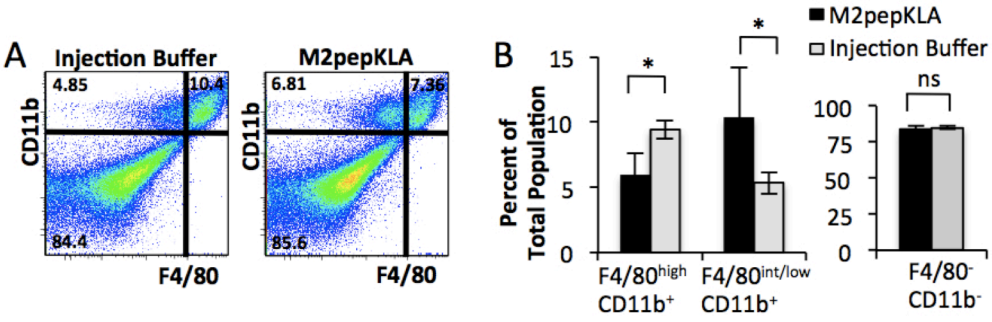

Figure 2.6: M2pepKLA mediates selective elimination of TAMs. (A) Following three injections of M2pepKLA or injection buffer, tumors were harvested, dissociated, and cells stained for flow cytometry analysis. M2pepKLA administration results in a reduction of $CD11b^{+}F4/80^{high}$ TAMs from 64% to 38% of all $CD11b^{+}$ cells. Dot plots are representative of mice (n=5) from each group. (B) M2pepKLA administration results in a decrease in $CD11b^{+}F4/80^{high}$ cells, an increase in $CD11b^{+}F4/80^{int/low}$ cells, and no change in $CD11b^{-}F4/80^{-}$ cells. * $p < 0.05$.

2.3.5 M2pepKLA Alters Populations of Tumor Infiltrating Lymphocytes and Extent of CD8+ T Cell Exhaustion with Little Efficacy

In a separate *in vivo* study, CT-26 tumor-bearing mice were injected with twice the dose of M2pepKLA, scM2pepKLA or Injection Buffer than in the TAMs Elimination Study described above. After the fourth day of injections, TAM elimination in the tumor microenvironment at this dose was confirmed by a similar flow cytometry analysis, and tumors also assayed for

changes in T cell populations. Specifically, tumor cell suspensions were stained for CD8, CD4, CD25 and FoxP3 to assess tumor infiltrating lymphocytes populations among treatment groups. While no statistical difference between groups was observed overall, a decrease in T Regulatory Cells ($CD4^+FoxP3^+CD25^+$) in the M2pepKLA treated group approached statistical significance (p = .174) when compared to Injection Buffer treated mice (Figure 2.7). This result suggests that decreases in TAMs diminish cues in the tumor microenvironment that contribute to the presence of tumor-promoting T regulatory cells.

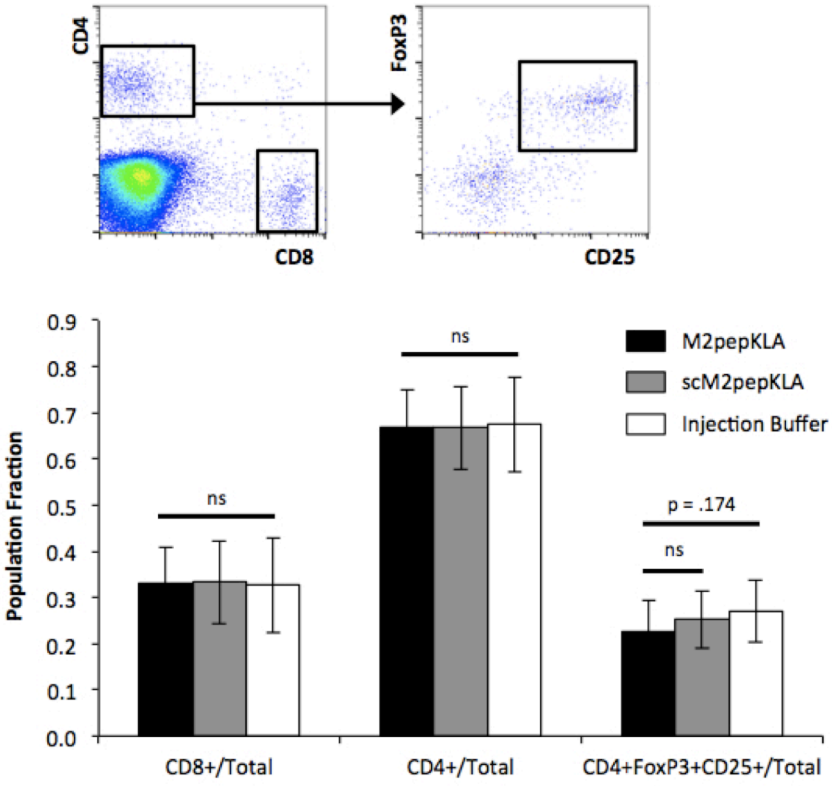

Figure 2.7: M2pepKLA treated mice show a decrease in T Regulatory Cells in the tumor environment. After four injections of M2pepKLA, scM2pepKLA, or Injection Buffer, cell suspensions from tumor-bearing mice were stained with CD8, CD4, FoxP3 and CD25, and analyzed by flow cytometry as shown in representative dot plots above. M2pepKLA treatment results in a trend towards decreased T Regulatory Cells in the tumor environment, though no values were statistically significant (n = 6 per group).

Tumor cell suspensions were also stained for CD8, PD-1 and TIM-3 to assess the extent of CD8+ T Cell exhaustion in the tumor among treated and untreated mice. At the time points

assayed, there was no statistical difference in CD8+ T Cell exhaustion among treatment groups (Figure 2.8).

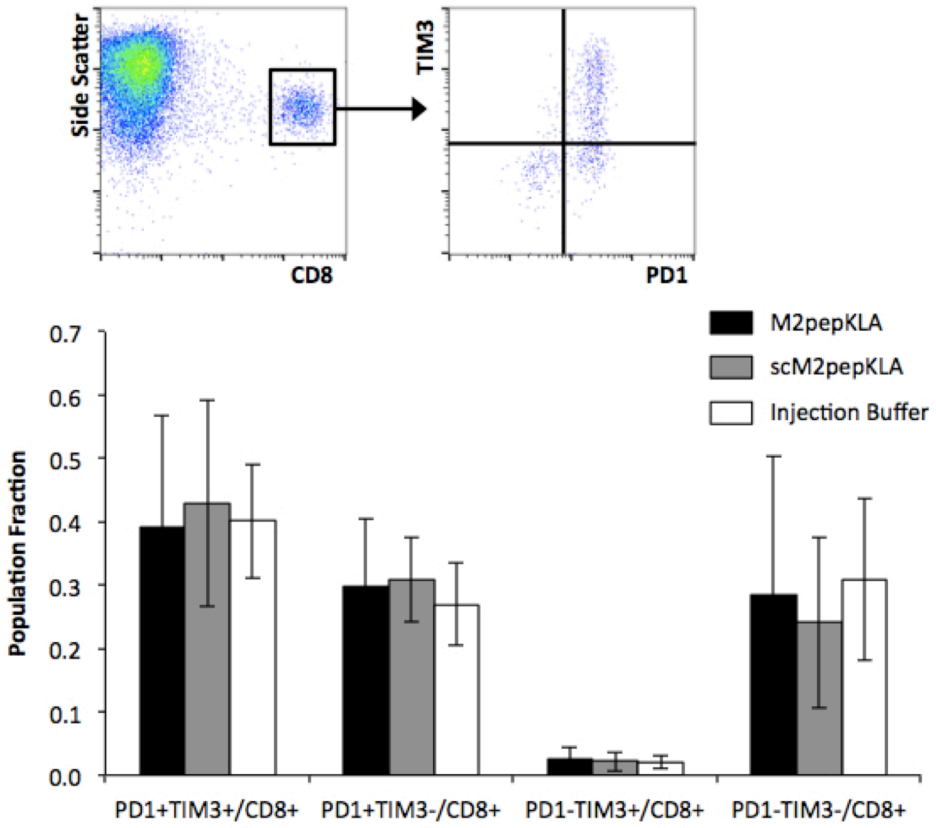

Figure 2.8: M2pepKLA treatment does not alter CD8+ T Cell exhaustion at the timepoints assayed. After four injections of M2pepKLA, scM2pepKLA, or Injection Buffer, cell suspensions from tumor-bearing mice were stained with CD8, PD-1 and TIM-3, and analyzed by flow cytometry as shown in representative dot plots above. There was no statistical difference among treatment groups (n = 6 per group).

2.3.6 M2pepKLA Exhibits Little Toxicity

Few toxic effects of M2pepKLA dosing were observed during *in vivo* studies, including no loss of animal weight or visible signs of animal distress. To confirm the lack of toxicity of M2pepKLA treatment, CT26 tumor-bearing mice were dosed with either Injection Buffer (PBS/5%DMSO) or M2pepKLA. At 6 and 24 hours post-injection, blood was collected and comprehensive hepatic blood panel performed. No statistical difference between Injection Buffer or M2pepKLA treated mice was observed at either 6 or 24 hours post-injection (Figure

2.9). In addition to the blood analysis, animal tissue (liver, spleen, lung, kidneys) was harvested from mice at the 24 hour time point and analyzed by a veterinary pathologist. The pathologist reported no difference in tissues between Injection Buffer and M2pepKLA treated mice.

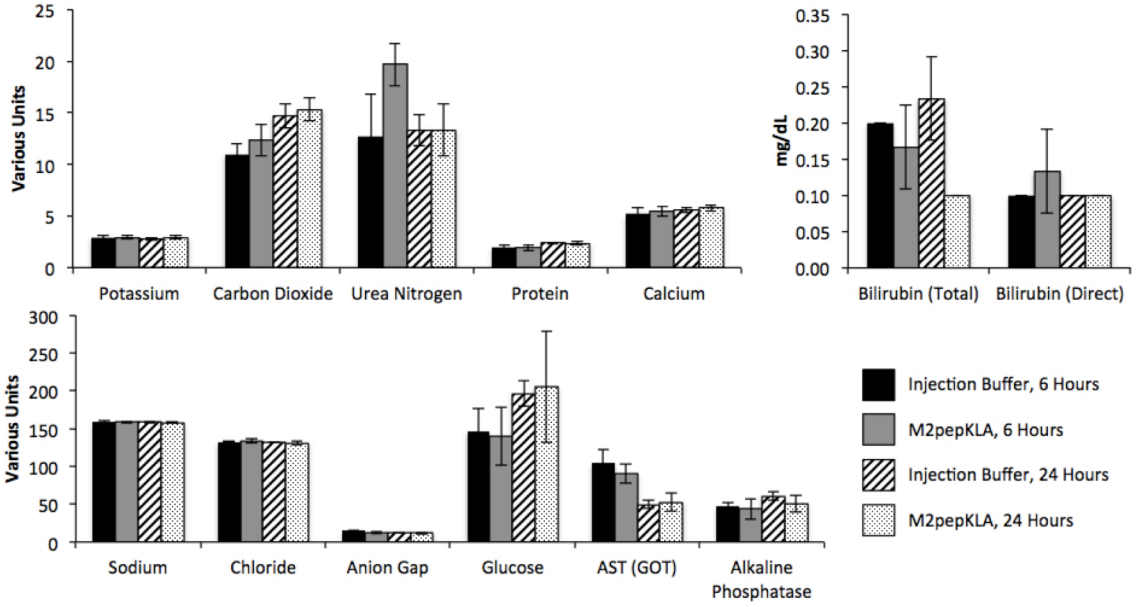

Figure 2.9: At 6 and 24 hours post injection of either buffer or M2pepKLA, a comprehensive hepatic blood panel analysis was performed (n = 3 per group). No statistical difference is observed between buffer and M2pepKLA treated mice. Units are as follows: mEq/L (Sodium, Potassium, Chloride, Carbon Dioxide), mg/dL (Glucose, Urea Nitrogen, Bilirubin, Calcium), U/L (AST, Alkaline Phosphatase), g/dL (Protein, Albumin).

2.4 Discussion

Associated with a shift to the M2 phenotype, TAMs have been shown to promote tumor cell growth, angiogenesis, metastasis and immune evasion through the recruitment of regulatory T-cells and promotion of the exhausted T cell phenotype [22, 38, 39]. Furthermore, TAMs can contribute to chemotherapy resistance in tumors [40, 41]. Work by Zeisberger and colleagues showed that the combination of anti-VEGF therapy and clodronate-encapsulated liposomes for selective knockout of macrophages resulted in delayed tumor progression in mice [42]. While the work demonstrated the utility of macrophage depletion in cancer therapy, the researchers

noted that the ability to better target liposomes to TAMs could decrease systemic toxic side effects.

The work described in this chapter provides *in vivo* evidence that M2pep preferentially binds to and accumulates in murine tumor-associated macrophages compared to other cells (e.g. resting macrophage, tumor epithelial cells, neutrophils, stromal cells), and can be used to deliver a therapeutic payload. Although binding to tumor isolates unexpectedly showed M2pep binding to a CD11b- population that is likely CT-26 tumor cells, *in vitro* binding studies showed no binding to or accumulation in CT-26 cells. Furthermore, no peptide accumulation in F4/80$^-$ tumor cells after intravenous injection and no change in the percent of CD11b- cells after M2pepKLA administration *in vivo* was observed. Taken together, these results suggest that M2pep-targeted constructs do not accumulate in CD11b- cells *in vivo*.

The lower binding affinity and faster blood clearance of most peptides compared to antibodies can be improved by peptide engineering approaches such as cyclization, artificial amino acids, multivalency, and polymer conjugation [37]. Although the binding affinity of M2pep is approximately 90 μM, similar to other peptides identified by library selection, *in vivo* targeting and activity of this peptide was observed. The rapid internalization of M2pep by TAMs may enhance accumulation in these target cells. For example, the DUP-1 peptide, identified by phage panning against PC-3 prostate cancer cells, binds it target with micromolar affinity, is rapidly internalized by cells and exhibits successful *in vivo* cell targeting [43].

In this chapter, M2pep was used to target and deliver a pro-apoptotic peptide to tumor-associated, murine macrophages *in vivo.* TAM-targeted delivery of the pro-apoptotic peptide alone, without an anti-cancer agent, was sufficient to delay mortality. Though selective killing of tumor-associated macrophages may aid in cancer regression, it is unclear whether macrophage-targeted therapy alone will limit cancer growth. In fact, other work has demonstrated that macrophage depletion alone may not effectively eliminate cancer [42]. However, this work that demonstrates a trend toward slower tumor growth in the M2pepKLA treatment group is

promising, indicating that targeted TAM depletion in conjunction with other anti-cancer agents may improve cancer therapy.

Existing literature reports that tumor-associated macrophages play a role in the exhaustion of CD8+ T cells, and knock out mouse models have demonstrated that depletion of TAMs results in reduction of exhausted CD8+ T cells in the tumor environment [32]. Thus it is surprising that depletion of TAMs via administration of M2pepKLA does not affect the phenotype of T cell populations. The fast-growing nature of the CT-26 syngeneic tumor-bearing mouse model requires mice be euthanized within two to three weeks of tumor inoculation, resulting in a short period of tumor burden to the mouse and interaction between tumor immune cells. In many studies exploring TAMs, mice are exposed to tumor burden for several weeks to several months, permitting the establishment of a diverse milieu of immune cells that change over time. For example, in recent work by Franklin and colleagues, at 8 weeks post tumor inoculation, resident macrophages and tumor-associated macrophages made up 30% and 12% of the tumor environment, respectively, in an MMTV-PyMT B6 tumor model. However, by 20 weeks, resident macrophages and tumor-associated macrophages made up 8% and 42% of tumor environment, respectively, indicating that tumor-associated macrophages play a greater role in tumor growth and maintenance over time and thus may have greater impact on other immune cells, like T cells, over time. In addition, Franklin and colleagues used cre-lox technology to get sustained elimination of TAMs and observed changes in T cell exhaustion, while M2pepKLA treatment only offers transient elimination of TAMs and thus may not have sufficient TAM depletion pressure to impact T cell subset phenotypes.

While delivery of KLA to TAMs requires additional optimization, the work in this chapter has important implications for methods development. The data presented here confirms that a macrophage-binding motif identified using an *in vitro* selection strategy is relevant for *in vivo* applications despite the heterogeneous and plastic nature of these cells. Therefore, application of a similar selection strategy to human macrophages has the potential to identify targeting ligands for human TAMs, and thus fulfill the need for a well-tolerated TAM-targeting approach for anti-cancer treatment.

2.5 Future Directions and Preliminary Data

Tumor-associated macrophage depletion via M2pepKLA was modest, with only a 50% reduction in TAMs. Thus, the development of alternative therapeutic cargo for M2pep may improve TAM elimination. Two potential alternative pro-apoptotic peptides to explore as M2pep cargo include the BIM and ATAP peptides discussed below. Data from preliminary experiments using untargeted and M2pep-targeted versions of BIM and ATAP peptides on M1 and M2 macrophages *in vitro* can be found in the appendix.

2.5.1 BH3 Peptides and the Use of BIM in Cancer Therapies

The Bcl-2 family of proteins plays a critical role in the balance of pro-apoptotic and anti-apoptotic signals in the cell. The anti-apoptotic components of the Bcl-2 family include Bcl-2, Bcl-x, Bcl-XL, Bcl-XS, Bcl-w, and Bag while the pro-apoptotic components include Bcl-10, Bax, Bak, Bid, Bad, Bik, Blk, and, of importance for this work, Bim [44]. These proteins have various mechanisms of action including binding interactions with each other as well as phosphorylation or dephosphorylation events that permit translocation across the mitochondrial membrane and result in the release of pro-apoptotic proteins such as cytochrome c.

The pro-apoptotic group of Bcl-2 family proteins are split into the Bax group and BH3-only group, which includes Bim. When activated by cytotoxic events, BH3-only proteins bind their anti-apoptotic counterparts via the BH3 protein domain, releasing pro-apoptotic proteins such as Bax and Bak. This binding interaction prepares the cell for apoptosis, which can then be initiated by the activation of Bax or Bak that induce the release of cytochrome c from mitochondria [45]. It remains controversial whether these BH3-only proteins act simply by neutralizing their pro-survival counterparts or if they play a direct role in Bax and Bak activation [46]. Of the BH3-only proteins, Bim is one of the most potent due to its ability to bind to several pro-survival proteins [45].

The BIM peptide has been employed as a pro-apoptotic agent for cancer therapeutics. In work by Hawkins and colleagues, the BIM peptide was fused to the TAT cell penetrating peptide and delivered to cancer cells *in vitro* and *in vivo* [47]. *In vitro,* TAT-BIM exhibited a dose-

dependent increase in apoptotic cells as assessed by the presence of active caspase-3, and presence of TAT facilitated improved delivery of BIM into cells. In an *in vivo* mouse model of cancer, intratumoral injections of TAT-BIM resulted in delayed tumor growth and improved survival of mice. Recently, Stayton and colleagues developed a pH-responsive diblock copolymer to improve targeting and intracellular delivery of BIM to tumor cells [48]. In this work, a polyethylene glycol block contained both streptavidin-bound anti-CD22 antibodies for tumor targeting and pyridylsulfide moieties for reversible conjugation of BIM peptides. A second diethylaminoethyl methacrylate and butyl methacrylate-containing block provided endosomal release capabilities for delivery. This CD22-targeted BIM polymer conjugate delivered intravenously in conjunction with a low dose of chemotherapy improved the survival of tumor-bearing mice compared to those treated with just chemotherapy or left untreated.

This work demonstrates the ability of BIM to be delivered intracellularly and mediate apoptosis *in vitro* and *in vivo.* Furthermore, the use of BIM conjugated to targeting agents suggests it could be successfully used with the M2pep targeting peptide for selective killing of M2 macrophages.

2.5.2 Amphipathic Tail-anchoring Peptide (ATAP) and Use in Cancer Therapies

While the BIM peptide has shown anti-cancer efficacy in the studies described above, research has shown that its efficacy may be greatly impacted by the concentration of the Bcl-2 family proteins in the cell. For example, over expression of Bcl-2 and Bcl-XL or low expression of Bax and Bak can diminish the pro-apoptotic effect of BIM due to lack of its target proteins present [49]. Thus, pro-apoptotic agents that act independently of apoptotic factors in the cell, such as the amphipathic tail-anchoring peptide (ATAP), are attractive alternatives.

ATAP is a 23 amino acid peptide derived from the C-terminus of the Bfl-1 anti-apoptotic protein. ATAP was identified after research demonstrated that deletion of residues from the N-terminus of Bfl-1, leaving the C-terminal ATAP portion remaining, eliminated the anti-apoptotic function of the protein [50]. Upon further investigation, it was predicted that ATAP forms an α-

helical structure, with charged residues lining one side of the helix providing the amphipathic properties of the peptide, and it was shown that these residues are critical for the pro-apoptotic function of the peptide [51]. Indeed, ATAP is able to form large pores in the mitochondrial membrane in the absence of any other cellular proteins, demonstrating its ability to act in a Bax or Bak –independent manner and avoid sensitivity to Bcl-2 family proteins [49].

Like BIM, ATAP has been used in conjunction with targeting moieties for delivery to cancer cells. In work by Ma and colleagues, the iRGD cell internalizing peptide sequence was fused to the C-terminus of the ATAP peptide to facilitate delivery into cells. The iRGD-ATAP construct demonstrated increased cytotoxicity compared to untargeted ATAP when incubated with various cancer cell lines *in vitro* [52]. In addition, intravenous administration of a stabilized version of the iRGD-ATAP construct to tumor-bearing mice resulted in a significant delay in tumor growth, with little toxicity to healthy tissue. This work suggests that, like BIM, ATAP may be successfully delivered to alternatively activated macrophages by M2pep.

2.5.3 Use of Pro-apoptotic Peptides in Selective Killing of Macrophages

While much work to date has characterized the impact of pro-apoptotic peptides such as KLA, BIM, and ATAP on cancer cells, few studies have assessed the cytotoxicity of these peptides to macrophages. The different mechanism each of these peptides employs to induce apoptosis could influence its cell killing capabilities in macrophages.

For example, KLA and ATAP are thought to induce apoptosis by accumulating at the mitochondrial membrane, causing mitochondrial membrane destabilization that releases cytochrome c. ATAP has been shown to induce pore formation in membranes in the absence of other factors, demonstrating it's utility in Bcl-2 family protein-independent apoptotic function. In contrast, BIM is thought to act in a Bcl-2 family protein-dependent manner, possibly through multiple mechanisms. The fully accepted method of BIM-induced apoptosis is through displacement of anti-apoptotic Bcl-2 family proteins that hold pro-apoptotic Bax and Bak proteins in check. Upon release, Bax and Bak can become activated to form an oligomer that

permeabilizes the mitochondrial membrane. The more controversial method of BIM-induced apoptosis is through direct binding of BIM to Bax and Bak, directly activating them to form oligomers. Thus there may be multiple mechanisms by which BIM is able to induce pore formation and potential amplification effects through protein-protein interactions, compared to KLA and ATAP which act through the single mechanism of accumulation at the mitochondrial membrane. In addition, it is unknown how the potency of pore formation via KLA or ATAP accumulation compares to the membrane permeabilization caused by the Bax/Bak oligomers, which could affect overall cell killing efficacy of each apoptotic cargo.

Because the action of BIM is dependent on other Bcl-2 family proteins in the cell, it could also be sensitive to differences in cellular concentrations of these proteins in M1 or M2 macrophages. The balance between pro- and anti-apoptotic proteins is key to homeostasis and thus cells are sensitive to changes in this ratio [53]. To date, there is little information about the balance of these proteins in M1 and M2 macrophages, and it is possible that differences in the level of expression of these Bcl-2 family proteins in M1 and M2 macrophages could make these cells more or less sensitive to the delivery of BIM.

In our model of activated macrophages, M1 macrophages were generated through exposure to interferon-γ and lipopolysaccharide while M2 macrophages were generated through exposure to interleukin-4 (IL-4). While scarce literature exists discussing regulation of apoptotic proteins in macrophages in response to IL-4 exposure, there is literature that suggests IL-4 can induce apoptosis in other types of cells. For example, Wedi and colleagues showed that eosinophils exposed to IL-4 underwent apoptosis after as little as 24 hours of exposure, with cell death increasing with extended exposure to IL-4 [54]. In addition, Shankaranarayanan and colleagues demonstrated that IL-4 induced apoptosis in A549 lung adenocarcinoma cells through multiple mechanisms [55]. A549 cells exposed to IL-4 had greater amounts of cleaved caspase-8 product and lower levels of anti-apoptotic protein Bcl-XL, while the pro-apoptotic Bax protein translocated from the cytoplasm to the mitochondrial membrane. While these studies suggest that IL-4 may prime other types of cells for apoptosis, it is unclear if IL-4 exposure, similar to the amount and duration used to generate bone marrow derived M2 macrophages,

would have a similar effect on macrophages. The concentrations of Bcl-2 family proteins may vary widely between different types of cells and thus the role of these proteins specifically in macrophages *in vitro* and *in vivo* warrants further exploration.

Other work has explored the role of the cell surface protein TREM-1 in pro-survival signaling in M1 macrophages. Triggering receptor expressed on myeloid cells 1 (TREM-1) is an immunoglobulin-like family member expressed on myeloid cells and plays a role in inflammation. Yuan and colleagues showed that knockdown of TREM-1 in RAW264.7 cells resulted in increased apoptosis and decreased expression of anti-apoptotic proteins Bcl-2 and Bcl-XL, among others [56]. In addition, overexpression of TREM-1 resulted in induction of Bcl-2. In separate work, Lo and colleagues showed that M1 macrophages (generated by differentiation with GM-CSF) exhibited higher expression of TREM-1 compared to M2 macrophages (generated by differentiation with M-CSF) [57]. Thus, it is possible that M1 macrophages have greater expression of anti-apoptotic Bcl-2 proteins and thus may be less sensitive to treatment with an agent like BIM, which relies on binding of these anti-apoptotic proteins to release sufficient Bax and Bak to induce apoptosis. The expression of various Bcl-2 proteins in M1 or M2 activated macrophages is not well studied, and future work to measure these proteins could identify the most potent pro-apoptotic agents specifically for M2 macrophage induced cell death.

2.6 Acknowledgements

Thank you to Jonathan Yu, Chayanon Ngambenjawong, Brynn Livesay, Christine Wang, and Leslie Chan for your assistance during animal experiments. Thank you to Michele Black for helpful discussions regarding selection of antibody panels and flow cytometry analysis. Thank you to Dr. Andrea Shietinger who contributed to the development of protocols for assessing tumor infiltrating lymphocyte and T Cell exhaustion populations. Thank you to Roma Yamul and Leslie Chan for assistance in developing the M2pepKLA cytotoxicity blood panel experiments. Thank you to Elaine Raines for helpful input regarding M1 and M2 macrophage regulation of Bcl-2 family proteins.

2.7 References

1. Schreiber RD, Old LJ, Smyth MJ (2011) Cancer Immunoediting: Integrating Immunity's Roles in Cancer Suppression and Promotion. Science Signaling 331:1565. doi: 10.1126/science.1203486

2. Mantovani A, Sica A (2010) Macrophages, innate immunity and cancer: balance, tolerance, and diversity. Curr Opin Immunol 22:231–237. doi: 10.1016/j.coi.2010.01.009

3. Jinushi M, Chiba S, Yoshiyama H, et al. (2011) Tumor-associated macrophages regulate tumorigenicity and anticancer drug responses of cancer stem/initiating cells. Proceedings of the National Academy of Sciences of the United States of America 108:12425–12430. doi: 10.1073/pnas.1106645108

4. Steidl C, Lee T, Shah SP, et al. (2010) Tumor-associated macrophages and survival in classic Hodgkin's lymphoma. N Engl J Med 362:875–885. doi: 10.1056/NEJMoa0905680

5. Chen J, Yao Y, Gong C, et al. (2011) CCL18 from tumor-associated macrophages promotes breast cancer metastasis via PITPNM3. Cancer Cell 19:541–555. doi: 10.1016/j.ccr.2011.02.006

6. Sica A, Mantovani A (2012) Macrophage plasticity and polarization: in vivo veritas. The Journal of Clinical Investigation 122:787–795. doi: 10.1172/JCI59643

7. Naito Y, Saito K, Shiiba K, et al. (1998) CD8+ T cells infiltrated within cancer cell nests as a prognostic factor in human colorectal cancer. Cancer Research 58:3491–3494.

8. Cullen SP, Brunet M, Martin SJ (2010) Granzymes in cancer and immunity. Cell Death Differ 17:616–623. doi: 10.1038/cdd.2009.206

9. Galon J (2006) Type, Density, and Location of Immune Cells Within Human Colorectal Tumors Predict Clinical Outcome. Science 313:1960–1964. doi: 10.1126/science.1129139

10. Tosolini M, Kirilovsky A, Mlecnik B, et al. (2011) Clinical Impact of Different Classes of Infiltrating T Cytotoxic and Helper Cells (Th1, Th2, Treg, Th17) in Patients with Colorectal Cancer. Cancer Research 71:1263–1271.

11. DeNardo DG, Andreu P, Coussens LM (2010) Interactions between lymphocytes and myeloid cells regulate pro- versus anti-tumor immunity. Cancer Metastasis Rev 29:309–316. doi: 10.1007/s10555-010-9223-6

12. Bellone G, Turletti A, Artusio E, et al. (1999) Tumor-Associated Transforming Growth Factor-β and Interleukin-10 Contribute to a Systemic Th2 Immune Phenotype in Pancreatic Carcinoma Patients. The American Journal of Pathology 155:537–547. doi: 10.1016/S0002-9440(10)65149-8

13. Sheu BC, Lin RH, Lien HC, et al. (2001) Predominant Th2/Tc2 polarity of tumor-infiltrating lymphocytes in human cervical cancer. J Immunol 167:2972–2978.

14. De Monte L, Reni M, Tassi E, et al. (2011) Intratumor T helper type 2 cell infiltrate correlates with cancer-associated fibroblast thymic stromal lymphopoietin production and reduced survival in pancreatic cancer. J Exp Med 208:469–478. doi: 10.1084/jem.20101876

15. Chen M-L, Pittet M, Gorelik L, et al. (2005) Regulatory T cells suppress tumor-specific CD8 T

cell cytotoxicity through TGF-beta signals in vivo. Proceedings of the National Academy of Sciences of the United States of America 102:419–424. doi: 10.1073/pnas.0408197102

16. Beyer M, Schultze JL (2006) Regulatory T cells in cancer. Blood 108:804–811. doi: 10.1182/blood-2006-02-002774

17. Cao X, Cai SF, Fehniger TA, et al. (2007) Granzyme B and Perforin Are Important for Regulatory T Cell-Mediated Suppression of Tumor Clearance. Immunity

18. Wolf D, Wolf AM, Rumpold H, et al. (2005) The Expression of the Regulatory T Cell–Specific Forkhead Box Transcription Factor FoxP3 Is Associated with Poor Prognosis in Ovarian Cancer. Clinical Cancer Research : an official journal of the American Association for Cancer Research 11:8326–8331.

19. Fu J, Xu D, Liu Z, et al. (2007) Increased regulatory T cells correlate with CD8 T-cell impairment and poor survival in hepatocellular carcinoma patients. Gastroenterology 132:2328–2339. doi: 10.1053/j.gastro.2007.03.102

20. Tang Q, Bluestone JA (2008) The Foxp3+ regulatory T cell: a jack of all trades, master of regulation. Nat Immunol 9:239–244. doi: 10.1038/ni1572

21. Wherry EJ (2011) T cell exhaustion. Nat Immunol 12:492–499. doi: doi:10.1038/ni.2035

22. Matsuzaki J, Gnjatic S, Mhawech-Fauceglia P, et al. (2010) Tumor-infiltrating NY-ESO-1-specific CD8+ T cells are negatively regulated by LAG-3 and PD-1 in human ovarian cancer. Proceedings of the National Academy of Sciences of the United States of America 107:7875–7880. doi: 10.1073/pnas.1003345107

23. Fourcade J, Sun Z, Benallaoua M, et al. (2010) Upregulation of Tim-3 and PD-1 expression is associated with tumor antigen–specific CD8+ T cell dysfunction in melanoma patients. J Exp Med 207:2175–2186.

24. Baitsch L, Baumgaertner P, Devevre E, et al. (2011) Exhaustion of tumor-specific CD8+ T cells in metastases from melanoma patients. The Journal of Clinical Investigation 121:2350–2360. doi: 10.1172/JCI46102

25. Wu K, Kryczek I, Chen L, et al. (2009) Kupffer cell suppression of CD8+ T cells in human hepatocellular carcinoma is mediated by B7-H1/programmed death-1 interactions. Cancer Research 69:8067–8075. doi: 10.1158/0008-5472.CAN-09-0901

26. Sakuishi K, Apetoh L, Sullivan JM, et al. (2010) Targeting Tim-3 and PD-1 pathways to reverse T cell exhaustion and restore anti-tumor immunity. J Exp Med 207:2187–2194. doi: 10.1038/nri1936

27. Zhou Q, Munger ME, Veenstra RG, et al. (2011) Coexpression of Tim-3 and PD-1 identifies a CD8+ T-cell exhaustion phenotype in mice with disseminated acute myelogenous leukemia. Blood 117:4501–4510. doi: 10.1182/blood-2010-10-310425

28. Gerner MY, Heltemes-Harris LM, Fife BT, Mescher MF (2013) Cutting Edge: IL-12 and Type I IFN Differentially Program CD8 T Cells for Programmed Death 1 Re-expression Levels and Tumor Control. J Immunol 191:1011–1015. doi: 10.4049/jimmunol.1300652

29. Shi F, Shi M, Zeng Z, et al. (2010) PD-1 and PD-L1 upregulation promotes CD8+ T-cell apoptosis and postoperative recurrence in hepatocellular carcinoma patients. Int J Cancer

128:887–896. doi: 10.1002/ijc.25397

30. Hsu M-C, Hsiao J-R, Chang K-C, et al. (2010) Increase of programmed death-1-expressing intratumoral CD8 T cells predicts a poor prognosis for nasopharyngeal carcinoma. Mod Pathol 23:1393–1403. doi: 10.1038/modpathol.2010.130

31. Brahmer JR, Tykodi SS, Chow LQM, et al. (2012) Safety and activity of anti-PD-L1 antibody in patients with advanced cancer. N Engl J Med 366:2455–2465. doi: 10.1056/NEJMoa1200694

32. Franklin RA, Liao W, Sarkar A, et al. (2014) The cellular and molecular origin of tumor-associated macrophages. Science 344:921–925. doi: 10.1126/science.1252510

33. Ellerby HM, Arap W, Ellerby LM, et al. (1999) Anti-cancer activity of targeted pro-apoptotic peptides. Nat Med 5:1032–1038. doi: 10.1038/12469

34. Mai JC, Mi Z, Kim SH, et al. (2001) A proapoptotic peptide for the treatment of solid tumors. Cancer Research 61:7709–7712.

35. Spence S, Fitzsimons A, Boyd CR, et al. (2013) Suppressors of cytokine signaling 2 and 3 diametrically control macrophage polarization. Immunity 38:66–78. doi: 10.1016/j.immuni.2012.09.013

36. Hamann FM, Brehm R, Pauli J, et al. (2011) Controlled modulation of serum protein binding and biodistribution of asymmetric cyanine dyes by variation of the number of sulfonate groups. Molecular Imaging 10:258–269.

37. Pollaro L, Heinis C (2010) Strategies to prolong the plasma residence time of peptide drugs. Med Chem Commun 1:319–324. doi: 10.1039/c0md00111b

38. Mantovani A, Allavena P, Sica A, Balkwill F (2008) Cancer-related inflammation. Nature 454:436–444. doi: 10.1038/nature07205

39. Lin EY, Pollard JW (2004) Role of infiltrated leucocytes in tumour growth and spread. Br J Cancer 90:2053–2058. doi: 10.1038/sj.bjc.6601705

40. Welford AF, Biziato D, Coffelt SB, et al. (2011) TIE2-expressing macrophages limit the therapeutic efficacy of the vascular-disrupting agent combretastatin A4 phosphate in mice. The Journal of Clinical Investigation 121:1969–1973. doi: 10.1172/JCI44562

41. Shree T, Olson OC, Elie BT, et al. (2011) Macrophages and cathepsin proteases blunt chemotherapeutic response in breast cancer. Genes Dev 25:2465–2479. doi: 10.1101/gad.180331.111

42. Zeisberger SM, Odermatt B, Marty C, et al. (2006) Clodronate-liposome-mediated depletion of tumour-associated macrophages: a new and highly effective antiangiogenic therapy approach. Br J Cancer 95:272–281. doi: 10.1038/sj.bjc.6603240

43. Mäkelä AR, Matilainen H, White DJ, et al. (2006) Enhanced baculovirus-mediated transduction of human cancer cells by tumor-homing peptides. J Virol 80:6603–6611. doi: 10.1128/JVI.00528-06

44. Elmore S (2007) Apoptosis: A Review of Programmed Cell Death. Toxicologic Path 35:495–516. doi: 10.1080/01926230701320337

45. Willis SN, Adams JM (2005) Life in the balance: how BH3-only proteins induce apoptosis. Current Opinion in Cell Biology 17:617–625. doi: 10.1016/j.ceb.2005.10.001

46. Mérino D, Giam M, Hughes PD, et al. (2009) The role of BH3-only protein Bim extends beyond inhibiting Bcl-2-like prosurvival proteins. J Cell Biol 186:355–362. doi: 10.1083/jcb.200905153

47. Kashiwagi H, McDunn JE, Goedegebuure PS, et al. (2007) TAT-Bim induces extensive apoptosis in cancer cells. Ann Surg Oncol 14:1763–1771. doi: 10.1245/s10434-006-9298-z

48. Berguig GY, Convertine AJ, Frayo S, et al. (2015) Intracellular Delivery System for Antibody-Peptide Drug Conjugates. Mol Ther. doi: 10.1038/mt.2015.22

49. Ko J-K, Choi K-H, Peng J, et al. (2011) Amphipathic tail-anchoring peptide and Bcl-2 homology domain-3 (BH3) peptides from Bcl-2 family proteins induce apoptosis through different mechanisms. J Biol Chem 286:9038–9048. doi: 10.1074/jbc.M110.198457

50. Ko J-K, Lee M-J, Cho S-H, et al. (2003) Bfl-1S, a novel alternative splice variant of Bfl-1, localizes in the nucleus via its C-terminus and prevents cell death. Oncogene 22:2457–2465. doi: 10.1038/sj.onc.1206274

51. Ko JK, Choi KH, Pan Z, et al. (2007) The tail-anchoring domain of Bfl1 and HCCS1 targets mitochondrial membrane permeability to induce apoptosis. J Cell Sci 120:2912–2923. doi: 10.1242/jcs.006197

52. De G, Ko J-K, Tan T, et al. (2014) Amphipathic tail-anchoring peptide is a promising therapeutic agent for prostate cancer treatment. Oncotarget 5:7734–7747.

53. Cory S, Huang DCS, Adams JM (2003) The Bcl-2 family: roles in cell survival and oncogenesis. Oncogene 22:8590–8607. doi: 10.1038/sj.onc.1207102

54. Wedi B, Raap U, Lewrick H, Kapp A (1998) IL-4-induced apoptosis in peripheral blood eosinophils. J Allergy Clin Immunol 102:1013–1020.

55. Shankaranarayanan P, Nigam S (2003) IL-4 Induces Apoptosis in A549 Lung Adenocarcinoma Cells: Evidence for the Pivotal Role of 15-Hydroxyeicosatetraenoic Acid Binding to Activated Peroxisome Proliferator-Activated Receptor Transcription Factor. J Immunol 170:887–894. doi: 10.4049/jimmunol.170.2.887

56. Yuan Z, Syed MA, Panchal D, et al. (2014) Triggering receptor expressed on myeloid cells 1 (TREM-1)-mediated Bcl-2 induction prolongs macrophage survival. J Biol Chem 289:15118–15129. doi: 10.1074/jbc.M113.536490

57. Lo T-H, Tseng K-Y, Tsao W-S, et al. (2014) TREM-1 regulates macrophage polarization in ureteral obstruction. 86:1177–1189. doi: 10.1038/ki.2014.205

Chapter 3

METHODS TO IDENTIFY A HUMAN M2 MACROPHAGE TARGETING PEPTIDE

Abstract

Targeting moieties that specifically bind human M2-like tumor-associated macrophages remain elusive. Phage display has been used to successfully identify murine M2 macrophage targeting peptide, M2pep, which was later shown to also bind murine tumor-associated macrophages. In this work, similar whole cell panning techniques were employed to identify a human M2 macrophage targeting peptide. Human M1 and M2 macrophages were generated by differentiating monocytes isolated from human peripheral blood mononuclear cells in to macrophages, and activated with IFNγ and LPS, or IL-4, respectively. M1 macrophages were then used as a negative selection step in phage panning while M2 macrophages were used as a positive selection step. Various elution methods were employed to isolate extracellularly or intracellularly bound phage. Phage panning on immobilized protein was also used to identify peptides exhibiting selective binding to human legumain or PD-L1 protein, both of which are known to be expressed on tumor-associated macrophages. Though several phage panning attempts were made, no human M2 macrophage specific peptide was identified.

3.1 Introduction and Rationale

3.1.1 Targeting Tumor-associated Macrophages in the Clinic

Tumor-associated macrophages are attractive cancer therapeutic targets due to the significant role they play in cancer progression and metastasis. The lack of targeting moieties that specifically bind these cells motivates the work described in this chapter. However, cancer therapeutics that target the role of macrophages in tumor progression are in their early stages of exploration in the clinic, demonstrating the importance of understanding the interplay between TAMs and tumor cells, as well as the interactions of TAMs with cancer therapeutics like chemotherapy. Current methods targeting TAMs in the clinic follow two schools of thought: 1) blocking the recruitment of TAMs into the tumor, or 2) reprogramming TAMs into a more anti-tumoral role [1, 2].

Inhibiting Recruitment of TAMs

While many TAM recruitment inhibition methods have been proposed and tested in animal models, few have been successful in the clinic. One example is the anti-CCL2 antibody, carlumab, which was hypothesized based on animal models to inhibit the CCL2/CCR2 signaling pathway that is responsible for inflammatory monocyte recruitment into tumors resulting in infiltration of tumor-promoting TAMs. In clinical trials of carlumab monotherapy or combination therapy with chemotherapy, carlumab failed to exert sustained inhibition of CCL2 signaling or demonstrate improved patient outcomes [3, 4].

Despite failures in inhibiting the CCL2/CCR2 signaling pathway for hindering TAM recruitment, macrophage colony-stimulating factor 1 receptor (CSF-1R) appears to be an attractive target. Macrophage colony-stimulating factor 1 (CSF-1) is the ligand that is responsible for the migration and differentiation of monocytes and macrophages that express its receptor, CSF-1R. Recently, anti-CSF-1R antibody RG7155 was intravenously administered alone or in combination with paclitaxel to patients with various solid tumors in a phase 1

clinical trial [5]. Patients who received the antibody drug had a significant reduction in CSF-1R+ cells and CD68+CD163+ macrophages within only 4 weeks of initial treatment.

Reprogramming TAMs for Anti-tumoral Response

One of the first attempts at skewing tumor-promoting TAMs towards an anti-tumor phenotype was the administration of interferon-γ (IFNγ) in an untargeted fashion over two decades ago. In these studies, ovarian cancer patients were intraperitoneally administered recombinant IFNγ as adjuvant cancer therapy following surgical resection [6]. In these treated patients, younger patients (<60 years old) responded better to IFNγ treatment when compared to older patients (42% versus 16% response rate, respectively). The study authors suggested that this result could be due to the decrease in responsiveness of intraperitoneal macrophages to IFNγ with increase in age.

In a recent clinical trial, a CD40 agonist antibody was administered in combination with gemcitabine to patients with pancreatic ductal adenocarcinoma with the hypothesis that activation of CD40, a member of the tumor-necrosis factor receptor superfamily, would result in T cell dependent anti-tumor immunity [7]. Indeed, patients receiving combination therapy had improved progression-free survival and overall survival, but tumor biopsies revealed no increase in infiltration of T cells, suggesting a different mechanism was responsible for tumor regression. Using a mouse model of pancreatic cancer, it was determined that the CD40 agonist antibody bound macrophages prior to their infiltration into the tumor, activating these macrophages to exhibit increased expression of MHC II and CD86 on their surface and acquire the ability to lyse tumor cells and degrade tumor matrix. Ultimately it was shown that the presence of these macrophages was required to observe tumor regression in this mouse model of disease, suggesting CD40 agonists as a new method of skewing tumor-associated macrophages towards an anti-tumor phenotype.

3.1.2 Legumain

Legumain is an acidic cysteine endopeptidase that was first identified in plants, but is evolutionarily conserved across species including humans. Its cleavage of peptides is very tightly controlled, recognizing an asparagine at the P1 location of the cleavage site and having optimal activity in the pH range of 4.2 to 5.5 [8]. Legumain is reported to be specifically upregulated on M2 macrophages and TAMs when compared to M1 macrophages and other healthy tissues [9], making it an attractive target for M2 macrophage selective therapies. Use of legumain as the target antigen in a DNA vaccine was reported to be effective in prolonging survival of tumor-bearing mice in both a prophylactic setting and after tumor onset [10]. In addition, legumain cleavable elements have been incorporated into doxorubicin prodrugs designed to only release active doxorubicin upon cleavage at the tumor site. In tumor-bearing mice administered this prodrug therapy, the doxorubicin prodrug was more effective than unmodified doxorubicin at delaying tumor growth and was also associated with lower toxicity to the animals [9]. In more recent work, a Y-shaped legumain-targeting construct made up of an [Ala-Ala-Asn-Leu] legumain cleavage domain targeting segment fused to a [His-Lys-$(His-Lys)_2$] functional segment, was used to deliver oxidized carbon nanotubes loaded with paramagnetic Fe_3O_4 nanoparticles for magnetic resonance imaging of TAMs within tumors [11].

Thus, legumain is an attractive TAM-selective target for several reasons. Its conservation across species provides ease of use during *in vivo* testing in animal models and rapid translation to human therapeutics. Its preferential activity in the low pH environment of a tumor suggests its use in a target site-specific manner. Its use as the target of a vaccine as well as prodrug therapy for cancer has proved effective in animal models, demonstrating its utility as a protein target. In addition, leugmain is also frequently upregulated on tumor cells [9, 12], suggesting that legumain-targeted cytotoxic therapy may also have some off target cancer-killing effects as well. Phage panning against immobilized legumain protein could potentially identify peptide sequences that bind legumain outside of its cleavage pocket.

3.1.3 PD-L1

Programmed Cell Death 1 Ligand, PD-L1 (also known as B7-H1), is one of the B7 family members that is a ligand for PD-1. PD-L1 is primarily expressed on antigen presenting cells such as macrophages and dendritic cells, but has also been found on T cells, B cells, natural killer cells, epithelial cells and endothelial cells [13]. In addition, the expression of PD-L1 is found to be increased in tumor cells [14]. Under normal conditions, PD-L1 plays an important role in regulating the balance between immune tolerance and autoimmunity, and thus its dysregulation has been implicated in disease [15-17].

As described in Chapter 2, PD-L1 displayed on antigen presenting cells may result in the exhaustion of CD8+ T cells and immune tolerance of tumors. Thus identification of a peptide that is able to selectively bind PD-L1 may facilitate the removal of not just tumor-associated macrophages, but all cells that facilitate T cell exhaustion and resulting immune tolerance of tumors. Furthermore, a peptide that is also able to block the interaction between PD-L1 and PD-1 may also be a viable cancer therapy similar to existing work with antibody therapies. These factors provide rationale for phage biopanning against immobilized PD-L1 protein as an attractive cancer therapy target.

3.2 Materials and Methods

3.2.1 Materials

K2 EDTA Vacutainer (BD); Ficoll Paque Plus (GE Healthcare); Modified Dulbecco's Phosphate Buffered Saline (DPBS) (Fisher); Bovine Serum Albumin (BSA) (Miltenyi) ethylenediaminetetraacetic acid (EDTA) (Fisher); Monocyte Isolation Kit II (Miltenyi); MACS Buffer (DPBS, 2mM EDTA, 0.5%BSA); LS Columns (Miltenyi); RPMI media; Fetal Bovine Serum (FBS) (Fisher); AbAm (Fisher); dimethyl sulfoxide (DMSO) (Sigma); recombinant human macrophage-colony stimulating factor (M-CSF) (Miltenyi); recombinant human interleukin-4 (R&D Systems); recombinant human interferon-γ (R&D Systems); lipopolysaccharide (LPS); anti-CD68 FITC (Miltenyi); anti-CD163 PE (Miltenyi); anti-CD86 PE (Miltenyi); anti-CD80 PE (Miltenyi);

anti-CD206 PE (Miltenyi); anti-HLA-DR PE (Miltenyi); anti-CD71 PE (Miltenyi); anti-CD23 PE (Miltenyi); PhD-12 Phage Library (New England Biolabs); PhD-C7 Phage Library (New England Biolabs); Hanks Balanced Salt Solution (HBSS) (Fisher); Nickel-coated plates (Pierce); human legumain protein with C-terminal his tag (Novoprotein); human PD-L1 protein with C-terminal his tag (Novoprotein); anti-M13 HRP (GE Healthcare); LIVE/DEAD Fixable Far Red Stain (Life Technologies); rabbit anti-M13 antibody (GE Healthcare); goat anti-rabbit CF405M antibody (Sigma); QIAprep Spin M13 Kit (QIAGEN); dNTPs (Qiagen); Phusion High Fidelity DNA Polymerase (New England BioLabs); Phusion High Fidelity buffer (New England BioLabs); AquaPor LE GTAC Agarose (National Diagnostics, Atlanta, GA, USA); QIAquick Gel Extraction Kit (QIAGEN); MiniPrep kit (QIAGEN); MinElute kit (QIAGEN); molecular biology grade H_2O (Corning); Acc65I (New England BioLabs); EagI (New England BioLabs); T4 DNA ligase (New England BioLabs); XL10-Gold ultracompetent cells (Agilent); Biotin-PEG NovaTag resin (EMD); streptavidin-FITC (eBioscience); streptavidin-PEcy7 (eBioscience)

3.2.2 Isolating Peripheral Blood Mononuclear Cells (PBMCs) from Human Blood Donors

Human subject blood samples were acquired with the approval of the Division of Human Subjects at the University of Washington. Blood samples were collected in EDTA-coated vacutainer tubes and processed immediately following collection. Blood was supplemented 1:10 (v/v) with 3.8% sodium citrate solution, followed by dilution 1:1 into DPBS supplemented with 2 mM EDTA. 15 mL of Ficoll Paque Plus was added to a 50 mL conical tube, followed by 35 mL of diluted blood sample layered above. Ficoll-blood tubes were centrifuged in a swinging bucket rotor at 400g for 40 minutes without breaking. Top plasma-containing layer was discarded and PBMC-containing layer transferred to a fresh 50 mL conical tube. Peripheral blood mononuclear cells (PBMCs) were diluted 1:1 with DPBS supplemented with 2mM EDTA, and pelleted by centrifugation for 10 minutes at 300g. Pellets were combined into one 50 mL conical tube and final volume brought to 50 mL with DPBS supplemented with 2 mM EDTA. PBMCs were again pelleted by centrifugation for 10 minutes at 300g, supernatant discarded, and pellet

resuspended in FBS. Cells were aliquoted to cyrovials and FBS supplemented with 20% DMSO added dropwise to a final composition of 10% DMSO with cells. Cells were frozen and stored in a liquid nitrogen dewar until use.

3.2.3 Isolating Monocytes from Human PBMC Samples and Human Macrophage Differentiation and Activation

Frozen aliquots of human PBMCs were quickly thawed at 37°C, transferred to a 15 mL conical tube and pelleted by centrifugation at 300g for 5 minutes. Cells were resuspended in MACS Buffer at a concentration of 10^7 cells per 30 μL and transferred to a 1.5 mL microcentrifuge tube. Next, 10 μL per 10^7 cells of Fc Blocking Agent and Biotin-antibody cocktail (Monocyte Isolation Kit II, Miltenyi) were added, pipetting up and down to mix. Cells were incubated with antibodies at 4°C for 10 minutes. Next 30 μL MACS Buffer per 10^7 cells was added, followed by 10 μL per 10^7 cells of anti-biotin microbeads. Cells were incubated with beads for 15 minutes at 4°C. Remaining tube volume was filled with MACS Buffer and cells were pelleted by centrifugation at 300g for 10 minutes. Supernatant was aspirated and cells were resuspended in 1 mL of MACS Buffer. Cell solution was applied to a primed LS Column and flow through collected. Column was washed 3 times with 1 mL of MACS Buffer. Cells were pelleted by centrifugation at 300g for 5 minutes, supernatant removed and resuspended in RPMI media supplemented with 10% FBS, 1% AbAm and 20 ng/μL recombinant human M-CSF. Cells were plated at 5 million cells per 100 mm petri dish. Four days following plating, additional M-CSF containing media was added to cell culture. For M2 macrophage activation, 6-day differentiated cells were washed once with warm HBSS and cultured for 2 days with media containing 25 ng/μL human IL-4. For M1 macrophage activation, 7-day differentiated cells were washed once with warm HBSS and cultured for 1 day with media containing 50 ng/μL human IFNγ and 10 ng/μL LPS.

3.2.4 Flow Cytometry Immunophenotyping of Human M1 and M2 Macrophages

Human M1 and M2 macrophages were generated as described in Section 3.2.3. To remove cells from the plate, cells were incubated with DPBS supplemented with 2 mM EDTA on ice for 30 minutes followed by removal by cell scraping. Cells were pelleted by centrifugation at 300g for 5 minutes, resuspended in PBS/1%BSA and aliquoted into a black round-bottom 96-well plate at 100,000 cells per well. Cells were pelleted and resuspended in 100 μL of PBS/1%BSA containing Human Fc Block (1:20 dilution) and one of the following antibodies: CD163 (1:5 dilution), CD80 (1:7 dilution), CD86 (1:15 dilution), CD206 (1:25 dilution), HLA-DR (1:100 dilution), CD71 (1:25 dilution) or CD23 (1:6 dilution). Cells were incubated with antibodies for 20 minutes at 4˚C and washed 3 times by pelleting and resuspending in PBS/1%BSA. For intracellular CD68 staining, cells were first fixed by incubation with 100 μL 4% paraformaldehyde for 15 minutes at 4˚C. Cells were pelleted, resuspended in ice-cold methanol and incubated at -20˚C for 10 minutes. Cells were then pelleted before staining with PBS/1%BSA containing Fc Block and CD68 antibody (1:10 dilution) for 20 minutes at 4˚C.

3.2.5 Cell Suspension Phage Biopanning Lacking Tween in Wash Buffers

Human M1 and M2 macrophages were plated as described in Section 3.2.3. Before use, media from each plate of cells was removed and replaced with pre-warmed RPMI for a 2 hour receptor clearing period. For an initial positive pan, M2 macrophages were scraped from the plate, pelleted by centrifugation and resuspended in PBS/1%BSA. 2 million cells were transferred to a microcentrifuge tube and PBS/1%BSA added to a total volume of 470 μL $2x10^{11}$ PFU of the PhD-12 and PhD-C7 Phage Libraries was added to the cell suspension, and incubated at 4˚C for 1 hour, rotating. Cells were washed five times by pelleting cells, removing supernatant and resuspending cells in 500 μL of PBS/1%BSA. For phage elution, cells were resuspended in 1 mL of 0.2 M Glycine-HCl pH 2.2 and incubated at 4˚C with shaking for 15 minutes. Solution was then neutralized with 150 μL 1 M Tris-Base pH 9.1, and cells underwent three freeze/thaw cycles to facilitate cell lysis. Resulting elution was titered and amplified according to the NEB

protocol. Three subsequent subtractive pans were performed in a similar manner, by first incubating phage with 1 million human M1 macrophages in suspension, then pelleting M1 macrophages and applying supernatant to 1 million M2 macrophages for the selective step. This panning method was employed to select for phage selectively binding human M1 or M2 macrophages.

3.2.6 Cell Suspension Phage Biopanning with Increasing Tween in Wash Buffers

Phage biopanning to identify a human M2 macrophage binding peptide sequence was performed similarly to that described in Section 3.2.5. To increase stringency in the pan, Tween 20 was added to the wash buffer with increasing concentration in each round. The wash buffer for the initial positive pan and first subtractive pan contained 0.1% Tween, the second subtractive pan wash buffer contained 0.3% Tween, and the third subtractive pan wash buffer contained 0.5% Tween.

3.2.7 Cell Suspension Phage Biopanning with Double M1 Macrophage Subtraction

Phage biopanning to identify a human M2 macrophage binding peptide sequence was performed similarly to that described in Section 3.2.5. In this pan, only the PhD-C7 library was used in an effort to select for cyclic peptides that would yield better *in vivo* stability. To increase stringency, a double subtraction with human M1 macrophages was performed. Briefly, phage was first applied to M1 macrophages in cell suspension. These cells were pelleted, and the supernatant applied to another tube of M1 macrophages in suspension. These cells were then pelleted and the supernatant applied to the M2 macrophages for the selective step.

3.2.8 Plate Phage Biopanning with Glycine-HCl Elution

Human M1 and M2 macrophages were plated as described in Section 3.2.3. Before use, media from each plate of cells was removed and replaced with pre-warmed RPMI for a 2 hour receptor

clearing period. For an initial positive pan, $2x10^{11}$ PFU phage from the PhD-12 and PhD-C7 Libraries (New England Biolabs) were added to 3.1 mL ice-cold HBSS/1%BSA. Then, RPMI media was aspirated from a plate of human M2 macrophages, and replaced with 3 mL of phage solution. The plate was incubated at 4˚C for 1 hour, followed by five 1-minute washes with HBSS/1%BSA. Phage was eluted from cells by adding 2 mL 0.2 M Glycine-HCl pH 2.2 to the plate, scraping cells and transferring solution to a 15 mL conical. 500 μL of 0.2 M Glycine-HCl was used to wash remaining cells from plate and transferred to the 15 mL conical. Cell elution solution was incubated for 10 minutes at 4˚C, before being neutralized with 375 μL of 1 M Tris-Base (pH 9.1) and undergoing 3 freeze/thaw cycles to facilitate cell lysis. Phage elution solution was then titered and amplified according to the NEB protocol. Three subsequent subtractive pans were performed in a similar manner by first incubating phage library with an empty non-tissue culture treated plate at room temperature for 1 hour to remove plastic binding phage. Plate supernatant was then transferred to a plate of human M1 macrophages for 1 hour at room temperature to eliminate M1 macrophage binding phage. Lastly, M1 macrophage plate supernatant was transferred to a plate of human M2 macrophages for the selective step.

3.2.9 Plate Phage Biopanning with Extracellular and Intracellular Recovery

Human M1 and M2 macrophages were plated as described in Section 3.2.3. Before use, media from each plate of cells was removed and replaced with pre-warmed RPMI for a 2 hour receptor clearing period. For an initial positive pan, $2x10^{11}$ PFU phage from the PhD-12 and PhD-C7 Libraries were pre-blocked in separate 3 mL aliquots of RPMI supplemented with 10% FBS for 1 hour at room temperature. Next, media was aspirated from M2 macrophages and replaced with blocked libraries for a 1 hour incubation at 4˚C with shaking. Cells were washed 4 times with ice-cold RPMI/10%FBS, for 3 minutes per wash with agitation. For extracellular elution, cells were incubated with 3 mL 0.2 M Glycine-HCl pH 2.2 for 15 minutes at 4˚C, with shaking. PhD-12 and PhD-C7 elutions were combined in a 15 mL conical tube and neutralized with 900 μL of 1 M Tris-Base pH 9.1. For intracellular elution, 10 mL of pre-warmed RPMI/10%FBS media was

applied to the cells and placed at 37˚C for 30 minutes to facilitate internalization of bound phage. Uninternalized phage were then eluted from the cell surface by incubating cells with 3 mL of 0.2 M Glycine-HCl pH 2.2 for 15 minutes at 4˚C, with agitation. Glycine-phage elution solution was discarded, cells trypsinized and transferred to a 15 mL conical tube. Cells were pelleted, resuspended in 500 μL of 100 mM Triethylamine and incubated for 10 minutes at room temperature to facilitate cell lysis. Triethylamine was neutralized with 1 mL of 1 M Tris-HCl pH 7. Both extracellular and intracellular elutions were titered and amplified according to the NEB protocol. Three subsequent subtractive rounds were performed in a similar manner by first incubating pre-blocked libraries with a plate of M1 macrophages for 1 hour at 4˚C. Plate supernatant was then transferred to plates seeded with M2 macrophages for the selective step.

3.2.10 Plate Phage Biopanning with Strong Binding Phage Elution

Human M1 and M2 macrophages were plated as described in Section 3.2.3 onto non-tissue culture treated 6-well plates. Before use, media from each plate of cells was removed and replaced with pre-warmed RPMI for a 2 hour receptor clearing period. For an initial positive pan, $2x10^{11}$ PFU phage from the PhD-12 Library was pre-blocked in 6 mL of RPMI/1%BSA for 1 hour at room temperature. Then 1 mL of block library was transferred to each well of an empty 6-well plate and incubated for 1 hour at room temperature, rocking. Supernatant from these wells was then transferred to wells of a plate seeded with human M2 macrophages and incubated for 1 hour at 4˚C with rocking. M2 macrophage wells were then washed five times with HBSS/1%BSA, 3 minutes per wash with rocking. Loosely bound phage were then eluted my incubating cells with 1 mL per well 0.2 M Glycine-HCl pH 2.2 for 10 minutes at 4˚C with rocking. Glycine elution solution was transferred to a 15 mL conical tube, neutralized with 1 mL of 1 M Tris-Base pH 8.2 and titered. M2 macrophages still adhered to the plate were quickly washed once with HBSS/1%BSA, and then incubated with 1 mL per well 30 mM Tris-HCl 1 mM EDTA pH 8 for 1 hour on ice with rocking to facilitate cell lysis. Then remaining cellular debris was scraped up from plate and elution solution transferred to a 15 mL conical tube. This elution

solution was titered and amplified for the next round of biopanning. Four subsequent subtractive rounds of panning were performed in a similar manner by including human resting and M1 macrophage subtractive steps before the human M2 macrophage selective step.

3.2.11 Phage Biopanning Against Immobilized Proteins Legumain and PD-L1 using Glycine-HCl Elution

For use in panning, His-tagged proteins legumain and PD-L1 were immobilized by incubating 100 μL of 10 μg/mL solution of protein on nickel-coated plates for 1 hour at room temperature with shaking. Solution was then removed by inverting on a paper towel, and wells blocked with PBS/1%BSA for 1 hour at room temperature with shaking. For an initial positive pan, $2x10^{11}$ PFU of the PhD-12 and PhD-C7 libraries in 150 μL of PBS/1%BSA were incubated in separate wells coated with target protein for 1 hour at room temperature with shaking. Then wells were washed 10 times by inverting plate onto a clean paper towel and adding 150 μL of PBS/1%BSA/0.1%Tween20 to the wells. Following washes, phage was eluted by incubation with 100 μL of 0.2 M Glycine-HCl pH 2.2 for 15 minutes at room temperature with shaking. PhD-12 and PhD-C7 elutions were combined, elution buffer neutralized with 30 μL of 1 M Tris-Base pH 9.1, and titered and amplified according to the NEB protocol. Three subsequent subtractive rounds of panning were conducted in a similar manner by first incubating the previous round's amplified library with poly-histidine coated wells as subtractive step, before incubating with the target protein as a selective step. Stringency was increased over time by increasing the amount of Tween20 in the wash buffer from 0.1% to 0.3% to 0.5% with each round of panning. Due to observed enrichment for histidine-containing peptide sequences following the legumain panning second subtractive round, an empty nickel-coated plate subtractive step was added beginning in the legumain third subtractive round and the PD-L1 second subtractive round.

3.2.12 Phage Biopanning Against Immobilized Proteins Legumain and PD-L1 using Imidizole Elution

For use in panning, target proteins were immobilized and pre-blocked on nickel-coated plates as described in Section 3.2.11. For an initial positive pan, $2x10^{11}$ PFU of the PhD-12 and PhD-C7 phage libraries in PBS/10mM Imidazole/1%BSA were incubated with empty nickel-coated plates for 1 hour at room temperature with shaking to eliminate plate binding phage. Then, plate supernatants were transferred to wells coated with target protein for a selective step. Then wells were washed 10 times by inverting plate onto a clean paper towel and adding 150 μL of PBS/10 mM Imidazole/1%BSA/0.1%Tween20 to the wells. Following washes, phage was eluted by incubation with 100 μL of PBS/300 mM Imidazole for 15 minutes at room temperature with shaking. PhD-12 and PhD-C7 elutions were combined, elution buffer neutralized with 30 μL of 1 M Tris-Base pH 9.1, and titered and amplified according to the NEB protocol. Three subsequent subtractive rounds were performed in a similar manner by first incubating phage libraries with an empty nickel-coated well, followed by incubation with a non-target protein coated well for subtractive steps. For example, when panning for a legumain binding phage clone, phage library was first incubated with PD-L1 as a subtractive step before being transferred to a well coated with legumain protein as the selective step. Stringency was increased over time by increasing the amount of Tween20 in the wash buffer from 0.1% to 0.3% to 0.5% with each subtractive round of panning.

3.2.13 Legumain and PD-L1 Phage Clone ELISA Binding Studies

Proteins were immobilized on nickel-coated plates as described in Section 3.2.11. 50 μL of $1x10^{5}$ PFU/μL of phage clones in PBS/1%BSA was incubated in wells for 1 hour at room temperature with shaking. Wells were washed 10 times with PBS/0.1%Tween, followed by incubation with anti-M13-HRP antibody (1:3000 dilution in PBS/1%BSA) for 30 minutes at 4˚C with shaking. Wells were washed 3 times with PBS/1%BSA followed by addition of substrate to develop ELISA. 50 μL stop solution was added to wells after 20 minutes of developing, and

ELISA absorbance read at 450 nm and 540 nm on a Safire^2 (Tecan) plate reader. 540 nm background signal was deducted from 450 nm signal for analysis.

3.2.14 Phage Clone Flow Cytometry Binding Studies

Human M1 and M2 macrophages were generated as described in Section 3.2.3. To remove macrophages from plates, cells were incubated with DPBS/2mM EDTA for 30 minutes on ice followed by scraping with a cell lifter. Cells were aliquoted 100,000 cells per well in a black, round bottom 96-well plate. Cells were pelleted and resuspended in 50 μL of 1x10^7 PFU/μL of phage clones and Fc Block in PBS/1%BSA. After a 30 minute incubation on ice, cells were washed twice by centrifuging at 300g to pellet cells, aspirating the supernatant and resuspending in PBS/1%BSA. Cells were stained with the LIVE/DEAD Fixable Far Red Stain according to manufacturers instructions. Cells were then fixed with 100 μL per sample 4% paraformaldehyde for 15 minutes on ice and washed once. Cells were then incubated with rabbit anti-M13 phage antibody for 20 minutes on ice, followed by one wash. Cells were then incubated with goat anti-rabbit secondary antibody for 20 minutes on ice, followed by one wash and analyzed on a flow cytometer.

3.2.15 Analysis of InHM2, ExHM2, and shM2 Enriched Libraries via Next Generation Sequencing

Single stranded DNA (ssDNA) was isolated from 1×10^{11} PFU of the amplified phage eluate from the second and third subtractive rounds of peptide phage display from the extracellular, intracellular and strong binding methods of whole cell panning using QIAprep Spin M13 Kit. 50 ng of ssDNA was amplified by PCR using primers containing Illumina-compatible sequencing adaptors and barcodes. The PCR reaction (50 μL) contained 500 nM of each primer, 250 μM dNTP, 1 U Phusion High Fidelity DNA Polymerase, and 1× Phusion High Fidelity buffer. Thirteen PCR cycles (10 s at 98˚C, 30 s at 59˚C, 30 s at 72˚C) were performed and PCR products were purified from a 2% agarose gel using QIAquick Gel Extraction Kit. The concentration of DNA was determined by a quantitation assay using a Qubit 3.0 Fluorometer (Life Technologies).

Purified PCR products prepared from the “unselected” and “selected” phage libraries were combined in a 5:1 molar ratio, respective to each individual “selected” sample, prior to sequencing.

Sequencing and analysis was performed using the approach described by ‘t Hoen *et al* with modifications [18]. Sequencing was performed on an Illumina MiSeq system in the presence of 7% PhiX control, using 150 bp single ended sequencing chemistries and custom sequencing primers (Read_1_primer, 5’- GCTCGACCTGTTCCTTTAGTGGTACCTTTCTATTCTCACTCT-3’; Index_read_primer, 5’- AGCAAAATCCCATACAGAAAATTCATTTACCGCAGGTCGCTCC -3’), according to manufacturer instructions.

Sequence reads that exactly matched the first 10 nucleotides of the flanking sequence immediately downstream of the library insert variable region (5’-GGTGGAGGTT- 3’) were retained for further analysis. Subsequences corresponding to the phage display variable region (excluding the terminal 3 glycines of the library insert) were extracted and translated into protein, substituting the amber stop codon with glutamine to reflect the nonsense suppression activity of *E. coli* K12 ER2738.

For each library, the count of sequence reads encoding each unique protein sequence was tabulated. The relative abundance of specific polypeptides was calculated as the fraction of total reads in the library that encoded the polypeptide. Sequencing results were represented in two formats: rank via raw number of phage peptide sequences appearing in the library or rank via fold enrichment in phage peptide sequence over the same sequence in a four-times amplified library without selection pressure. Libraries from the third subtractive rounds of panning of each biopanning strategy were analyzed for the appearance of peptides across all three libraries as well as with at least 2-fold enrichment over the unselected library. From this list, those peptides that lacked common plastic-binding motifs were analyzed for their enrichment value in each library and the presence of other similar peptide sequences that may reveal the emergence of a common binding motif. The Clustal Omega (European Bioinformatics Institute) online sequence alignment program was used to identify these potential binding motifs. A second, less stringent analysis method identified those sequences that only appeared

in one of the three analyzed libraries, but had ten-fold or higher enrichment values over the unselected library. This method was used to ensure that if one biopanning method was more successful at selecting for M2 macrophages specific peptides than another, these peptide sequences would still be identified. Candidate peptide sequences were then cloned into the phage for testing for binding to human M2 macrophages.

3.2.16 Cloning of Candidate Peptide Sequences into Phage

Vector isolation. The M13KE dsDNA vector was isolated and purified from a 1:100 dilution of an overnight culture of ER2738 *E. coli* grown with a phage clone for 4.5 h using a MiniPrep kit.

Insert preparation. Oligonucleotides encoding the peptides of interest were designed with 5' overhangs and an overlap region with T_m ~55-60 ˚C and synthesized by Integrated DNA Technologies. Oligonucleotide pairs were allowed to hybridize at 95 ˚C for 5 min and then gradually cooled to room temperature over 1 h. After, the 5' overhangs were filled with Klenow (30 min at 37 ˚C, 20 min at 75 ˚C), and the reaction was purified using a MinElute kit and eluted in molecular biology grade H_2O. Concentrations were quantified by NanoDrop (Thermo Scientific).

Restriction digest and ligation. In separate reactions, the dsDNA vector and the dsDNA insert were simultaneously digested with Acc65I and EagI for 2.5 h at 37 ˚C. The dsDNA insert was purified using a MinElute kit and eluted in molecular biology grade H_2O. The digested dsDNA vector was isolated by 0.8% agarose gel electrophoresis, purified using a Gel Purification kit, and eluted in molecular biology grade H_2O. Concentrations were quantified using NanoDrop. After, the vector and insert were ligated using T4 DNA ligase at a 1:100 vector:insert mole ratio for 1 h at room temperature.

Transformation. Plasmids were transformed into competent XL10-Gold ultracompetent cells according to the manufacturer's instructions with modifications. Briefly, transformations were performed using 50 μL of cells using LB broth, and cells were titered from 10^0-10^2 dilutions according to the New England BioLabs Ph.D. manual. The resulting plaques were used for

amplification and production of phage. Peptide sequences were confirmed by DNA sequencing (GENEWIZ).

3.2.17 Peptide Synthesis

Peptides with a C-terminal PEG-Biotin tag were synthesized using standard Fmoc solid phase peptide synthesis on a PS3 peptide synthesizer (Protein Technologies) using a Biotin-PEG NovaTag resin.

3.2.18 Peptide Flow Cytometry Binding Studies

For each binding study, 10^5 cells were incubated with 200 μM of peptide for 30 minutes at 4°C. Cells were washed three times and fixed with 4% paraformaldehyde for 15 minutes at 4°C. Cells were then washed once and probed with either Streptavidin-FITC or Streptavidin-PEcy7 and antibodies. Cells were analyzed on a BD Canto flow or Miltenyi MACSQuant cytometer.

3.3 Results

3.3.1 In Vitro Generated Human M1 and M2 Macrophages Exhibit Typical Immunophenotypes

For use in phage panning methods, human M1 and M2 macrophages were generated by isolating monocytes from human donor peripheral blood mononuclear cells, and differentiating into macrophages for 7 days. Activation of these human macrophages into M1 and M2 phenotypes was tested by flow cytometry immunophenotyping. All cells exhibited expression of the general macrophage markers CD68 and CD163 as expected (Figure 3.1). Human M1 macrophages also exhibited the expected higher expression of markers CD80, CD86 and HLA-DR, and M2 macrophages exhibited higher expression of CD206, CD71 and CD23 [19].

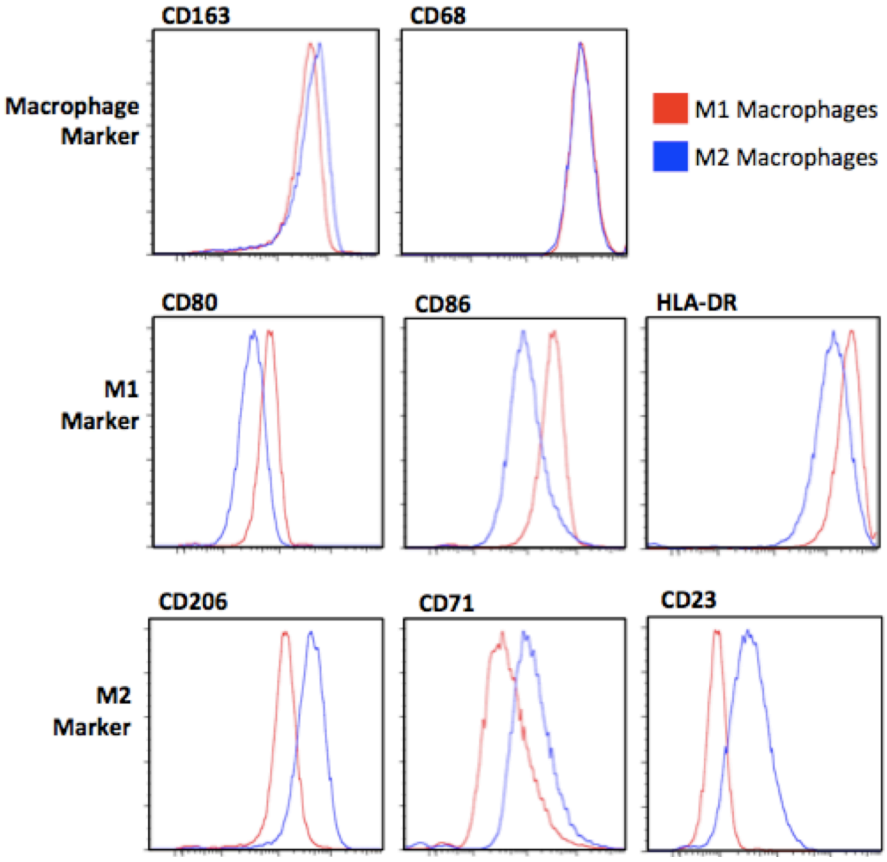

Figure 3.1: Immunophenotyping of human M1 and M2 macrophages derived from donor peripheral blood mononuclear cells. Histograms are representative of two experiments.

3.3.2 Biopanning in Cell Suspension with Glycine-HCl Elution Results in Potential Human M1 Binding Clone hM1pep and General Macrophage Binding Clone hMpep

Initially, biopanning against human M1 and M2 macrophages was performed using methods similar to those used to identify the murine M2 macrophage binding peptide, M2pep. Briefly, human M1 and M2 macrophages were generated from human peripheral blood monocytes. The PhD-C7 and PhD-12 libraries were panned against these cells, using cells of the opposite polarization as a subtractive pan. Target cell-bound phage were eluted using a low pH Glycine-HCl solution.

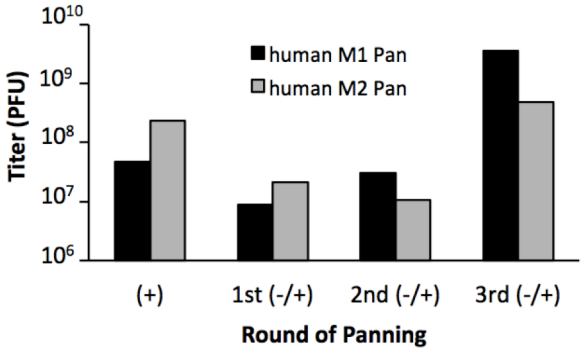

Figure 3.2: Titers for biopanning against human M1 and M2 macrophages increase in the third subtractive round.

Following each round of panning, eluted phage were titered and amplified. Following the first subtractive pan, phage titer in both the M1 and M2 pans decreased as is expected with the increased stringency of a subtractive step (Figure 3.2). In the subsequent second and third subtractive pans, M1-targeted panning resulted in increased titers each round, while M2-targeted panning only resulted in increased titer after the third subtractive pan. This increase in titers suggested that amplified phage libraries were becoming enriched with phage that exhibit preferential binding to their target, and thirty clones from each pan were sequenced (Figure 3.3).

Sequencing of human M1 pan clones yielded two consensus sequences, DLWSSYKWPTMN and DLFHGRAPWDD, which appeared 4/28 and 3/28 times, respectively. Sequencing of human M2 pan clones yielded no M2-specific consensus sequences. One sequence, SSDMFRFHPWFT, was observed in both pans, appearing in the M1 and M2 pans 18/28 and 21/30 times, respectively. DLWSSYKWPTMN and SSDMFRFHPWFT were named hM1p.1.1 and hMp.1, respectively, and tested for binding to human M1 and M2 macrophages.

hM1p.1.1, hMp.1 and a few other identified phage clones were tested via flow cytometry for binding to human M1 and M2 macrophages. hMp.1 phage bound strongly to both M1 and M2 macrophages while hM1p.1.1 phage bound slightly-preferentially to M1 macrophages (Figure 3.4). Most other clones tested lacked preferential binding to M1 or M2 macrophages.

hM1p Sequencing Results		
Clone ID	**Sequence**	**Frequency**
hMp.1	SSDMFRFHPWFT	18/28
hM1p.1.1	DLWSSYKWPTMN	4/28
hM1p.1.2	DLFMHGRAPWDD	3/28
hM1p.1.3	NWGLPWMVTPWR	2/28
	SLWDWFSQPITR	1/28

hM2p Sequencing Results		
Clone ID	**Sequence**	**Frequency**
hMp.1	SSDMFRFHPWFT	21/30
hM2p.1.1	SAITLLGHMLNL	1/30
hM2p.1.2	NTIIQSAAQNLL	1/30
	LMNNLTNTWYPL	1/30
	SPIIEPTFEWRS	1/30
	TTRNADSQPLWE	1/30
	DHYLAKSHPHSD	1/30
	YPMMTFHPHSSL	1/30
	YFENFTDLSWPD	1/30
	ACPWWQSWFC	1/30

Figure 3.3: Sequencing clones from the 3rd Subtractive Round of human M1 and M2 panning yield a potential human M1 binding peptide sequence and a potential general human macrophage binding sequence.

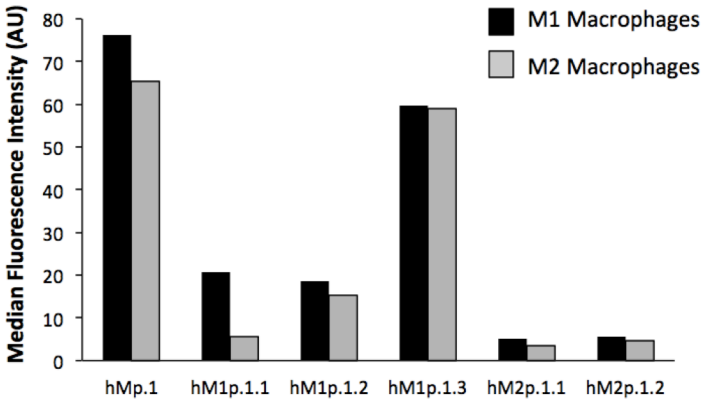

Figure 3.4: A flow cytometry binding study of phage clones identified from the third subtractive round of panning suggest that hM1p.1.1 is a human M1 macrophage-specific phage and that hMp.1 binds both types of polarized macrophages.

Due to its high binding to both M1 and M2 macrophages, the hMp.1 peptide sequence, and a scrambled version, MFFPTHRDSWSF, were synthesized with C-terminal PEG-Biotin tag and tested for binding to human M1 and M2 macrophages (Figure 3.5A). When the hMpep version of

the peptide did not exhibit binding to human M1 or M2 macrophages, an alternative version with five amino acids from the phage coat protein, EVTEA, added to the C-terminus was synthesized and named hexMpep. This extended form of the peptide also did not exhibit binding to either cell type (Figure 3.5B).

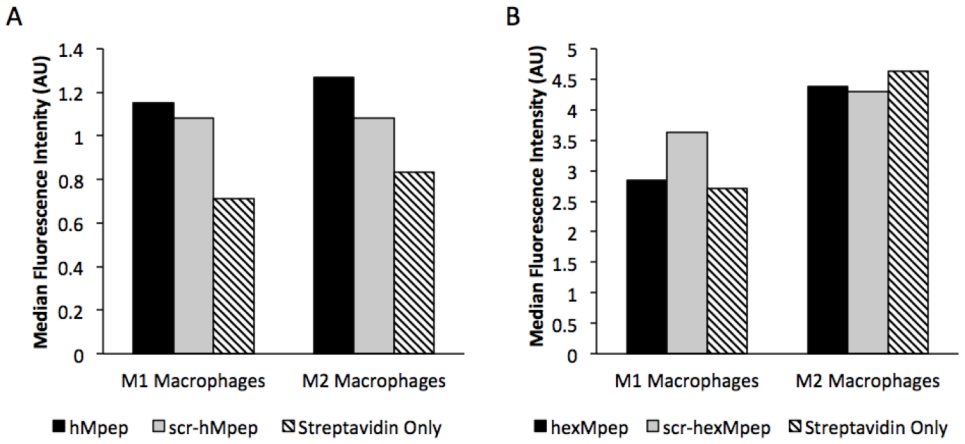

Figure 3.5: hMp.1 synthesized peptide sequence lacks binding to human M1 or M2 macrophages. (A) hMp.1 peptide sequence was synthesized with a C-terminal PEG-Biotin tag and termed hMpep. (B) The hMp.1 peptide sequence was synthesized with an additional C-terminal five amino acids, EVTEA, derived from the phage coat protein and termed hexM1pep.

Due to its preferential binding to human M1 macrophages, as shown in Figure 3.4, the hM1p.1.1 peptide sequence, and a scrambled version, TKSMYLSPDWNW, were synthesized with C-terminal PEG-Biotin tag and tested for binding to human M1 and M2 macrophages (Figure 3.6A). When the hM1pep version of the peptide did not exhibit binding to human M1 macrophages, an alternative version with 5 amino acids, EVTEA, from the phage coat protein added to the C-terminus was synthesized and named hexM1pep. This extended form of the peptide also did not exhibit binding to either cell type (Figure 3.6B).

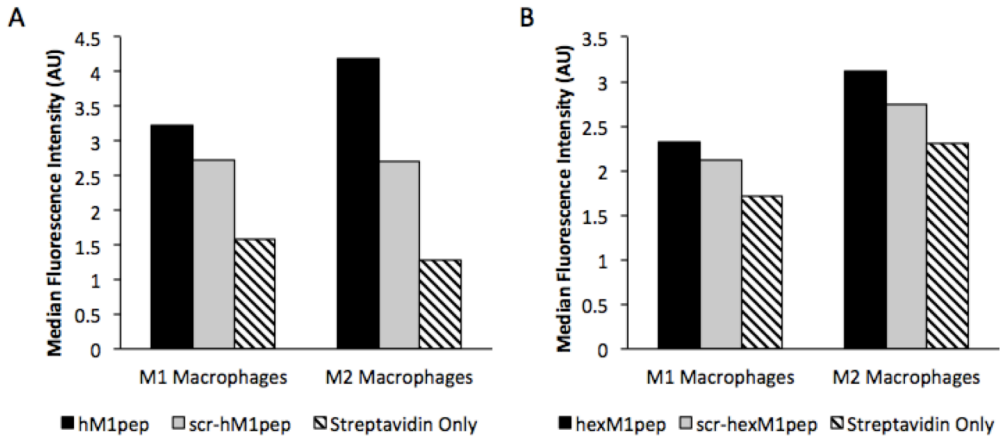

Figure 3.6: hM1p.1.1 synthesized peptide lacks preferential binding to human M1 macrophages. (A) hM1p.1.1 peptide sequence was synthesized with a C-terminal PEG-Biotin tag and termed hM1pep. (B) The hM1p.1.1 peptide sequence was synthesized with an additional C-terminal five amino acids, EVTEA, derived from the phage coat protein and termed hexM1pep.

3.3.3 Biopanning in Cell Suspension with Increased Stringency of Washes Yields No New Consensus Sequences

In a second attempt at panning for a human M2 macrophage binding peptide on cells in suspension, a similar method was employed and stringency increased by adding Tween 20 to the wash buffer. Tween 20 concentration was increased from 0.1% to 0.3% to 0.5% with each successive subtractive round of panning. Elution titers increased only in the third subtractive round of panning, suggesting that the amplified library from this round may be enriched with M2 macrophage binding phage (Figure 3.7A). Sequencing of 29 of the clones from the third subtractive round of panning yielded no new consensus sequences (Figure 3.7B). In addition, testing the binding of several of the clones from this pan via flow cytometry yielded no preferential M2 macrophage binding phage peptides (Figure 3.8).

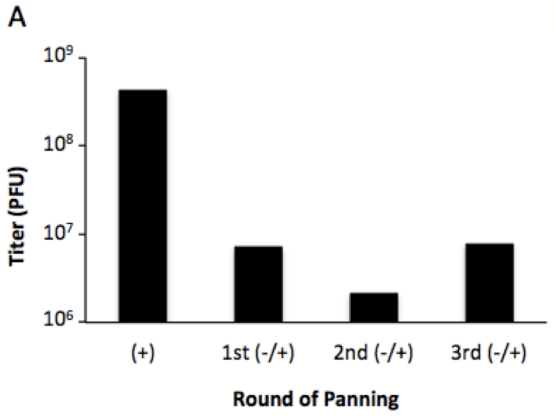

B

Clone ID	Sequence	Frequency
hM2p.2.1	YPISPSLVAHPV	1/29
hM2p.2.2	HTNSNFAALWER	2/29
hM2p.2.3	LPYAFDSYTPDS	1/29
hM2p.2.4	ACLPALPATC	1/29
hM2p.2.5	TTPRVNTFDVMA	1/29
hM2p.2.6	ACALAWPYTC	1/29
hM2p.2.7	GANANLMDRKEL	1/29
hMp.1	SSDMFRFHPWFT	21/29

Figure 3.7: Biopanning against human M2 Macrophages with increased stringency of washes results in no new consensus sequences.

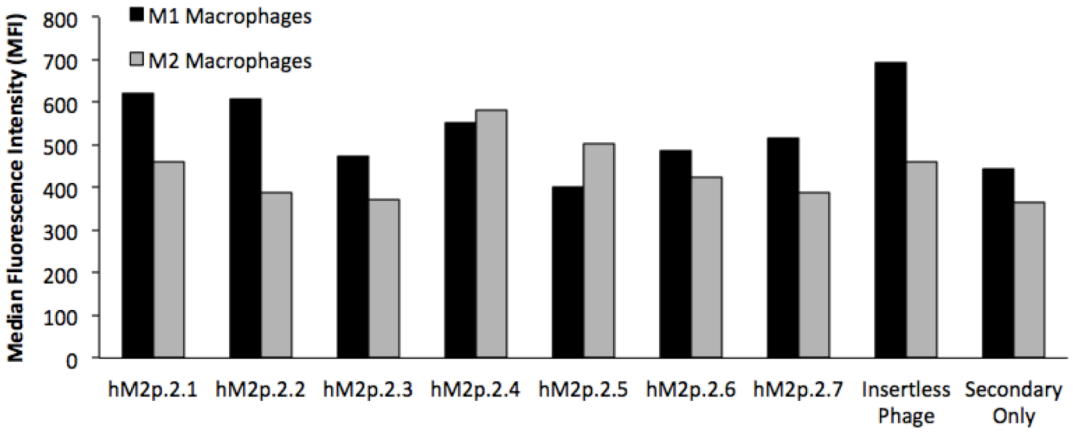

Figure 3.8: A flow cytometry binding study of phage clones identified from the third subtractive round of panning identifies no human M2 macrophage specific targeting peptides.

3.3.4 Biopanning of PhD-C7 Library in Cell Suspension with Double M1 Macrophage Subtraction Yields No New Consensus Sequences

In a third attempt at phage panning, increasing the stringency of the subtractive pan was employed. Briefly, the PhD-C7 library was applied to M1 macrophages twice as a double subtraction before being applied to M2 macrophages for the selective pan. The cyclic-7 library

was used in an attempt to select for peptides that would have better *in vivo* stability. Unfortunately, after both the third and fourth subtractive rounds of panning, no consensus sequences emerged (Figure 3.9). None of these peptides were consequently tested for binding.

3rd -/+	4th -/+
ACDWAARNTC	ACLPVHQPMC
ACSDYMPLLC	ACLKEFGRSC
ACPALGKTNC	ACTKNKDPFC
ACPLAADRVC	ACPNTPFLFC
ACSTRDNYEC	ACPYDWVFGC
ACDGHRHMHC	
ACYGSDMALC	
ACSSPVWPSC	
ACHVSKTPHC	
ACRTTATHSC	
ACPNLYMKFC	
ACSANISLVC	
ACLNYDLNLC	
ACMHVRSQQC	
ACSHQSLAVC	
ACSNTRWPMC	
ACWMSDLDHC	
ACSQSAYLMC	
ACNNSHWRLC	

Figure 3.9: Biopanning against human M2 macrophages using a double subtractive M1 macrophage pan to increase stringency yields no new M2-selective phage clones.

3.3.5 Biopanning on Adherent Cells with Glycine-HCl Elution Yields Two Potential Human M1 Macrophage Binding Phage but No Human M2 Macrophage Binding Phage

The three previous panning attempts used phage panned against cells in suspension. Following scraping of the human macrophages from the cell culture plate in these studies, significant cell death was observed via trypan blue staining and may have contributed to the lack of M2 macrophage-selective phage identified. To avoid causing significant cell death, panning was performed on adherent cells in this fourth attempt at biopanning. Briefly, for

human M2 macrophage binding phage selection, PhD-C7 and PhD-12 libraries were applied to human M1 macrophages cultured on a petri dish. Any unbound phage was then incubated with human M2 macrophages cultured on a petri dish. Adherent M2 macrophages were then washed five times, followed by phage elution with a low pH Glycine-HCl buffer, scraping of cells and eluted phage from the plate and freeze/thaw cycles to lyse cells that may have internalized phage. Panning to select for a human M1 macrophage selective phage was performed in parallel.

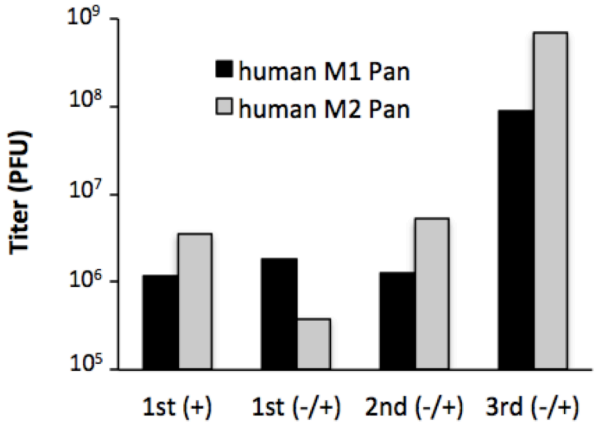

Figure 3.10: Titers for biopanning against human M1 and M2 macrophages increase in the third subtractive round.

As expected, panning for a human M2 macrophage binding peptide demonstrated a loss in phage titer between the initial positive pan and first subtractive pan, but then exhibited increasing titers with each subtractive round. Surprisingly, panning for a human M1 macrophage binding peptide demonstrated an increase in phage titer between the initial positive pan and the first subtractive pan, followed by a decrease in titer in the second subtractive and again an increase in titer in the third subtractive pan (Figure 3.10). The significant increase in titer after the third subtractive pan for both targets suggested library enrichment for target binding phage and phage clones from each library were sequenced.

Sequencing of clones from the third subtractive pan of the human M1 macrophage biopanning yielded two consensus sequences, AQSPFYFHPWFG AND AWYLPWLEGTRL, which

appeared 4/16 and 7/16 times, respectively (Figure 3.11). AWYLPWLEGTRL also appeared 1/18 times in the human M2 macrophage pan. Sequencing of clones from the human M2 macrophage pan yielded one consensus sequence, WNDLYLSSWFNP, which appeared 14/18 times. Due to its significant amplification in the third subtractive round of panning, the phM2.1 phage clone was tested for binding in a flow cytometry study, but did not demonstrate selective binding to human M2 macrophages (Figure 3.12).

phM1p Sequencing Results		
Clone ID	**Sequence**	**Frequency**
phM1.1	AQSPFYFHPWFG	4/16
phM1.2	AWYLPWLEGTRL	7/16 *
	ACNEPKPRLC	1/16
	GSAPLLTVDTSK	1/16
	ACDTSTKYLC	1/16
	AAKSGDLIWYGY	1/16
	ISWGSFAAWGYA	1/16

phM2p Sequencing Results		
Clone ID	**Sequence**	**Frequency**
phM2.1	WNDLYLSSWFNP	14/18 ↯
phM1.2	AWYLPWLEGTRL	1/18 *
	GASFQALNVSWE	1/18
	ACMNMALSSC	1/18
	SSILTPFRGVNN	1/18

Figure 3.11: Biopanning against adherent human M1 or M2 macrophages yields two human M1 macrophage consensus sequences and one human M2 macrophage consensus sequence. * appears in both the M1 and M2 pan. ↯ also appears in Figure 3.16 below.

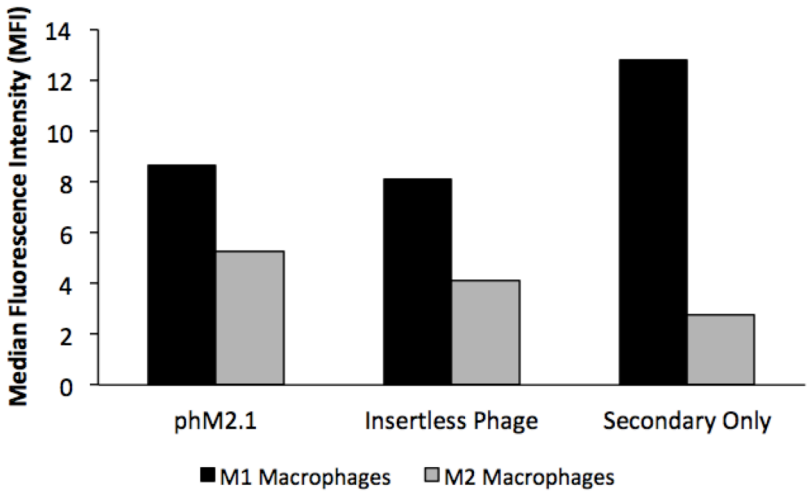

Figure 3.12: A flow cytometry binding study of phM2.1 phage clone identified from the third subtractive round of panning exhibits no selective binding to human M2 macrophages.

A flow cytometry binding study of the two human M1 macrophage phage clones, phM1.1 and phM1.2, demonstrated preferential binding of both clones to M1 macrophages over M2 macrophages. However, both phage clones also exhibited high binding to resting macrophages, though lower than the binding to M1 macrophages (Figure 3.13).

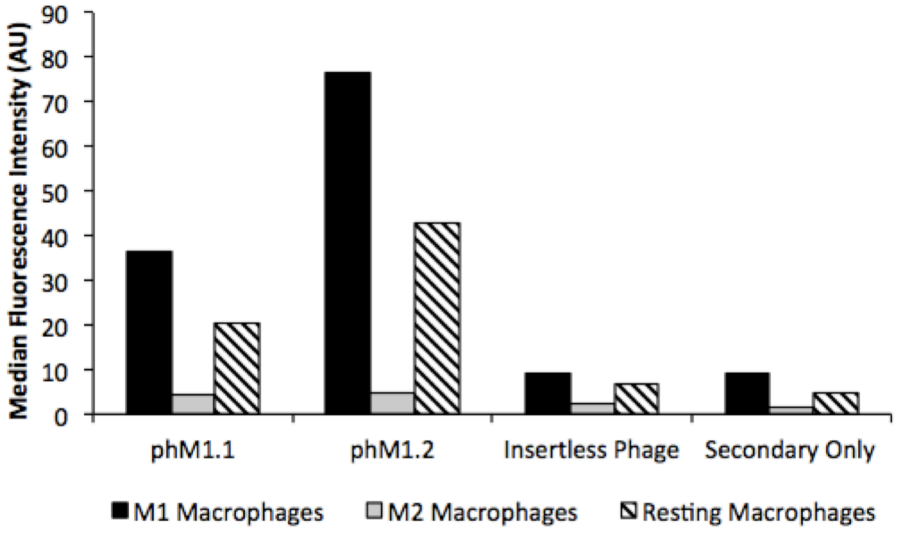

Figure 3.13: A flow cytometry binding study of phage clones identified from the third subtractive round of panning identifies two potential human M1 macrophage-selective phage.

The phM1.1 and phM1.2 clones appeared quite promising as selective human M1 macrophage binding peptide sequences, and their peptide form was synthesized with a C-terminal PEG-Biotin tag. A binding study of the phM1.1 and phM1.2 peptides exhibited no selective binding to human M1 macrophages (Figure 3.14A). To mimic the display of the peptide on the phage coat, five additional amino acids from the phage coat protein, EVTEA, were added to the C-terminus the peptide and synthesized with a C-terminal PEG-Biotin tag. A binding study of these pHexM1.1 and pHexM1.2 peptides exhibited no selective binding to human M1 macrophages (Figure 3.14B).

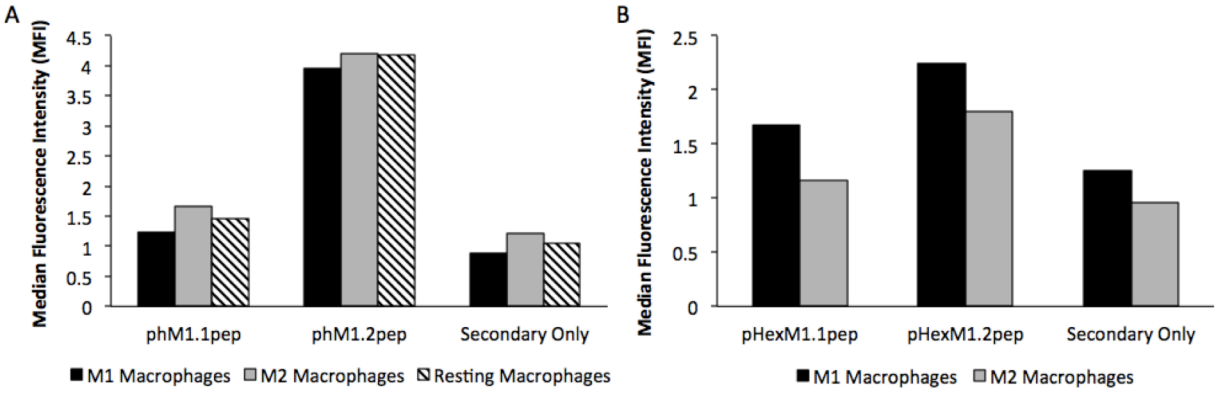

Figure 3.14: phM1p.1 and phM1.2 synthesized peptides lack preferential binding to human M1 macrophages. (A) phM1p.1 and phM1.2 peptides were synthesized with a C-terminal PEG-Biotin tag. (B) The phM1p.1 and phM1.2 peptide sequence was synthesized with an additional C-terminal five amino acids, EVTEA, derived from the phage coat protein and termed pHexM1.1pep and pHexM1.2pep.

3.3.6 Biopanning on Adherent Cells Using Intracellular and Extracellular Recovery Yields No New Human M1 or M2 Macrophage Binding Phage

A literature search for alternative panning methods identified a method utilized by Marks and colleagues to identify peptides that bind extracellularly to a target cell or become internalized by cells [20]. The goal of this fifth panning method tested was to identify phage clones that appear in both the extracellular pan (can bind target cells) and the intracellular pan (can be internalized after binding target). Furthermore, in an ideal method, the intracellular method of panning would eliminate the amplification of plastic binding phage. Briefly, two pans against human M2 macrophages with M1 subtraction were performed in parallel. In the pan to identify extracellularly bound phage, human M2 macrophage bound phage were eluted with a low pH Glycine-HCl buffer. In the pan to identify internalized phage, phage-bound human M2 macrophages were incubated for 30 minutes at 37˚C to facilitate internalization. Then any uninternalized phage were eluted from the cell surface using a low pH Glycine-HCl buffer, cells trypsinized and lifted from the plate, and then lysed in solution using a buffer containing triethylamine. As expected, both the extracellular and intracellular method of panning resulted in a decrease in phage titer between the initial positive pan and the first subtractive pan,

followed by increasing titers with each round of subtractive panning (Figure 3.15). Due to this increase in titer suggesting library enrichment for target binding phage, phage clones from the third subtractive round of each pan were sequenced.

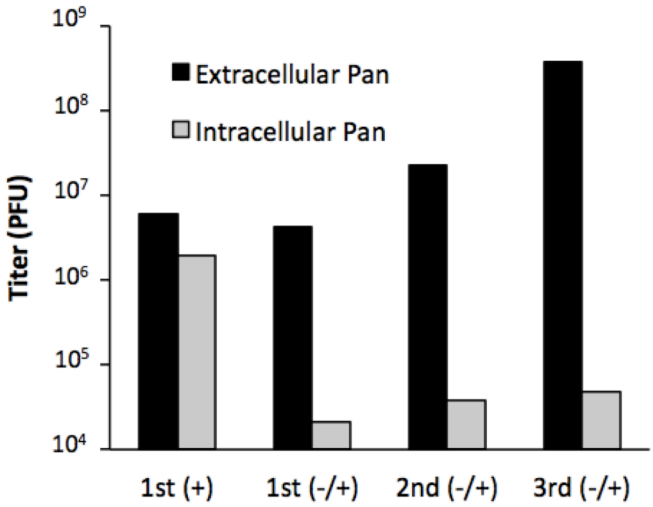

Figure 3.15: Titers for biopanning against human M2 macrophages to select for extracellularly bound or internalized phage increase with each subtractive round of panning.

Sequencing of phage clones from the third subtractive round of both the extracellular and intracellular pan did not yield any sequences in common between pans, but did identify consensus sequences (Figure 3.16). Sequencing of the extracellular pan identified one consensus sequence, WNDLYLSSWFNP, which appeared 13/18 times. This sequence is the same as phM2.1 identified in Section 3.3.5 that exhibited no selective binding to human M2 macrophages in phage form. Sequencing of the intracellular pan identified four consensus sequences, TSSTSINYVRFS, HPLTWNLRSSPA, YESMPRAGSHVA, AND VVSPDMNLLLTN, which appeared 3/13, 3/13, 2/13 and 2/13 times, respectively.

The four consensus phage clones identified via the intracellular panning method were selected for testing via a flow cytometry binding study. Unfortunately, none of the phage clones exhibited selective binding to human M2 macrophages over M1 macrophages (Figure 3.17).

ExHM2p Sequencing Results		
Clone ID	Sequence	Frequency
phM2.1	WNDLYLSSWFNP	13/18 ↯
	SPILGPWWGLPL	1/18
	AVWHLASPPVFA	1/18
	NPLPLNFSSPGT	1/18
	WVTDLHAYFSSI	1/18
	WPTDHQMLRIPM	1/18

InHM2pep Sequencing Results		
Clone ID	Sequence	Frequency
InHM2p.1	TSSTSINYVRFS	3/13
InHM2p.2	HPLTWNLRSSPA	3/13
InHM2p.3	YESMPRAGSHVA	2/13
InHM2p.4	VVSPDMNLLLTN	2/13
	HGAPHRINDAVE	1/13
	MSSSLEHRSTPF	1/13
	DRWVARDPASIF	1/13

Figure 3.16: Biopanning against adherent human M2 macrophages using an extracellular and intracellular pan yields five human M2 macrophage consensus sequences, but no common sequences between the two panning methods. ↯ also appears in Figure 3.11 above.

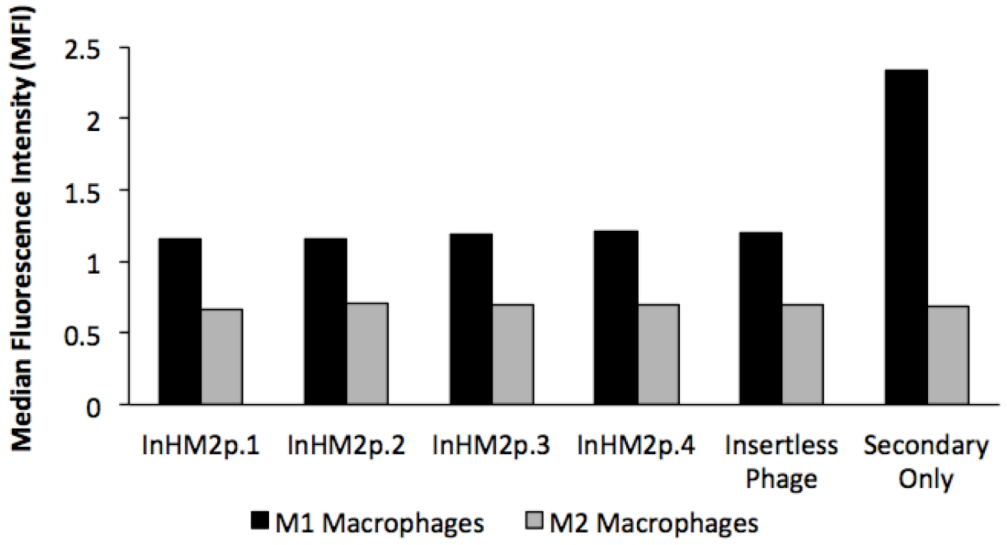

Figure 3.17: A flow cytometry binding study of phage clones identified from the third subtractive round of intracellular phage panning exhibits no selective binding to human M2 macrophages.

Because phM2.1 appeared for a second time in a separate panning method, the peptide form was synthesized with a PEG-Biotin tag and tested for binding, despite the lack of binding observed in its phage form (Figure 3.12). Unfortunately, phM2.1 peptide did not exhibit any binding to human M1 or M2 macrophages (Figure 3.18).

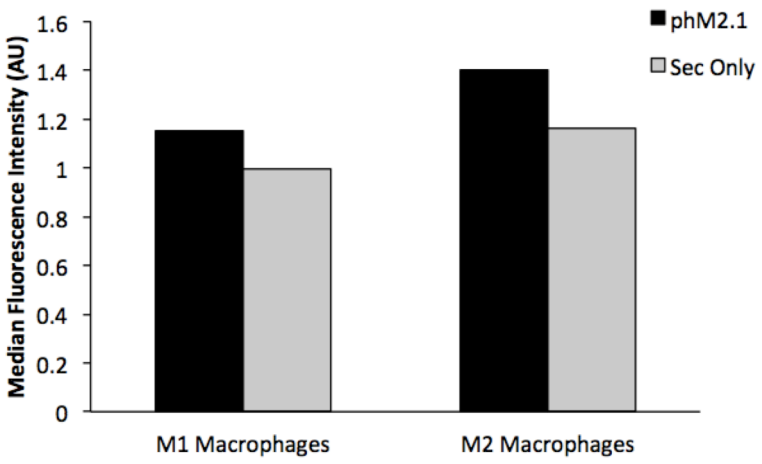

Figure 3.18: Flow cytometry binding study of the phM2.1 synthesized peptide with a C-terminal PEG-Biotin tag exhibits lack of binding to human M2 macrophages.

3.3.7 Biopanning on Adherent Cells Using Strong/Weak Elution Recovery Yields No New Human M1 or M2 Macrophage Binding Phage

Work by Baker and colleagues suggested that low pH Glycine-HCl elution may not be eluting strong preferential binding phage, resulting in amplification of weak cell binding phage or plastic binding phage [21]. Thus a method was employed to amplify only those phage that are strongly associated with M2 macrophages. Briefly, after subtractive pans on resting and M1 macrophages, phage weakly associated with M2 macrophages were eluted using a low pH Glycine-HCl buffer. Remaining strongly-bound phage were eluted by cell lysis and scraping from the culture plate. Both elutions were titered for analysis, but only the strongly bound phage elution was amplified for subsequent rounds of panning. Surprisingly, phage titers from both elutions increased between the initial positive pan and the first subtractive pan (Figure 3.19A). Furthermore, phage elution titers continued to decrease in the second and third subtractive rounds of panning. Despite this phage titer decrease, clones from the third subtractive pan were sequenced and yielded no consensus sequences (Figure 3.19B). In an attempt to further enrich the panning libraries, a fourth subtractive round of panning was performed. Both the

weak and strong elutions from this round of panning exhibited a drastic increase in titer, and phage clones were sequenced. Only one sequence, SGVYKVAYDWQH, appeared 2/12 times while all other sequences appeared only once.

A

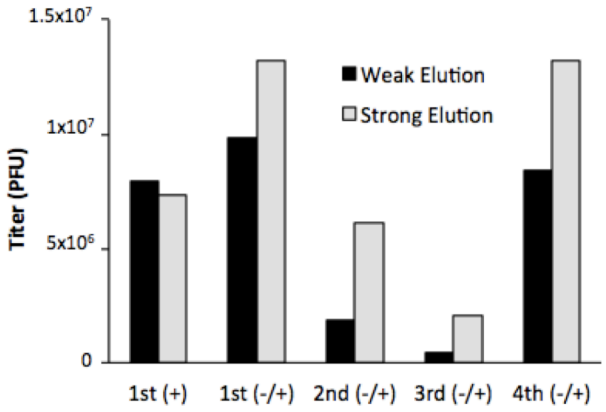

B

shM2p Sequencing Results	
3rd (-/+)	4th (-/+)
SGVYKVAYDWQH	SGVYKVAYDWQH (2/12)
MHPNAGHGSLMR	TVLWTPYPLAPH
NWYCDRCGPNYV	VAARTGEIYVPW
SYGAMITSPMMK	MASVVESTPGHG
NYTVLGALPRYG	SNSWNTNEQRFG
HNPDYFHKGMSV	AAHAPNLMSTVN
SMGPNTSYSLAH	ADLPWSWYPAIN
ADIPRNLGARTN	MDARSWVTNGPA
DINYWRSARGMV	NNLNNTPLRFSS
SGASGTGHWSTL	YPISVTTKFYAM
SSPLSIASEGLN	NDSHVWSTMRAV
VAARTGEIYVPW	
QCFNSVCLHTNP	
MGSNFPLPTSVF	

Figure 3.19: Biopanning against adherent human M2 macrophages using a strong binding selection method yields no new M2 macrophage selective phage candidates. (A) Phage elution titers do not increase until a fourth subtractive round of panning. (B) Sequencing of clones from the third and fourth subtractive rounds of panning yield no new consensus sequences.

To determine if any phage clones identified in the third or fourth round of subtractive panning should be individually tested for human M2 macrophage binding, whole libraries from each round of panning were tested for binding to human M1 and M2 macrophages. An increase in binding of the whole library to human M2 macrophages would suggest enrichment of specific M2 macrophage-binding phage in the library. Unfortunately, libraries from each round of panning appear to have the same, low level binding to both human M1 and M2 macrophages (Figure 3.20).

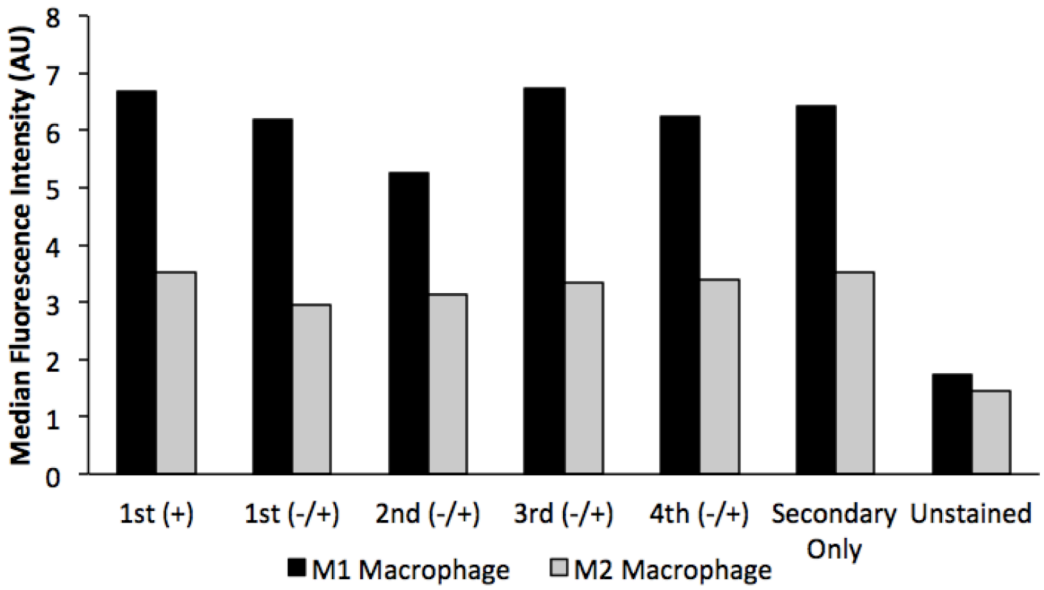

Figure 3.20: Phage libraries from each round of panning exhibit low binding to human M2 macrophages, suggesting lack of enrichment of M2 macrophage-specific phage clones.

3.3.8 Analyzing Enriched Intracellular, Extracellular and Strong Panning Libraries via Next Generation Sequencing Yields No Human M2 Macrophage Selective Phage Clones

Given the lack of M2 macrophage selective sequences identified through sequencing of just a few dozen phage clones, the third subtractive round of panning from the extracellular (Section 3.3.6), intracellular (Section 3.3.6), and strong binding (Section 3.3.7) panning methods were submitted for next generation sequencing. A four times amplified PhD-12 library was also submitted and provided a reference for identifying phage clones that are preferentially amplified by bacteria. While the next generation sequencing returned a list of thousands of peptide sequences, restricting the list to those peptides that were present in all three panning methods, shortened the list to 88 candidates. Increasing the stringency of the filter to require a two-fold enrichment in the peptide sequence when compared to the four-times amplified library reduced the candidate list to 39, and eliminating sequences commonly associated with plastic plate binding further reduced the list to 26 candidates. These 26 candidates where then analyzed for their enrichment value in each pan as well as the presence of other peptide sequences identified in the next generation sequencing that also contained similar amino acid

motifs. Using this method, four clones (YVPD, VSNL, TELH, and VARD) were selected for testing (Figure 3.21A). In the event that requiring a sequence to appear in all three pans was too stringent, a similar filter was used that looked separately at each panning method results for peptide sequences that exhibited a ten-fold or higher enrichment over the four times amplified library. Using this filter, two more sequences (SFR and SVN) were selected for testing. Selected peptide sequences were cloned into phage and tested for binding to human M1 and M2 macrophages. Unfortunately, none of the six clones tested exhibited binding to human M2 macrophages (Figure 3.21B).

A

Next Generation Sequencing Candidates	
Clone ID	**Sequence**
YVPD	SGRYVPDEHLYT
VSNL	AVSNLQILHRNA
TELH	IEGRGAFTELHV
VARD	DRWVARDPASIF
SFR	SFRHIDLSGSIH
SVN	SVNHLYLDRSQA

B

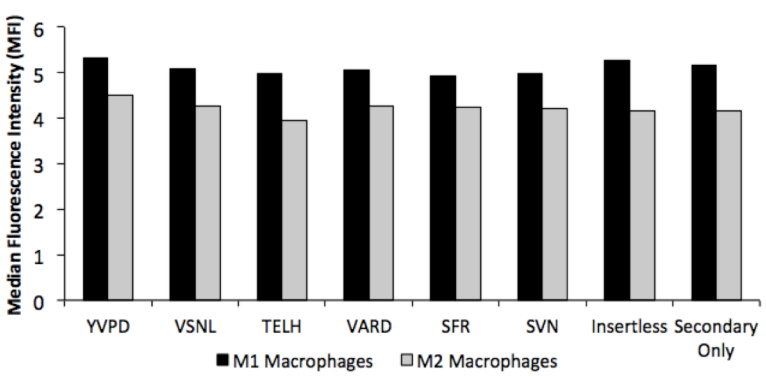

Figure 3.21: Third round subtractive pan libraries from the intracellular, extracellular and strong binding panning methods were submitted for next generation sequencing and six candidates identified for testing. (A) Candidate peptide sequences and their ID. (B) Binding study using phage-displayed peptides demonstrates that no sequence has preferential binding to human M2 macrophages.

3.3.9 Biopanning on Immobilized Legumain and PD-L1 Using Glycine-HCl Elution Yields No Protein-Specific Binding Phage

Whole cell phage display is challenging due to the heterogeneity of proteins on the cell surface, while panning against immobilized proteins is typically more successful due a homogenous target population. After several unsuccessful attempts at whole cell phage display to identify a human M2 macrophage specific binding peptide, biopanning against immobilized legumain and PD-L1 protein was employed. These proteins were selected as panning targets due to their expression on tumor-associated macrophages and role tumor progression (Sections 3.1.2 and 3.1.3). Briefly, his-tagged legumain or PD-L1 were bound to nickel-coated 96-well

plates. Then PhD-C7 and PhD-12 phage libraries were incubated with target protein, using Poly-His coated wells as subtractive pans. As expected, the elution titer between the initial positive legumain pan and the first subtractive round of panning decreased, while then elution titer increased with each subsequent subtractive round of panning (Figure 3.22). Surprisingly, there was a large increase in titer between the initial PD-L1 positive pan and the first subtractive pan. Concerned that unbound nickel coated on the plates may be enriching the libraries for histidine-containing peptides, the third subtractive round of legumain panning and the second and third subtractive rounds of PD-L1 panning also contained an additional subtractive step with uncoated plates. This additional subtractive step may explain the decrease in phage titer between the first and second subtractive PD-L1 pan.

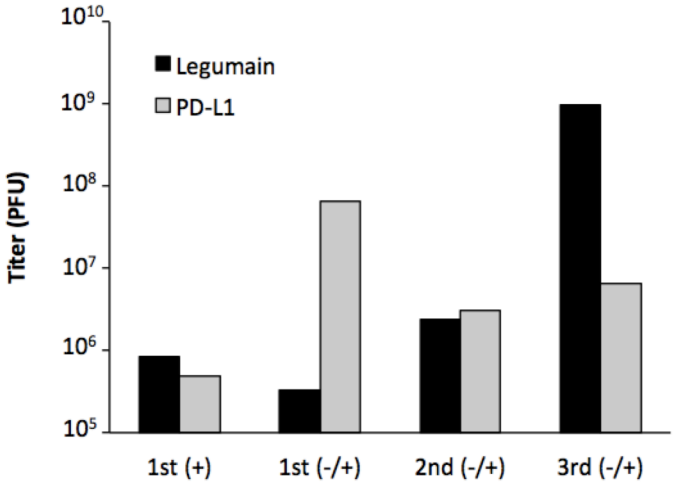

Figure 3.22: Phage elution titers following each round of panning against immobilized legumain or PD-L1 protein.

Phage clones from the third subtractive round of the legumain and PD-L1 pans were sequenced (Figure 3.23). Sequencing phage clones from the legumain pan identified one consensus sequence, HYEYTRLKHDSV, which appeared 8/20 times. Sequencing of phage clones from the PD-L1 pan identified one consensus sequence, SAGTNQQSTSRV, which appeared 4/19 times. Both pans identified clone VHWDFRQWWQPS, which also appeared in the sequencing

results of other panning attempts in the laboratory at the time, suggesting that it was a contaminant in the stocks of phage libraries.

HYEYTRLKHDSV (Leg01) and SAGTNQQSTSRV (PD-L1-01) phage were selected to test for binding to immobilized legumain and PD-L1 protein in an ELISA assay. In these assays, Leg01 unexpectedly exhibited higher binding to PD-L1 than legumain, but also exhibited high background binding to the uncoated nickel plate (Figure 3.24A). PD-L1-01 also exhibited high background binding to the nickel plate, indicating that neither phage clone candidate is promising as a selective binding peptide sequence (Figure 3.24B).

Legumain Sequencing Results

Clone ID	Sequence	Frequency
Leg01	HYEYTRLKHDSV	8/20
Contaminant	VHWDFRQWWQPS	2/20
	NRETDFELSVSH	1/20
	ACVQMPAHSC	1/20
	SPSHQRYQAETR	1/20
	LAGSVPAPTGLA	1/20
	RDKSAGTTDLKK	1/20
	GYSWWPSVWAWA	1/20
	HRSPSYHPDTYT	1/20
	ADWYHWRSHSSS	1/20
	STSHWYTNAIDG	1/20
	HKIPYSPSPIKL	1/20

PD-L1 Sequencing Results

Clone ID	Sequence	Frequency
PD-L1-01	SAGTNQQSTSRV	4/19
Contaminant	VHWDFRQWWQPS	7/19
	NSDAMRLMFFGY	2/19
	DKISRNQRPELP	2/19
	HGTHRPPHYSHL	1/19
	FMNGATFSRNRS	1/19
	FFPLTFPWTYYD	1/19
	NMNPILMERPIT	1/19

Figure 3.23: Sequencing of phage clones from the third subtractive round of panning yields one legumain consensus sequence, one PD-L1 consensus sequence and a contaminant sequence that appeared in the sequencing results of other panning attempts in the laboratory.

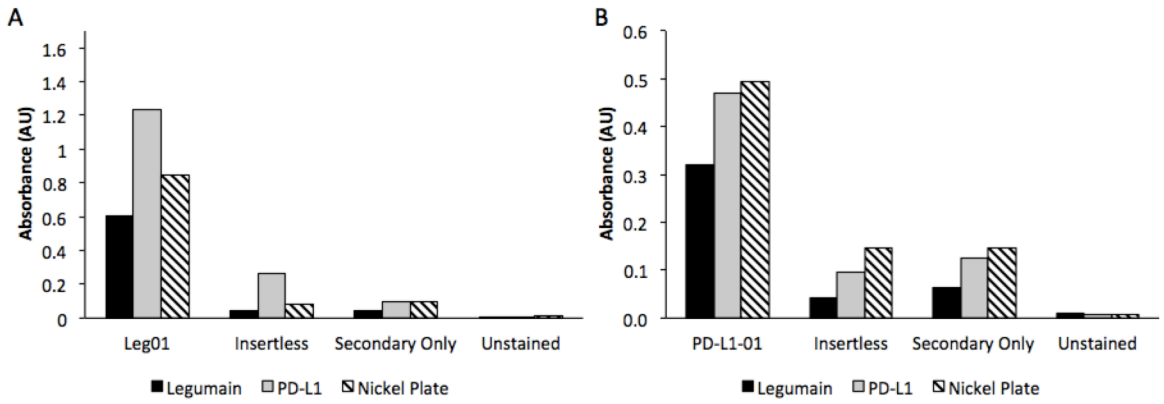

Figure 3.24: ELISA binding assay of (A) Leg01 and (B) PD-L1-01 phage binding to immobilized legumain or PD-L1 protein show lack of binding of either phage candidate.

3.3.10 Biopanning on Immobilized Legumain and PD-L1 Using Imidazole Elution Yields No Protein-Specific Binding Phage

Concerned that low pH Glycine-HCl elution was resulting in amplification of low affinity or plastic binding peptides, an imidazole elution technique was used in five rounds of panning. Briefly, high concentration of imidazole is able to elute His-tagged protein bound to nickel. Thus, following incubation with phage library, 300 mM imidazole was used to elute protein bound to the plate, which is bound by phage. These phage were then amplified for several rounds of selection. As expected, phage elution titers decreased between the initial positive pan and the first subtractive round of panning (Figure 3.25). As expected, legumain phage elution titers increased in the third round of subtractive panning, though this increase in titer was small. Surprisingly, PD-L1 phage elution titers decreased in the third subtractive round of panning, despite increasing after the second subtractive round of panning.

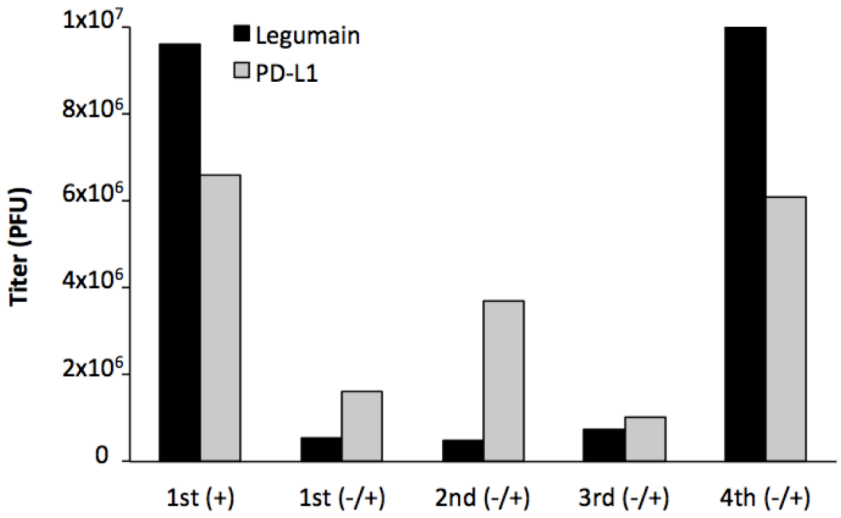

Figure 3.25: Phage elution titers of imidazole elution phage panning against legumain and PD-L1 increase in the fourth subtractive round of panning.

Despite the low phage elution titers in the third subtractive round of panning, phage clones were sequenced for the legumain and PD-L1 pan (Figure 3.26). Sequencing of legumain libraries identified one clone, RTAQLDRPMLDE, that appeared 4/16 times in the third subtractive round of panning. Sequencing of PD-L1 libraries identified no new consensus sequences. Because no PD-L1 consensus sequences were identified, a fourth subtractive round of panning was performed on both legumain and PD-L1. Phage elution titers following this fourth subtractive round of panning increased for both legumain and PD-L1 (Figure 3.25). Sequencing phage from the fourth subtractive round of panning confirmed the third subtractive round legumain consensus sequence which now appeared 13/19 times, and also identified a PD-L1 consensus sequence, LDWHALWHQTVL, which appeared 5/19 in the PD-L1 pan and 1/19 times in the legumain pan (Figure 3.27).

Legumain 3rd -/+ Sequencing Results		
Clone ID	Sequence	Frequency
Leg 11	RTAQLDRPMLDE	4/16
	ALWPTFPFWWMS	1/16
	ACHPNPKLSC	1/16
	HYPWPWLQHWVT	1/16
	WPYSLQWFWPNV	1/16
	HFWWHPHHVLA	1/16
	ACHEVHANKC	1/16
	HFPWDMWLSRTP	1/16
	SPWLQSWFWPFK	1/16
	LDWHALWHQTVL	1/16
	HWNLSPFLFHFN	1/16
	ACPLADNQKC	1/16
	SWYHPRSLYFDV	1/16

PD-L1 3rd -/+ Sequencing Results		
Clone ID	Sequence	Frequency
	RKQHAIPLIWPA	2/18
	HWHTPAWWSFFA	2/18
Contaminant	VHWDFRQWWQPS	1/18
	ACENKHTWGC	1/18
	VDTVKHSHGLTR	1/18
	TTMDQPGFWSYR	1/18
	MPWNWFDIQATA	1/18
	ACNHHAWNAC	1/18
	VFPFTYSYTYPR	1/18
	HWSIWLGNPHLH	1/18
	ACHNSTGFGC	1/18
	SPFNRFMVSSTY	1/18
	FPSFWNSWFGQP	1/18
	STHLQLKIEPIP	1/18
	HSQGILGSKSAF	1/18
	ITITVLPMGLTY	1/18

Figure 3.26: Sequencing of phage clones from the third subtractive round of panning yields one legumain consensus sequence and no new PD-L1 consensus sequences.

Legumain 4th -/+ Sequencing		
Clone ID	Sequence	Frequency
Leg 11	RTAQLDRPMLDE	13/19
	ALWPTFPFWWMS	2/19
PD-L1-11	LDWHALWHQTVL	1/19
	SNWANAMRSWWW	1/19
	WPYSLQWFWPNV	1/19
	WDFRSPWHYFYL	1/19

PD-L1 4th -/+ Sequencing Results		
Clone ID	Sequence	Frequency
PD-L1-11	LDWHALWHQTVL	5/19
Contaminant	VHWDFRQWWQPS	4/19
	HWTWWLGVPFHG	1/19
	GLHTSATNLYLH	1/19
	WPYSWDMYLKLF	1/19
	YNWGPWVWWAGQ	1/19
	ACNAGHLSQC	1/19
	HWYQWFQMNQYF	1/19
	GFGFGAWLTTLR	1/19
	ACPVVLGQKC	1/19
	HCEXFGYWFSPC	1/19
	HWHTPAWWSFFA	1/19

Figure 3.27: Sequencing of phage clones from the fourth subtractive round of panning identifies the same legumain consensus sequence and one new PD-L1 consensus sequence.

RTAQLDRPMLDE (Leg11) and LDWHALWHQTVL (PD-L1-11) were then selected to test for binding to immobilized legumain and PD-L1 in an ELISA assay (Figure 3.28). Both Leg11 and PD-L1-11 exhibited high background binding to the uncoated nickel plate, suggesting that neither are legumain or PD-L1 selective binding phage clones.

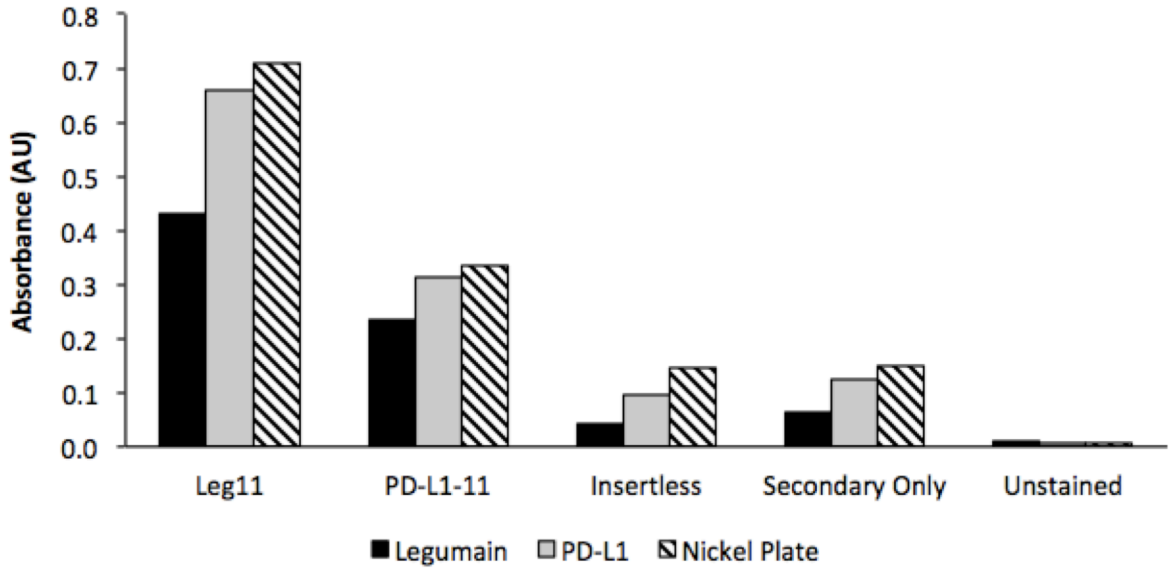

Figure 3.28: ELISA binding assay of Leg11 and PD-L1-11 phage binding to immobilized legumain or PD-L1 protein show lack of binding of either phage candidate.

3.4 Discussion

Whole cell panning as a method to identify cell-specific targeting agents is challenging due to the heterogeneity of proteins on the surface of cells. Despite these challenges, whole-cell panning has successfully been used to identify peptides that target cells [21-23]. In this work, whole cell panning was particularly difficult because differences between M1 or M2 polarized human macrophages may be quite subtle, compared to, for example, the large scale changes in protein expression observed in cancer cells compared to healthy cells. Thus, it is not surprising that identification of a human M2 macrophage specific targeting peptide remains elusive. Work

towards identification of a human M2 macrophage or tumor-associated macrophage targeting agent is ongoing in the laboratory. Additional panning methods that may be employed to identify an M2-targeting moiety are discussed here.

In this work to date, whole cell panning has been performed using human M1 and M2 macrophages derived from PBMCs from human donors. While using these cells may provide a reproducible set of target proteins for each round of panning, they do not exactly reflect the phenotype of our target cells for therapeutic applications: tumor-associated macrophages. Thus biopanning against TAMs isolated from human tumor biopsies may yield more disease-specific targeting peptides. Currently, the lab is authorized to receive tumor biopsies from ovarian cancer patients. These tumors may be dissociated with a collagenase cocktail and tumor-associated macrophages isolated using anti-CSF1R and anti-CCR2 antibodies. These cells can then be used as the selective target cell type while MD cells, a human macrophage cell line, can be used as a negative selection step to remove general macrophage binding phage. This panning method may yield additional protein targets that were not present on the *in vitro* generated M2 macrophages that could have been responsible for the failure to identify a targeting peptide.

There are also additional ways to improve the panning strategies against known proteins legumain and PD-L1. Panning against a known protein target offers the opportunity to conduct mirror phage display, which results in identification of targeting peptides made of D-amino acids that are more resistant to peptidase degradation *in vivo*. Mirror phage display is a technique in which phage-displayed peptides that are made up of L-amino acids, are panned against a protein that has been synthesized using D-amino acids. Because of the mirroring properties of D-amino acids, a peptide identified via mirror phage display that is synthesized using D-amino acids will bind its target synthesized with the naturally, occurring L-amino acids [24, 25]. In addition to the use of mirror phage display, different immobilization methods can be used to secure the protein panning target. In this current work, His-tagged protein was immobilized to nickel coated plates. In initial rounds of panning it was discovered that peptides containing histidines were being preferentially selected, and phage clone candidates later tested often had high background binding to the nickel coated plate. These results suggest that use of

nickel coated plates added to the selective pressure for nickel or plastic binding phage rather than target protein selective phage. Immobilizing protein on nickel-coated magnetic beads may decrease this background binding.

Lastly, peptide phage display has been the primary tool for identifying peptides selective for human M2 macrophages in this work. However, other targeting moieties, like aptamers, have shown promise as targeting agents in the literature. Aptamers are attractive targeting agents because their rounds of selection can be done entirely *in vitro* for ease of use, they bind their target in the nanomolar to picomolar range, and they can accommodate a variety of chemical modifications for functionalization [26]. Furthermore, the diversity of an aptamer library can be five to six orders of magnitude greater than the diversity of a phage library, providing additional components in the library that may bind cells of interest. As others in the lab have begun to optimize aptamer selection methods for other therapeutic targets, aptamers represent a new avenue for the development of a human M2 macrophage targeting moiety for this work.

3.5 Acknowledgements

Thank you to Brynn Livesay for further characterizing the synthesized peptide form of hMp. Thank you to Jonathan Yu for conducting plate panning against human M1 and M2 macrophages as well as panning against immobilized Legumain and PD-L1 proteins. Jonathan Yu also synthesized hM1pep, phM1.1pep, phM1.2pep, pHexM1.1pep, and pHexM1.2pep peptides. Thank you to Gary Liu, Brynn Livesay and Emi Lutz for optimizing the next generation sequencing submission protocol. Thank you to Nataly Kacherovsky for cloning the next generation sequencing candidate sequences into phage.

3.6 References

1. Bronte V, Murray PJ (2015) Understanding local macrophage phenotypes in disease: modulating macrophage function to treat cancer. Nat Med 21:117–119. doi: 10.1038/nm.3794

2. Mantovani A, Allavena P (2015) The interaction of anticancer therapies with tumor-associated macrophages. J Exp Med 212:435–445. doi: 10.1158/1078-0432.CCR-10-1343

3. Sandhu SK, Papadopoulos K, Fong PC, et al. (2013) A first-in-human, first-in-class, phase I study of carlumab (CNTO 888), a human monoclonal antibody against CC-chemokine ligand 2 in patients with solid tumors. Cancer Chemother Pharmacol 71:1041–1050. doi: 10.1007/s00280-013-2099-8

4. Brana I, Calles A, LoRusso PM, et al. (2015) Carlumab, an anti-C-C chemokine ligand 2 monoclonal antibody, in combination with four chemotherapy regimens for the treatment of patients with solid tumors: an open-label, multicenter phase 1b study. Target Oncol 10:111–123. doi: 10.1007/s11523-014-0320-2

5. Ries CH, Cannarile MA, Hoves S, et al. (2014) Targeting Tumor-Associated Macrophages with Anti-CSF-1R Antibody Reveals a Strategy for Cancer Therapy. Cancer Cell 25:846–859. doi: 10.1016/j.ccr.2014.05.016

6. Pujade-Lauraine E, Guastalla JP, Colombo N, et al. (1996) Intraperitoneal recombinant interferon gamma in ovarian cancer patients with residual disease at second-look laparotomy. J Clin Oncol 14:343–350.

7. Beatty GL, Chiorean EG, Fishman MP, et al. (2011) CD40 agonists alter tumor stroma and show efficacy against pancreatic carcinoma in mice and humans. Science 331:1612–1616. doi: 10.1126/science.1198443

8. Chen JM, Dando PM, Rawlings ND, et al. (1997) Cloning, isolation, and characterization of mammalian legumain, an asparaginyl endopeptidase. J Biol Chem 272:8090–8098.

9. Liu C, Sun C, Huang H, et al. (2003) Overexpression of legumain in tumors is significant for invasion/metastasis and a candidate enzymatic target for prodrug therapy. Cancer Research 63:2957–2964.

10. Luo Y, Zhou H, Krueger J, et al. (2006) Targeting tumor-associated macrophages as a novel strategy against breast cancer. J Clin Invest 116:2132–2141. doi: 10.1172/JCI27648

11. Yan L, Gao Y, Pierce R, et al. (2014) Development of Y-shaped peptide for constructing nanoparticle systems targeting tumor-associated macrophages in vitro and in vivo. Materials Research Express 1–15. doi: 10.1088/2053-1591/1/2/025007

12. Murthy RV, Arbman G, Gao J, et al. (2005) Legumain expression in relation to clinicopathologic and biological variables in colorectal cancer. Clinical Cancer Research : an official journal of the American Association for Cancer Research 11:2293–2299. doi: 10.1158/1078-0432.CCR-04-1642

13. Butte MJ, Peña-Cruz V, Kim M-J, et al. (2008) Interaction of human PD-L1 and B7-1. Molecular Immunology 45:3567–3572. doi: 10.1016/j.molimm.2008.05.014

14. Soliman H, Khalil F, Antonia S (2014) PD-L1 expression is increased in a subset of basal type breast cancer cells. PLoS ONE 9:e88557. doi: 10.1371/journal.pone.0088557

15. Shi F, Shi M, Zeng Z, et al. (2010) PD-1 and PD-L1 upregulation promotes CD8+ T-cell apoptosis and postoperative recurrence in hepatocellular carcinoma patients. Int J Cancer 128:887–896. doi: 10.1002/ijc.25397

16. Rodríguez-García M, Porichis F, de Jong OG, et al. (2011) Expression of PD-L1 and PD-L2 on human macrophages is up-regulated by HIV-1 and differentially modulated by IL-10. J Leukoc Biol 89:507–515. doi: 10.1189/jlb.0610327

17. Franceschini D, Paroli M, Francavilla V, et al. (2009) PD-L1 negatively regulates CD4+CD25+Foxp3+ Tregs by limiting STAT-5 phosphorylation in patients chronically infected with HCV. J Clin Invest 119:551–564. doi: 10.1172/JCI36604

18. 't Hoen PAC, Jirka SMG, Broeke Ten BR, et al. (2012) Phage display screening without repetitious selection rounds. Anal Biochem 421:622–631. doi: 10.1016/j.ab.2011.11.005

19. Rey-Giraud F, Hafner M, Ries CH (2012) In Vitro Generation of Monocyte-Derived Macrophages under Serum-Free Conditions Improves Their Tumor Promoting Functions. PLoS ONE 7:e42656. doi: 10.1371/journal.pone.0042656

20. Heitner T, Moor A, Garrison JL, et al. (2001) Selection of cell binding and internalizing epidermal growth factor receptor antibodies from a phage display library. J Immunol Methods 248:17–30.

21. Nicklin SA, White SJ, Watkins SJ, et al. (2000) Selective targeting of gene transfer to vascular endothelial cells by use of peptides isolated by phage display. Circulation 102:231–237.

22. Li M, Anastassiades CP, Joshi B, et al. (2010) Affinity peptide for targeted detection of dysplasia in Barrett's esophagus. Gastroenterology 139:1472–1480. doi: 10.1053/j.gastro.2010.07.007

23. McGuire MJ, Samli KN, Johnston SA, Brown KC (2004) In vitro selection of a peptide with high selectivity for cardiomyocytes in vivo. J Mol Biol 342:171–182. doi: 10.1016/j.jmb.2004.06.029

24. Schumacher TNM, Mayr LM, Minor DL, et al. (1996) Identification of D-Peptide Ligands Through Mirror-Image Phage Display. Science 271:1854–1857. doi: 10.1126/science.271.5257.1854

25. Wiesehan K, Willbold D (2003) Mirror-image Phage Display: Aiming at the Mirror. Chem Eur J of Chem Bio 4:811–815. doi: 10.1002/cbic.200300570

26. Nimjee SM, Rusconi CP, Sullenger BA (2005) Aptamers: An Emerging Class of Therapeutics. Annu Rev Med 56:555–583. doi: 10.1146/annurev.med.56.062904.144915

Chapter 4

MAJOR FINDINGS AND FUTURE DIRECTIONS

Abstract

This final section summarizes the major findings of this thesis work and presents two proposed research projects as follow-up work to these findings.

4.1 Summary of Major Findings

4.1.1 Identification of M2pep Murine M2 Macrophage Targeting Ligand

Prior to this work, there existed no peptide targeting ligands able to specifically target M2 macrophages. This work utilized peptide-phage display to identify M2pep, which specifically binds and is internalized by murine bone marrow derived M2 macrophages. This peptide was also shown to retain specific binding to M2 macrophages in mixed populations of cells, demonstrating its potential utility in targeting therapeutic cargo. This work has motivated the use of whole-cell phage display to identify physiologically relevant targeting peptides.

4.1.2 Modest Depletion of TAMs in a Tumor-bearing Mouse Model

M2pep was shown to also bind tumor-associated macrophages isolated from mice bearing CT-26 colon carcinoma tumors. This crossover in binding to a therapeutically relevant cell type suggests the future use of model cells, like the *in vitro*-generated M2 macrophages, to identify targeting ligands that bind in diseased tissues. Fluorescently labeled M2pep was also shown to preferentially accumulate within TAMs in tumors. Fusing the pro-apoptotic KLA peptide sequence to the M2pep targeting peptide resulted in selective depletion of TAMs *in vivo,* as well as improved survival and delay of tumor growth in these mice. While depletion of TAMs appeared promising, there were no statistically significant changes in tumor-infiltrating T cell populations or the state of CD8+ T cell exhaustion within the tumors at the treatment time points tested. The ability of M2pepKLA to deplete TAMs and improve outcomes in mice provides rationale for the identification of a similar M2 macrophage targeting peptide for human macrophages. In addition, the modest TAM depletion observed suggests that alternative therapeutic cargo for M2pep delivery should be investigated.

4.1.3 Human M2 Macrophage Targeting Ligand Remains Elusive

A variety of whole-cell phage display techniques, similar to those used to identify murine M2pep, were used to identify a human M2pep targeting peptide. These whole-cell panning methods included protocols to isolate phage peptides that are bound extracellularly or intracelluarly, or exhibit strong-binding characteristics. Panning against immobilized Legumain or PD-L1 proteins was also performed twice. Despite these attempts, no human M2 macrophage-selective targeting agent was identified, and this work is on going.

4.2 Proposed Research Projects

4.2.1 Blocking T Cell Exhaustion Through Polymer Displayed Checkpoint Peptides

Immune checkpoint therapy, the targeted blockade of protein-protein interactions responsible for dampening a cytotoxic T cell response to cancer antigens, has gained traction in the last decade as successful cancer treatment. To date, antibodies targeting two checkpoint pathways, CTLA-4 and PD-1, have been FDA approved. An anti-CTLA-4 antibody, ipilimumab, was approved by the FDA in 2011 for treatment of patients with melanoma, after clinical trials demonstrated increased overall survival of treated patients, with a subset of patients surviving over ten years [1]. Two anti-PD-1 antibodies, pembroluzimab and nivolumab, were approved in 2014 for different indications. Pembroluzimab has been approved for patients with advanced stage melanoma while nivolumab has been approved for patients with metastatic melanoma or previously treated advanced or metastatic non-small cell lung cancer.

Due to their independent success, combination therapies of checkpoint antibodies have been proposed and tested in initial clinical trials. In addition, targeting other checkpoint pathway proteins such as TIM-3 and LAG-3 have been proposed and begun testing in preclinical studies. For example, work by Sakuishi and colleagues in mice demonstrated that T cells co-expressing PD-1 and TIM-3 exhibited the greatest exhausted phenotype, and that co-inhibition of both checkpoint pathways is the most effective in delaying tumor growth, compared to monotherapy

[2]. These results motivate the use of simultaneous multiple checkpoint pathway inhibition in cancer therapy.

While to date, methods of blocking these checkpoint pathways in the clinic have been limited to antibodies, peptides can also be effective in blocking protein-protein interactions. For example, Gao and colleagues recently reported effective blocking of PD-1/PD-L1 interactions by a small peptide that binds PD-L1, resulting in anti-tumor effects in a CT-26 tumor mouse model [3].

Polymers decorated with peptides that bind various checkpoint proteins may be a viable method of simultaneously targeting multiple checkpoint pathways, and provide a platform for investigating the optimum combination of checkpoint pathways to target.

To date, peptides that specifically bind checkpoint proteins CTLA-4, PD-1, TIM-3, and LAG-3 have not been reported. Thus peptide phage display biopanning against purified protein targets can be used to identify new targeting peptides that bind these checkpoint proteins. Through competition binding assays, it can be determined what peptide candidates are able to inhibit the interaction of each protein with its ligand and thus identify peptide candidates for polymer grafting.

The Pun Lab has extensive experience synthesizing peptide-polymer conjugates. Most recently, the lab developed a fibrin cross-linking hemostatic polymer made of a (hydroxyethyl)methacrylate (HEMA) and *N*-hydroxysuccinimide methacrylate (NHSMA) polymer backbone that displayed fibrin binding peptides [4]. A similar polymer displaying checkpoint blockade peptides may be synthesized, incorporating one type of peptide or a combination of peptides into the polymer. Preclinical testing of these different polymer constructs in mouse tumor models can identify, 1) the number of peptides per polymer that achieve sufficient tumor regression, and 2) the combination of blocking peptides that best inhibits tumor growth. This peptide polymer construct could provide the opportunity to further elucidate checkpoint blockade mechanisms as well as produce a clinically translatable material that is fully synthetic, thus avoiding manufacturing challenges associated with antibody production. Lastly, development of a single peptide-polymer conjugate that targets multiple checkpoint pathways

may simplify patient dosing regimens compared to dosing multiple antibodies that each target a single pathway.

4.2.2 Utilizing FcγIII Receptors for TAM-targeted Therapy

The categorization of polarized macrophages as M1 "classically activated" or M2 "alternatively activated" is a convenient description of the extreme ends of what is really a spectrum of activation states [5]. As such, activated macrophages found in disease take on diverse phenotypes that often exhibit overlapping M1 and M2 characteristics. For example, recent work by Grugan and colleagues compared expression of markers of activation and different Fcγ Receptors in tumor-associated macrophages with those in bone marrow derived M1 or M2 macrophages [6]. One hallmark of M2 macrophages, when compared to M1 macrophages, is the down regulation of Fc receptors. Despite the classification of TAMs as M2-like, TAMs were actually shown to retain expression of many Fc Receptors, exhibiting slightly higher expression of FcγRIIa and FcγRIIb compared to M1 macrophages and much higher expression of FcγRIII compared to M1 macrophages. It appears that, despite other tumor-promoting characteristics, TAMs retain Fc-mediated immune effector function, explaining the recent clinical success of tumor-targeted mAbs.

The upregulation of FcγRIII on TAMs can potentially be utilized in the development of TAM-targeted therapies. First, FcγRIII is considered a low-affinity Fc receptor, exhibiting low to negligible binding to monomeric IgG (in the micromolar range) and relying on avidity of immune complexes for binding [7]. Thus, constructs targeting this Fc receptor will not compete with monomeric IgG in the tumor environment. Second, FcγRIII is primarily found on natural killer cells and is heavily upregulated on monocytes and macrophages after activation, suggesting that off-target effects will be limited to natural killer cells that can also aid in tumor eradication upon activation. Third, recent work demonstrated that phage libraries can be used to identify peptides that mimic the activating role of IgG1 binding to FcγRI [8]. Conjugating these peptides onto the surface of nanoparticles or divalently displaying them in a fusion

peptide was shown to be sufficient to cause macrophages to generate superoxides and trigger phagocytosis.

It has been suggested that large differences in the binding region of FcγRIII compared to other Fc regions may make it an attractive target for developing a peptide that is selective only for FcγRIII [7]. Thus it may be feasible to use phage display to identify activating peptides that bind FcγRIII, similar to the peptides identified against FcγRI in work by Bonetto and colleagues discussed above. FcγRIII-targeting peptides can then be formulated onto nanoparticles or synthesized as a divalent construct. These constructs may be used to induce superoxide formation and phagocytosis in tumor-associated macrophages *in vivo*, aiding in tumor-eradication and priming of an immune response against tumor cells.

4.3 References

1. Schadendorf D, Hodi FS, Robert C, et al. (2015) Gauging the Long-Term Benefits of Ipilimumab in Melanoma. Journal of Clinical Oncology. doi: 10.1200/JCO.2014.59.5041

2. Sakuishi K, Apetoh L, Sullivan JM, et al. (2010) Targeting Tim-3 and PD-1 pathways to reverse T cell exhaustion and restore anti-tumor immunity. J Exp Med 207:2187–2194. doi: 10.1038/nri1936

3. Gao Y, Liu B, Chang H, et al. (2014) Small peptides elicit anti-tumor effects in CT26 model through blocking PD-L1/PD-1 (TUM2P.900). J Immunol 192:71.24.

4. Chan LW, Wang X, Wei H, et al. (2015) A synthetic fibrin cross-linking polymer for modulating clot properties and inducing hemostasis. Sci Transl Med 7:277ra29. doi: 10.1126/scitranslmed.3010383

5. Mosser DM, Edwards JP (2008) Exploring the full spectrum of macrophage activation. Nat Rev Immunol 8:958–969. doi: 10.1038/nri2448

6. Grugan KD, McCabe FL, Kinder M, et al. (2012) Tumor-Associated Macrophages Promote Invasion while Retaining Fc-Dependent Anti-Tumor Function. J Immunol 189:5457–5466. doi: 10.4049/jimmunol.1201889

7. Hogarth PM, Pietersz GA (2012) Fc receptor-targeted therapies for the treatment of inflammation, cancer and beyond. Nat Rev Drug Discov 11:311–331. doi: 10.1038/nrd2909

8. Bonetto S, Spadola L, Buchanan AG, et al. (2008) Identification of cyclic peptides able to mimic the functional epitope of IgG1-Fc for human Fc RI. The FASEB Journal 23:575–585. doi: 10.1096/fj.08-117069

Chapter 5

APPENDIX

This chapter provides data from preliminary experiments testing untargeted and M2pep-targeted KLA, ATAP, and BIM peptides on mouse M1 and M2 macrophages *in vitro.*

5.1 Materials and Methods

5.1.1 Materials

AnnexinV Staining Kit (eBioscience); AnnexinV-eFluor450 (eBioscience); AnnexinV-APC (eBioscience); propidium iodide (Sigma); CellTrace Violet Cell Proliferation Kit (Life Technologies); SYTOX Green (Life Technologies)

5.1.2 Apoptotic Peptide Synthesis

Apoptotic peptides Mp2pepKLA, ATAP, M2pepATAP, BIM and M2pepBIM were purchased from GL Biochem (Shanghai, China). Peptide sequences are as follows: M2pepKLA (YEQDPWGVKWWY-GGGS-$_{D}$[KLAKLAK]$_{2}$), ATAP (KFEPKSGWMTFLEVTGKIAEMLSLLKQYC), M2pepATAP (YEQDPWGVKWWY–GGGS–KK–KFEPKSGWMTFLEVTGKIAEMLSLLKQYC), BIM (MRPEIWIAQELRRIGDEFNAYC), M2pepBIM (YEQDPWGVKWWY–GGGS–MRPEIWIAQELRRIGDEFNAYC). KLA peptide ($_{D}$[KLAKLAK]$_{2}$) was synthesized via standard Fmoc solid phase peptide synthesis using a NovaPEG Rink Amide resin and purified at >95% purity by RP-HPLC in house. 10 mg/mL stock solutions of KLA and ATAP and 5 mg/mL stock solutions of BIM in H2O/10%DMSO were made, and these concentrated stocks diluted into RPMI for use in cytotoxicity assays.

5.1.3 Cell Suspension Cytotoxicity Assay on Pure Populations of M1 and M2 Macrophages

Murine M1 and M2 macrophages were generated as described in Chapter 1. Cells were removed from their cell culture plate via a cell lifter and 100,000 cells per sample aliquoted into a 96-well black, round bottom plate. Cells were incubated with 0, 5, 10 and 15 μM apoptotic peptides (KLA, M2pepKLA, ATAP, M2pepATAP, BIM, M2pepBIM) in RPMI at 37˚C for 30 minutes. Cells were briefly resuspended by pipetting and then pelleted by centrifugation at 300g for 5 minutes. Supernatant was removed and cells resuspended in pre-warmed RPMI/10%HorseSerum. Cells were incubated for an additional 1.5 hours at 37˚C. Cells were

again resuspended via pipetting and pelleted via centrifugation. Cells were then stained with AnnexinV-eFluor450 and propidium iodide via the manufacturers instructions and analyzed on a MACSQuant Flow cytometer (Miltenyi).

5.1.4 Cell Suspension Cytotoxicity Assay on Mixed Populations of M1 and M2 Macrophages

Murine M1 and M2 macrophages were generated as described in Chapter 1. M1 macrophages were removed from their cell culture plate via a cell lifter, pelleted via centrifugation at 300g and stained with CellTrace violet via the manufacturers instructions. M2 macrophages were also lifted from their cell culture plate and mixed 1:1 with CellTrace-stained M1 macrophages. 200,000 total M1 and M2 macrophages per sample were aliquoted into a 96-well black, round bottom plate. Cells were incubated with 0, 5, 10 and 15 μM apoptotic peptides (KLA, M2pepKLA, ATAP, M2pepATAP, BIM, M2pepBIM) in RPMI at 37˚C for 30 minutes. Cells were briefly resuspended by pipetting and then pelleted by centrifugation at 300g for 5 minutes. Supernatant was removed and cells resuspended in pre-warmed RPMI/10%HorseSerum. Cells were incubated for an additional 1.5 hours at 37˚C. Cells were again resuspended via pipetting and pelleted via centrifugation. Cells were then stained with AnnexinV-APC and propidium iodide via the manufacturers instructions and analyzed on a MACSQuant Flow cytometer (Miltenyi).

5.1.5 Adherent Cytotoxicity Assay on Pure Populations of M1 and M2 Macrophages via Incucyte Imaging

M1 and M2 macrophages were generated as described in Chapter 1 and cultured in 24-well plates. Adherent macrophages were incubated with 0 or 5 μM of M2pepKLA, M2pepATAP or M2pepBIM for 30 minutes at 37˚C. Then peptide-containing media was removed and replaced with pre-warmed RPMI/10%HorseSerum containing 50 μM SYTOX Green. Imaging of each well via an IncuCyte imager began 20 minutes following the conclusion of peptide incubation with peptides. Nine phase-contrast and green fluorescence images per well were taken once per hour

for 20 hours. Images were quantified for confluence of green (dead) cells and confluence of all cells via the IncuCyte software package.

5.2 Results

5.2.1 In Pure Cell Populations, M2pepKLA Mediates Selective Elimination of M2 Macrophages at Low Concentrations while ATAP and BIM Constructs Mediate Selective Elimination of M2 Macrophages Independent of Targeting Moiety

KLA, M2pepKLA, ATAP, M2pepATAP, BIM and M2pepBIM peptides were tested for their ability to mediate selective elimination of M2 macrophages in pure cell populations. Briefly, murine M1 and M2 macrophages were incubated in suspension with 5, 10 and 15 μM of peptides in RPMI media for 30 minutes at 37˚C. Then, unbound peptide was removed and replaced with RPMI media containing 10% Horse Serum. Cells were incubated for an additional 1.5 hours at 37˚C before being stained with AnnexinV and propidium iodide and analyzed on a flow cytometer. Viability was assessed as (Live) x (AnnV- PI-) and normalized to the untreated control for its respective cell type (Figure 5.1).

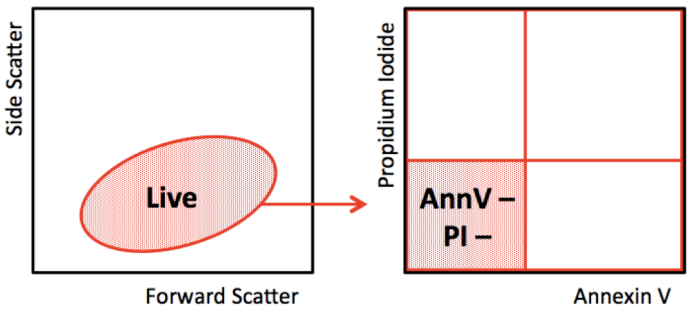

Figure 5.1: Gating strategy for assessing viability of pure populations of M1 and M2 macrophages treated with pro-apoptotic peptides. Viability is measured as (Live) x (AnnV- PI-) and normalized to the untreated control.

Untargeted KLA exhibited little to no toxicity to either M1 or M2 macrophages at any concentration tested while M2pepKLA exhibited limited selectivity for M2 macrophage at low concentrations (Figure 5.2A). When treated with 5 μM M2pepKLA, M2 macrophages exhibited

lower viability (66%) when compared to M1 macrophages (94%). However, at the higher 10 μM and 15 μM concentrations, viability of M1 macrophages (56% and 37%, respectively) was lower when compared to M2 macrophages (73% and 60%, respectively). These results indicate that *in vitro* M2pepKLA lacks the desired selectivity of an M2-specific cytotoxic agent.

Both the ATAP and M2pepATAP peptides exhibited selectivity in depletion of M2 macrophages (Figure 5.2B). At all 5, 10 and 15 μM concentrations tested, ATAP-treated M2 macrophages exhibited a decrease in viability (54%, 59%, and 67%, respectively) when compared to ATAP-treated M1 macrophages (104%, 106%, and 118%, respectively). At the lower 5 and 10 μM concentrations tested, M2pepATAP-treated M2 macrophages exhibited a decrease in viability (59% and 46%, respectively) when compared to M2pepATAP-treated M1 macrophages (116% and 93%, respectively). However, at the higher 15 μM concentration, M2pepATAP-treated M2 macrophage viability (49%) was similar to M2pepATAP-treated M1 macrophage viability (65%). These results suggest that at lower concentrations, M2pepATAP may be used as an M2 macrophage-selective cytotoxic agent. Surprisingly, these results also suggest that untargeted ATAP may also be a promising agent for selective M2 macrophage depletion.

The BIM and M2pepBIM peptides exhibited similar cytotoxicity profiles to the ATAP peptides. At all 5, 10 and 15 μM concentrations tested, BIM-treated M2 macrophages exhibited decreases in viability (65%, 59%, and 65%, respectively) compared to M1 macrophages (98%, 90%, and 95%, respectively). Likewise, at the 5, 10 and 15 μM concentrations tested, M2pepBIM-treated M2 macrophages exhibited decreases in viability (59%, 50%, and 58%, respectively) compared to M1 macrophages (98%, 86%, and 85%, respectively). These results indicate that M2pepBIM may also be used as an M2 macrophage selective cytotoxic agent, though the M2 macrophage depletion is not as great as that demonstrated in M2 macrophages treated with M2pepATAP. It is also surprising that untargeted BIM shows selective depletion of M2 macrophages, suggesting its use also in M2 macrophage-targeted therapy.

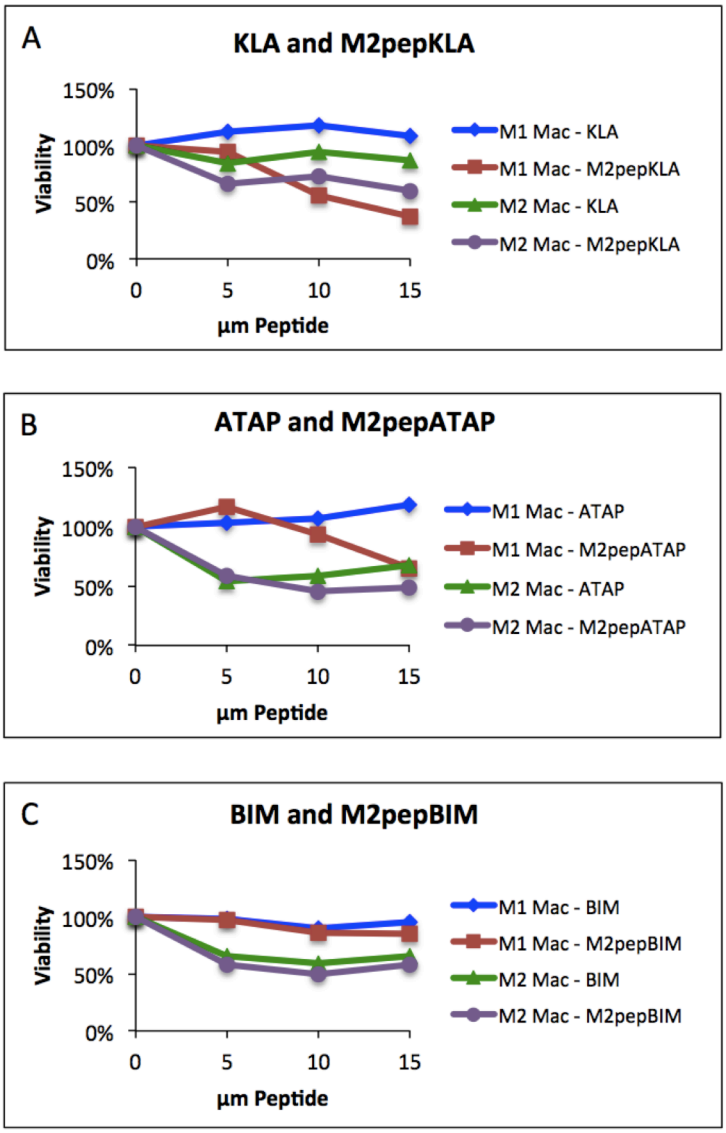

Figure 5.2: Viability of pure populations of M1 and M2 macrophages treated with pro-apoptotic peptides. M1 or M2 macrophages were treated with 5, 10, or 15 µM of (A) KLA or M2pepKLA, (B) ATAP or M2pepATAP, or (C) BIM or M2pepBIM. Viability was assessed as described in Figure 5.1.

Exposure of pure populations of cells to M2pep-targeted pro-apoptotic peptides lacks similarity to an *in vivo* environment where peptides will encounter a diverse milieu of cells. Thus, the lack of selectivity exhibited by the M2pepKLA construct on pure cell populations may be due to non-specific uptake by M1 macrophages exposed to a high concentration of peptide without competition. Likewise, the selectivity of the M2pepATAP and M2pepBIM constructs may

be abrogated by the presence of other cells competing for uptake of the peptides, and untargeted ATAP and BIM my lose selectivity in mixed cell populations. To test these hypotheses, mixed populations of M1 and M2 macrophages were exposed to the pro-apoptotic peptides.

5.2.2 In Mixed Cell Populations, M2pepBIM is Most Selective in Elimination of M2 Macrophages

To test the targeted and untargeted pro-apoptotic peptides in mixed populations of macrophages, M1 macrophages were first labeled with CellTrace Violet before being mixed in a 1:1 ratio with M2 macrophages. These mixed cell populations were then exposed to pro-apoptotic peptides as described in Section 5.2.1 and analyzed on a flow cytometer, utilizing the CellTrace Violet dye to identify M1 versus M2 macrophages in the mixed cell population. Viability was assessed as (M1 or M2) x (AnnV- PI-) and normalized to the untreated control for its respective cell type (Figure 5.3).

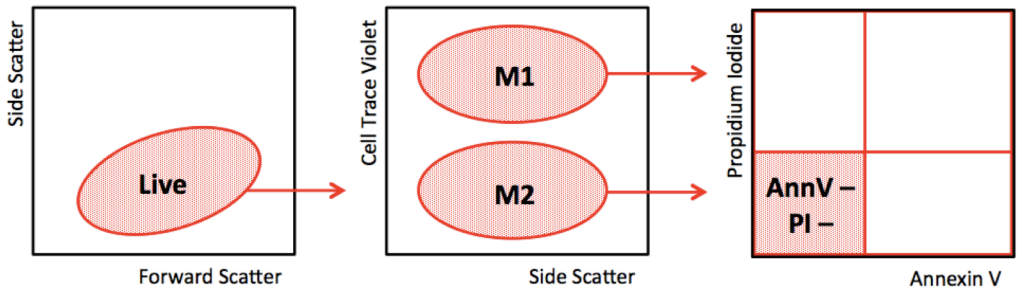

Figure 5.3: Gating strategy for assessing viability of mixed populations of M1 and M2 macrophages treated with pro-apoptotic peptides. Viability is measured as (M1 or M2) x (AnnV- PI-) and normalized to the untreated control for each cell type.

Similar to the results found in pure populations of M1 or M2 macrophages, untargeted KLA shows little to no toxicity on macrophages in mixed population of cells (Figure 5.4A). Again, at the low concentration of peptide, 5 μM, M2pepKLA demonstrates slightly higher toxicity on M2 macrophages (78% viability) over M1 macrophages (84% viability). At the higher 10 μM and 15 μM peptide concentrations, M1 macrophages show lower viability (63% and 21%, respectively) compared to M2 macrophages (77% and 33%, respectively). These results suggest that

M2pepKLA is more toxic to both M1 and M2 macrophages when incubated in a mixed cell population. However, the results mirror those shown in pure cell populations exposed to M2pepKLA and indicate that *in vitro* M2pepKLA does not exhibit the desired M2 macrophage-specific cytotoxicity.

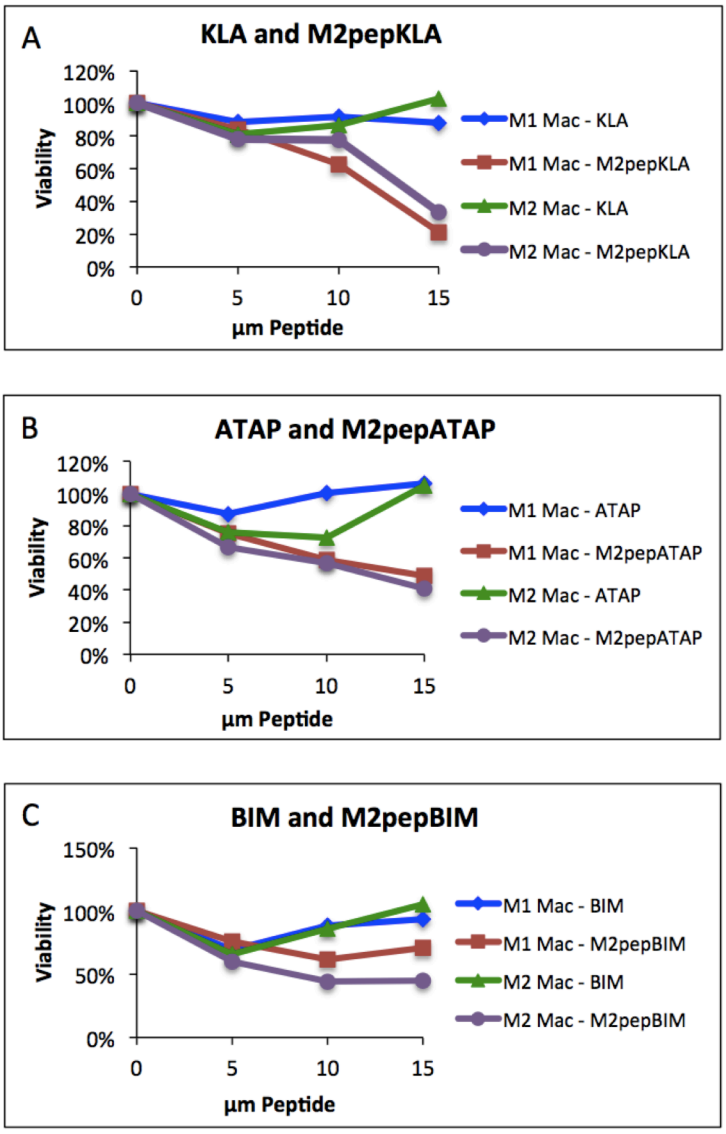

Figure 5.4: Viability of mixed populations of M1 and M2 macrophages treated with pro-apoptotic peptides. M1 or M2 macrophages were treated with 5, 10, or 15 µM of (A) KLA or M2pepKLA, (B) ATAP or M2pepATAP, or (C) BIM or M2pepBIM. Viability was assessed as described in Figure 5.3.

While in pure populations of M1 and M2 macrophages, untargeted and M2pep-targeted ATAP exhibited preferential M2 macrophage cytotoxicity, in mixed populations of cells, cell death between M1 and M2 macrophages is similar for each peptide type (Figure 5.4B). For example, at each ATAP peptide concentration 5, 10 and 15 μM, viability of M1 macrophages (87%, 100% and 106%, respectively) was slightly higher than M2 macrophages (76%, 72%, and 105%). At each M2pepATAP peptide concentration 5, 10 and 15 μM, viability of M1 macrophages (75%, 59%, and 49%, respectively) was very similar to M2 macrophages (67%, 56%, and 41%, respectively). These results suggest that in mixed populations of cells, ATAP and M2pepATAP exhibit diminished M2 macrophage depletion properties.

While in the study using pure populations of macrophages, untargeted and M2pep-targeted BIM displayed M2 macrophage-selective depletion properties, in mixed populations of cells only M2pepBIM demonstrated M2 macrophage selectivity (Figure 5.4C). At each BIM peptide concentration 5, 10 and 15 μM, viability of M1 macrophages (69%, 88%, and 94%, respectively) was very similar to the viability of M2 macrophages (66%, 86%, and 105%, respectively). However, with increasing concentration of M2pepBIM, viability of M2 macrophages (60%, 44%, and 45%, respectively) decreased compared to viability of M1 macrophages (76%, 62%, and 71%, respectively). These results suggest that M2pepBIM may be a viable alternative to the well-characterized M2pepKLA construct to selectively deplete M2 macrophages.

While the methods described above represent cell death through staining with the Annexin V and propidium iodide markers of cell death, another indication of cell death is changes in the composition of the mixed population of cells. For example, results showing a decrease in the percent of cells in a mixed population that are M2 macrophages would suggest that the treatment was selectively killing M2 macrophages. To test this, the percent of cells that fall in the M1 or M2 gate in Plot 2 as a proportion of all events in Plot 1 was measured for mixed populations of M1 and M2 macrophages treated with pro-apoptotic peptides (Figure 5.5). These percentages were then normalized to the untreated controls for each cell type.

This alternative method of assessing cell viability supported many of the conclusions of the Annexin V and propidium iodide staining, and provided additional insight into the extent of cell death and the initiation of apoptosis in cells. All untargeted constructs of KLA, ATAP and BIM exhibited no decrease in proportion of M1 or M2 macrophages within the mixed cell population (Figure 5.6), supporting the conclusion of the Annexin V and propidium iodide staining which also indicated little initiation of apoptosis in these cells as well (Figure 5.4).

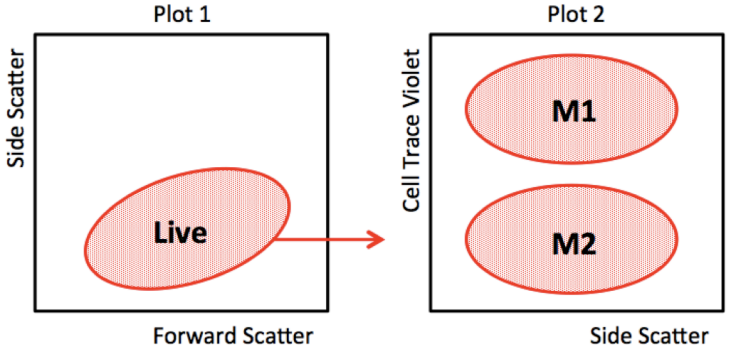

Figure 5.5: Gating strategy for assessing the selective cell killing of M1 or M2 macrophages in mixed populations of cells exposed to pro-apoptotic peptides. A cell is considered live if it falls within the M1 or M2 gate in Plot 2, and percent live M1 or M2 cells is represented as a percentage of all events in Plot 1. Percentages were then normalized to the untreated control for each cell type.

With increasing concentration of M2pepKLA (5, 10 and 15 μM) the proportion of M1 macrophages (95%, 88%, and 66%, respectively) decreased compared to the proportion of M2 macrophages (97%, 102%, and 94%, respectively), which remained unchanged (Figure 5.6A). This result, compared with that shown with Annexin V and propidium iodide staining, indicates that M2pepKLA treated M1 macrophages have both disappeared from the cell populations after death (Figure 5.6A) and are actively dying (Figure 5.4A), whereas M2 macrophages are still present in the population (Figure 5.6A) but have begun the process of apoptosis (Figure 5.4A). Again, this work indicates that, *in vitro,* the M2pepKLA construct does not offer the M2 macrophage selective cytotoxicity desired.

With increasing concentrations of M2pepATAP (5, 10, and 15 μM), the proportion of M1 macrophages (92%, 74%, and 70%, respectively) or M2 macrophages (90%, 69%, and 66%,

respectively) decreased to a similar extent (Figure 5.6B). This result mirrors that shown with Annexin V and propidium iodide staining (Figure 5.4B), suggesting that extent of cell death and initiation of apoptosis is similar between M1 and M2 macrophages.

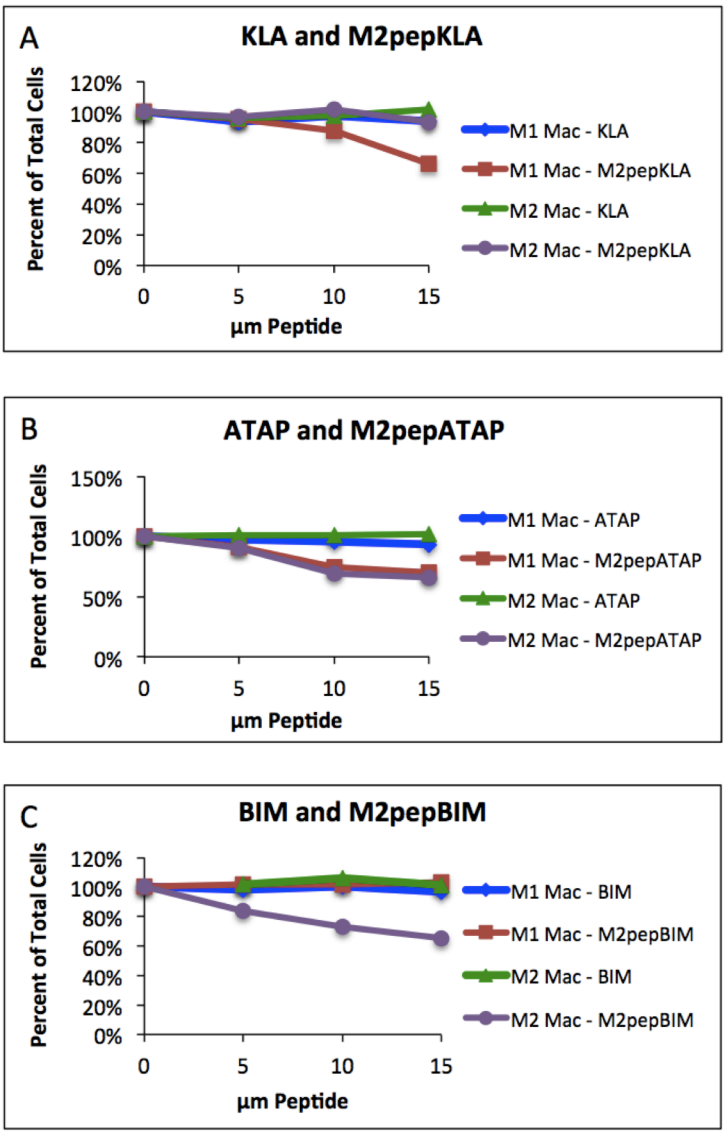

Figure 5.6: Selective cell killing in mixed populations of M1 and M2 macrophages treated with pro-apoptotic peptides. M1 or M2 macrophages were treated with 5, 10, or 15 µM of (A) KLA or M2pepKLA, (B) ATAP or M2pepATAP, or (C) BIM or M2pepBIM. Cell death was assessed as described in Figure 5.5.

Lastly, with increasing concentrations of M2pepBIM (5, 10 and 15 µM) the proportion of M2 macrophages (84%, 73%, and 65%, respectively) decreases compared to the proportion of M1

macrophages (101%, 101%, and 104%, respectively), which remains unchanged. These results suggest that M2pepBIM-treated M2 macrophages have both disappeared from the cell population (Figure 5.6C) and initiated apoptosis (Figure 5.4C), while M1 macrophages are still present in the cell population (Figure 5.6C) but have begun the process of apoptosis (Figure 5.4C). This work demonstrates that M2pepBIM is an effective agent in mixed cell populations, and again indicates that M2pepBIM is a viable candidate for selective depletion of M2 macrophages.

5.2.3 Overall M1 Macrophage Cell Death is Higher when Coincubated in a Mixed Population of Cells with M2 Macrophages

Further analysis of the results of the pure and mixed cell population studies of apoptosis indicated lower viability of M1 macrophages when incubated in a mixed population with M2 macrophages than alone in a pure cell population. For example, Figure 5.7 shows the viability of M1 macrophages for each treatment group at 15 μM, demonstrating decreased viability in mixed populations. This trend was also consistent for the other concentration points tested, with the exception of cells treated with 10 μM M2pepKLA, which showed slightly higher viability in the mixed population.

The reason for this bystander M1 macrophage cell death effect of incubation with healthy or apoptotic M2 macrophages is unclear. It is known that M1 and M2 macrophages possess different efferocytosis capabilities [1]. Due to their role in the resolution of inflammation and clearance of cellular debris, M2 macrophages have increased levels of efferocytosis function accompanied by increased expression of receptors, like CD36, that mediate engulfment of apoptotic cells. The low level of similar receptors on M1 macrophages makes them less responsive to apoptotic cells. Research has shown that macrophage cell surface CD36 binding of oxidized phosphatidylserine on apoptotic or viable cells can induce macrophage efferocytosis [2]. Thus it is possible that incubation of M1 macrophages with M2 macrophages that exhibit higher efferocytosis function can result in greater engulfment of M1 macrophages

by M2 macrophages and higher levels of M1 macrophage cell death. This is in contrast to when M1 macrophages are incubated in a pure population, surrounded by other M1 macrophages that overall exhibit low efferocytosis function. Overall, additional research into the pro-apoptotic bystander effect of M1 and M2 macrophage coincubation is warranted.

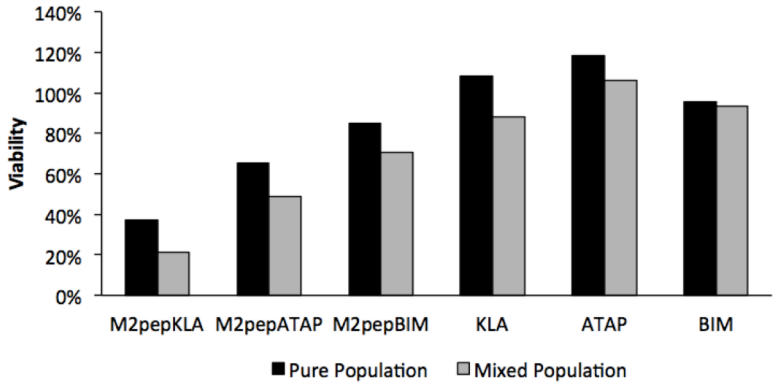

Figure 5.7: M1 macrophages exhibit lower viability when treated with 15 μM pro-apoptotic peptides in mixed cell populations of M1 and M2 macrophages than in a pure cell population.

5.2.4 M2pepATAP and M2pepBIM are Promising Candidates for M2 Macrophage Elimination on Adherent Cells

While the work described above demonstrates the cytotoxic effects of the pro-apoptotic peptides on M1 and M2 macrophages in a cell suspension, live cell imaging via an IncuCyte imager provided information about the cytotoxicity of the peptides on adherent cells. Briefly, M1 and M2 macrophages plated in 24 well plates were treated for 30 minutes at 37˚C with 5 μM M2pepKLA, M2pepATAP or M2pepBIM. Then, media was replaced with RPMI containing 10% Horse Serum and Sytox Green. Cells were incubated at 37˚C for 20 more hours, and fluorescently imaged for Sytox Green staining (dead cells) and phase contrast imaged for cell confluence once per hour. Percent of cells that are dead at each time point was calculated by dividing Sytox Green cells per area by all cells per area, and then was normalized to the untreated control.

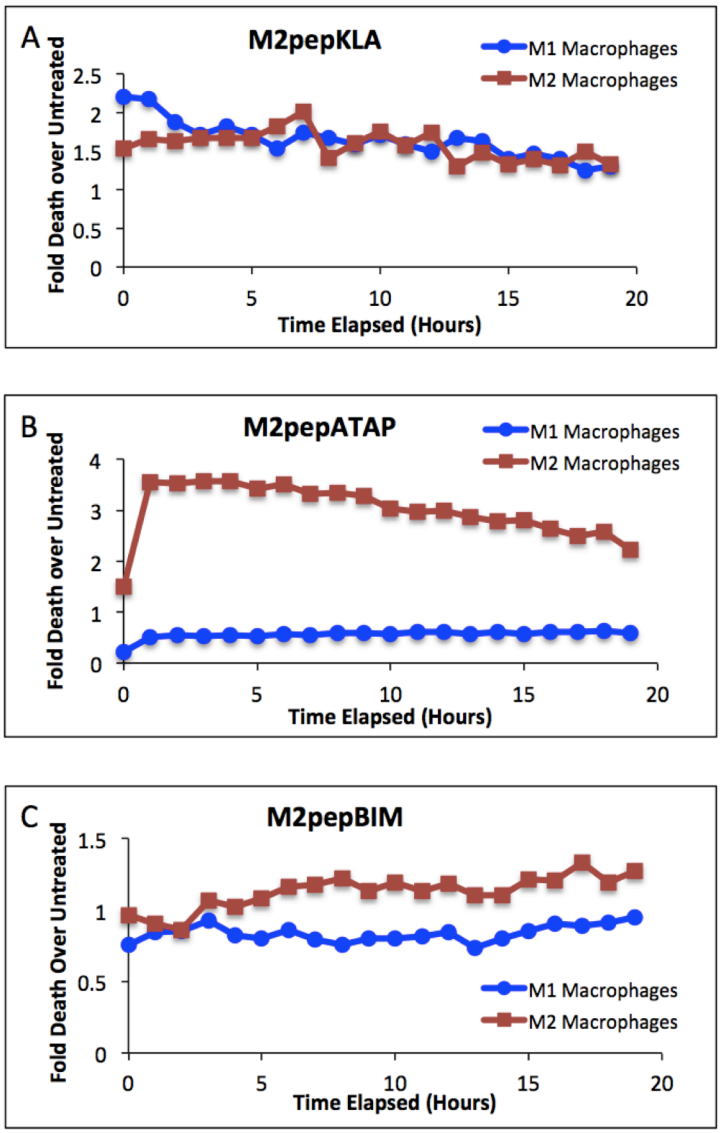

Figure 5.8: Viability of adherent M1 and M2 macrophages. M1 and M2 macrophages were treated for 30 minutes with 5 μM (A) M2pepKLA, (B) M2pepATAP, or (C) M2pepBIM, followed by imaging via an IncuCyte for 20 hours. Fluorescent images identified dead cells via a Sytox Green stain and phase contrast imaging measured overall cell confluence. Percent of total cells that are dead was calculated and normalized to an untreated control.

Plots of the fold death of treated M1 or M2 macrophages over their untreated controls provided similar results to the pure cell population flow cytometry assay on cells in suspension (Figure 5.2). Over the 20 hour time period, M2pepKLA treated M1 or M2 macrophages displayed little difference in cytotoxicity (Figure 5.8A). In addition, cell death varied roughly between 1.5

and 2 times the untreated samples, low level cytotoxicity that is similar to that seen at the 5 μM concentration on cells in suspension.

M2pepATAP treated M2 macrophages exhibited a large three to four fold increase in cell death compared to M1 macrophages over the 20 hour time period (Figure 5.8B). This result is very similar to the results seen on pure populations of macrophages in suspension, where M2pepATAP treatment resulted in a roughly 50% depletion of M2 macrophages compared to M1 macrophages. However, untargeted ATAP incubation with macrophages in suspension also resulted in a marked decrease in M2 macrophage viability. Without the untargeted ATAP control in this cytotoxicity experiment on adherent macrophages, it is difficult to determine if the M2pep targeting agent is responsible for this selective M2 macrophage cell killing.

Lastly, M2pepBIM treatment exhibited selective M2 macrophage killing four hours after peptide exposure, and maintained higher cell death in M2 macrophages over M1 macrophages over the remaining 16 hours of cell imaging (Figure 5.8C). These results mirrored the results of M2pepBIM treatment on cell suspensions where M2 macrophages exhibited roughly 40% reduction in viability compared to M1 macrophages. However, like the ATAP peptide, untargeted BIM treatment on cells in suspension also resulted in preferential M2 macrophage cytotoxicity and thus without this untargeted control, it is difficult to discern if the M2pep targeting peptide is responsible for M2pepBIM's cytotoxicity towards adherent M2 macrophages.

While the results of this cytotoxicity experiment on adherent macrophages suggest that M2pepBIM remains a viable alternative to M2pepKLA for selective killing of M2 macrophages, the assay can be further optimized for future work. As discussed above, the addition of the untargeted peptides as controls would provide additional insight into the role of M2pep in selective M2 macrophage depletion. In addition, cell death appears to be already elevated at the 0 hour time point and change little over time. This suggests that more frequent images, for example every 15 minutes, may offer additional information regarding the kinetics of cell death. Lastly, the Incucyte imager takes nine images per well and averages the cell death and confluence data over these nine images. In review of the images, cell density and response to

peptides appears to vary greatly among the nine images from a single well. Work to more evenly distribute cell density across the well may improve the reproducibility of the results.

5.3 Acknowledgements

Thank you to Dr. Patrick Stayton for his thoughtful discussions regarding the BIM peptide. Also, thank you to Chayanon Ngambenjawong who optimized many M2pepKLA cell viability assays and provided helpful discussions during interpretation of data. Lastly, thank you to Dr. Andrew Oberst for the helpful discussion regarding our preliminary data, and for the use of the IncuCyte Imager.

5.4 References

1. Korns D, Frasch SC, Fernandez-Boyanapalli R, et al. (2011) Modulation of macrophage efferocytosis in inflammation. Front Immunol 2:57. doi: 10.3389/fimmu.2011.00057

2. Greenberg ME, Sun M, Zhang R, et al. (2006) Oxidized phosphatidylserine-CD36 interactions play an essential role in macrophage-dependent phagocytosis of apoptotic cells. J Exp Med 203:2613–2625. doi: 10.1084/jem.20060370